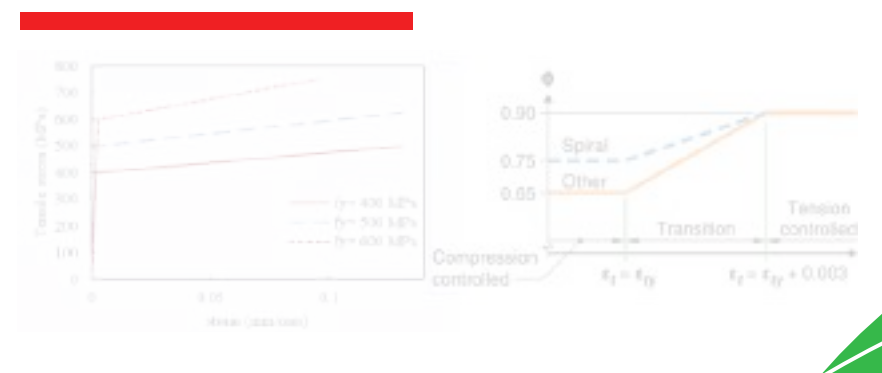
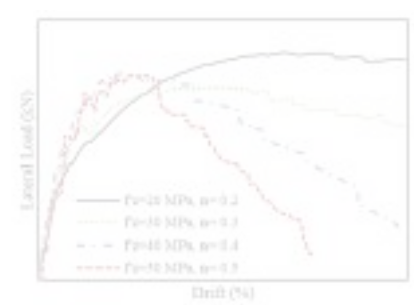
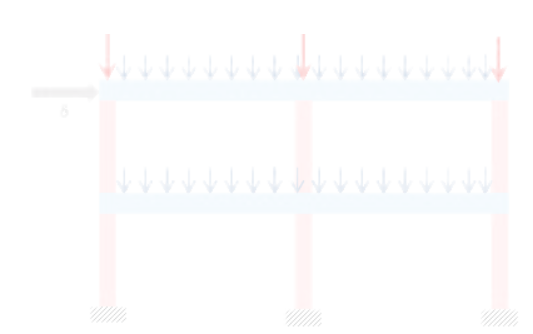




Study on Concrete Compatibility and Other Aspects for Application of High—Strength Rebar in Reinforced Concrete Building Design







Prepared under
A Memorandum of Understanding between
Public Works Department and GPH Ispat Limited

December 2024

Disclaimers

This report was prepared for the Public Works Department (PWD) and GPH Ispat Limited under the project contract aimed at investigating the use of high-strength steel reinforcement in reinforced concrete building design in Bangladesh. The contents of this publication do not necessarily reflect the views and policies of PWD or Government of Bangladesh.

The report was produced by the research team as part of a collaborative effort. While every attempt has been made to ensure the accuracy and practicality of the information, the research team, authors, and reviewers assume no liability for, nor express or imply any warranty concerning, the information provided. Users of this report assume all responsibility for any consequences arising from its use.

Various commercial software and tools have been utilized during the preparation of this report. Their mention here is not intended as an endorsement or recommendation by PWD, nor does it suggest that they are necessarily the most suitable or effective options available for the intended purposes.

In alignment with international practices, the preferred units of measurement in this report are metric units, though other systems may be referenced where relevant.

Study on Concrete Compatibility and Other Aspects for Application of High-Strength Rebar in Reinforced Concrete Building Design

PUBLIC WORKS DEPARTMENT GPH Ispat Limited

Prepared under
A Memorandum of Understanding between
Public Works Department and GPH Ispat Limited

DECEMBER 2024

© Public Works Department

All rights reserved. No part of this publication shall be reproduced, stored in a retrieval system, reprinted, or transmitted in any form by any means electronic, mechanical, photocopying, recording, or otherwise without permission in writing from the Additional Chief Engineer, Planning and Special Project, Public Works Department.

Published by: Public Works Department Purta Bhaban, Segunbagicha Dhaka-1000

Utmost care has been taken to avoid printing and other mistakes, but there may always be chances of unintended mistakes.

Any mistakes and suggestions to update/revise may please be addressed to: The Additional Chief Engineer, Planning and Special Project Public Works Department.

Acknowledgement

AUTHORS

Jahid Hasnain, Sub-divisional Engineer, Design Division-2, PWD S.A.M Nassif Zubayer, Sub-divisional Engineer, Design Division-6, PWD Muhammad Salah Uddin Sumon, Sub-divisional Engineer, Design Division-5, PWD

Md. Samiul Basar, Sub-divisional Engineer, Design Division-6, PWD Mohammad Elias, Assistant Engineer, Special Design Unit-2, PWD

RESEARCH ASSOCIATE

Minhajul Bari Prince, B.Sc. in Civil Engineering

PANEL OF SUPERVISORS

PWD side

Md. Rafiqul Islam Superintending Engineer, Design Circle-1, PWD

Md. Sohel Rahman Superintending Engineer, Design Circle-2, PWD

GPH side

Md. Ahsan Habib, PEng

ACADEMIC EXPERT

Dr. Md. Tarek Uddin, PEng Professor Department of Civil & Environmental Engineering Islamic University of Technology

Background

Public Works Department (PWD), under the Ministry of Housing and Public Works, is the pioneer in construction arena of Bangladesh. Over about two centuries, PWD could successfully set the trend and standard in the country's infrastructural development. It plays a pivotal role in the implementation of government construction projects.

GPH Ispat Ltd. is one of the leaders in steel manufacturing in Bangladesh ensuring the quality products following various international and national standards. GPH Ispat Ltd. is a Public Limited Company by share under the Companies Act, 1994 seeking to improve understanding between their respective organization and to establish mutually beneficial collaborations.

During structural design and implementation, engineers from PWD encounter several practical issues which can be mitigated by proper research. So, both the PWD and GPH Ispat Ltd. agreed on 22 November, 2023 to establish a Memorandum of Understanding (MoU) as a framework to develop their mutual interests and collaborative research program, where honorable Chief Engineer of PWD signed on behalf of PWD.

High-strength steel reinforcement has gained popularity in construction due to its cost-effectiveness and ability to reduce rebar congestion in joints, allowing for better concreting. According to the provision of the Bangladesh National Building Code (BNBC 2020), the yield strength limit of steel reinforcing bar is 550 MPa (80 ksi) in the general case and 420 MPa (60 ksi) in the case of special moment frames. In contrast, the latest American standard, ACI 318-19 allows the use of 690MPa (100 ksi) in general cases, and 550MPa (80 ksi) in special moment frames for yield strength upper limit of the rebar yield strength, reflecting a trend of adaptation toward higher-strength steel reinforcement. Under the direction of the Additional Chief Engineer, P&SP (PWD), a collaborative research initiative was taken by forming two research teams composed of PWD engineers to explore the applicability of high-strength reinforcement considering technical and economic aspects. This report covers the findings on concrete compatibility and other technical aspects related to design strength, serviceability, and seismic performance of high-strength reinforcement for application in Reinforced Concrete Building Design.

Table of Contents List of Figuresviii List of Tablesxi Abstract xiii 1 1.2 1.3 Purpose and Scope1 2 3 Use of High-Strength Reinforcement in RC Design5 3.1 3.2 Availability of High-Strength Reinforcement in Bangladesh6 3.3 3.4 Material Grade & properties applicable as per Building Codes......6 3.5 Comparison of reinforcements properties available in Bangladesh......9 3.6 Required minimum compressive strength of concrete11 3.7 4 4.1 Flexural Capacity of Beam13 4.1.1 4.1.2 4.1.3 Maximum rebar spacing and serviceability stress condition.......24 Column capacity (axial load-moment interaction)26 4.1.4 4.1.5 Confinement requirement for Column27 Bond and Development Length Demand33 4.1.6 5 5.1 5.1.1 Behavior of Hysteresis loop due to cyclic load test......43 5.2 Discussion 67 6 6.1 Comparison of Structural Member Design Parameters......67 6.2 Structural member Performance comparison against Lateral Load69 7 7.1 Challenges72 7.2 7.3 Recommendations 73 7.4

List of Figures
Figure 1: Tri-Linear presentation of Stress-strain diagram of Grade 500CWR Rebar9
Figure 2:Tri-Linear presentation of Stress-strain diagram of Grade 500DWR Rebar9
Figure 3:Tri-Linear presentation of Stress-strain diagram of Grade 600DWR Rebar9
Figure 4: Stress-strain curve for ASTM A1035 Grade 100 and Grade 120 reinforcement (Wiss Janney Elstner Associates, Inc., Copyright 2008)
Figure 5: Stress-strain curve for USD685A reinforcement (Ousalem et al., 2009)11
Figure 6: Span length, Loading and RC member detail for Flexural capacity comparison13
Figure 7: Strain limit states and relation to Strength reduction factor, ϕ (ACI 318-19)14
Figure 8: Relation of Beam Deflection with Reinforcement ratio, Beam depth & Concrete grade
Figure 9: Geometrical basis of Crack width in flexural member [25]
Figure 10:Beam section used for crack width analysis
Figure 11: Comparison of crack width at various serviceability limit state according to (a) ACI 318-95 (b) Eurocode 1992-1-1:2004 (c) NZ 3101.1:2006 (d) IS 456:200023
Figure 12: Maximum allowable serviceability stress limit (f_s =% f_y) for various rebar grade at different crack width based on exposure condition (as per ACI 318-95)24
Figure 13: Maximum rebar spacing required for crack control at serviceability limit state24
Figure 14: Flow diagram for checking rebar spacing limit for crack control25
Figure 15: Column section used for nominal capacity analysis
Figure 16: Comparison of Column nominal capacity using Different Rebar grade and using constant " $A_s f_y$ "
Figure 17: Effect of Confinement on concrete capacity [27]
Figure 18: of column specimens for confinement calculation
Figure 19: Comparison of confinement requirement (a) according to different building codes, (b) variation with respect to f'c for different rebar grade according to ACI 318-1932
Figure 20: Comparison of confinement ratio according to ACI 318-19 with different rebar grade (a) for various concrete grade with C-500x500 (b) for various column size with $f^*c = 30MPa$ 33
Figure 21: Development length of straight deformed bar, 1 _d requirement for different grade of concrete and rebars
Figure 22: Comparison of Development length requirement according to BNBC 2020 and ACI 318-1936
Figure 23: Standard hook geometry for bar development in tension
Figure 24: Hooked Development length, l _{dh} requirement for different grade of concrete and rebars
Figure 25: Hooked Development length, l _{dh} requirement for different grade rebars by varying concrete's grade according to ACI 318-19 with 25mm dia bar
Figure 26: Headed deformed bar extension within column (ACI 318-19, 25.4.4)40

Figure	27: Headed bar Development length, l _{dt} requirement for different grade of concrete and rebars41
Figure	28: Typical end detailing of Beam-Column exterior joint
Figure	29: Reinforcement details and test set up for beam specimens [3]44
Figure	30: Measured shear versus drift ratio (a) Specimen with Grade 60 reinforcement; and (b) Specimen with Grade 97 reinforcement.
Figure	31: Test sample and experimental parameters for column capacity test [29]45
Figure	32: Tensile Strain vs Drift ratio for Reinforcement Grade 415, 550 and 700MPa [29]45
Figure	33: Test sample and experimental parameters for column capacity test [30]46
Figure	34: Effect of axial load ratio on (a) Strength and deformation capacity, (b) Stiffness degradation [30]46
Figure	235: Effect of Equal Strength reinforcement replacement (constant $A_s f_y$) (a) Strength and deformation capacity, (b) Stiffness degradation [30]47
Figure	236: Hysteresis response specimen(a) NS-30, (b) RHS-30, (c) NS-70 and (d) RHS-70 [31]48
Figure	37: Stiffness degradation pattern for frame specimens [31]
Figure	38: Stress-strain relationship in Flexural member section in uncracked section [25]50
Figure	39: Stress-strain relationship in Flexural member in cracked section [25]50
Figure	40: Idealized bi-linear curve for moment-curvature relationship50
Figure	41: Concrete material properties used for Concrete Damage Plasticity (CDP) model [34] (a) compressive behavior (b) tensile behavior51
Figure	42: Bilinear steel model (for Class:D according to BDS-ISO 6935-2-2021)52
Figure	43: Typical load-deformation curve of RC structural members [35]52
Figure	44: Definition of yield drift and ultimate drift [36]52
Figure	45: Details of Reference RC frame [33]
Figure	46: Geometric FE modelling of reference specimen in ABQUS54
Figure	47: Load and boundary conditions of FEM according to reference RC specimen54
Figure	48: Details of reference RC column specimen [8] (all dimensions are in mm)55
Figure	49: Finite element modeling of reference RC column in ABQUS55
Figure	50: Comparison between backbone curve of FEM approach and experiment56
Figure	51: Schematic diagram of RC frame used for FEM parametric study56
Figure	52: Backbone curve of analytical specimens varying rebar's grade59
Figure	53: Stiffness degradation curve of analytical specimens varying rebar's grade59
Figure	54: Damage of concrete due to tension for different specimens at 2% drift for Grade 400, 500 & 600MPa60
Figure	55: Stress level of reinforcement for different specimens at 2% drift for Grade 400, 500 & 600MPa
Figure	56: Backbone curve of analytical specimens varying concrete's grade61
Figure	57: Stiffness degradation curve of analytical specimens varying concrete's grade61

Figure 58: Damage of concrete due to tension for different specimens at 2% drift for Grade 20, 30 & 50MPa concrete	
Figure 59: Backbone curve of analytical specimens varying axial load ratio for fy=600MPa	63
Figure 60: Stiffness degradation curve of analytical specimens varying axial load ratio	.64
Figure 61: Backbone curve of analytical specimens varying concrete's grade	.65
Figure 62: Stiffness degradation curve varying concrete's grade	.65

List of Tables

Table 1: Comparison of required material properties of reinforcing bars of maximum grade allowed according to different standards
Table 2: Comparison of applicable reinforcement grade as per ACI 318-19 for different seismic applications (limited ASTM standards for deformed bars have been considered)
Table 3: Comparison of applicable concrete grade as per ACI 318-19 for different seismic applications
Table 4: Material grade comparison specified in different building codes for RC building design considering seismic application (only longitudinal reinforcement considered here)
Table 5: Permissible limit of compressive strength of concrete according to ACI 318-1912
Table 6: Material Properties for various concrete grades
Table 7: Flexural Capacity of Beam section using f'c = 20MPa15
Table 8: Flexural Capacity of Beam section using f'c = 30MPa13
Table 9: Flexural Capacity of Beam section using f'c = 40MPa13
Table 10: Deflection of Beam section using f'c = 20MPa10
Table 11: Deflection of Beam section using f'c = 30MPa10
Table 12: Deflection of Beam section using f'c = 40MPa10
Table 13: Beam depth demand for target deflection control with different graded reinforcement
Table 14: Guideline for reasonable flexural crack width under service load as per ACI 224R-01
Table 15: Recommended maximum surface crack width at serviceability limit state as per NZS 3101:2006 [23]
Table 16: Recommended values of maximum crack width limit as per Eurocode 2 (EN 1992-1-1) [24]
Table 17: Comparison of Crack width compliance for different stress level of various yield strength of Reinforcement based on formula shown with ACI (clear cover=40mm) .23
Table 18: Trend of Column nominal capacity increase for Different Rebar grade and increasing concrete compressive strength, f'c
Table 19: Transverse reinforcement for columns of SMF
Table 20: Properties of analytical specimens for confinement calculation
Table 21: Material properties used for analytical study of development length for straight bar
Table 22: Material properties used for analytical study of development length for hooked bar
Table 23: Comparative end column dimensions for different combinations of concrete and rebar grades using hooked and headed deformed bar
Table 24: Properties of reference specimen for Beam-Column Joint experiment [31]48
Table 25: Material properties of reference experiments for FEM validation

Table 26: Variation of different parameters for FEM study	57
Table 27: Lateral behavior of analytical specimens varying rebar's grade	58
Table 28: Lateral behavior of analytical specimens varying concrete's grade	61
Table 29: Lateral behavior of analytical specimens varying axial stress ratio on column	62
Table 30: Lateral behavior of analytical specimens varying concrete's grade	65

Abstract

Practicing in structural design & construction of RCC structures in Bangladesh started and evolved with concrete compressive strength of around 15MPa and plain steel reinforcement of 275MPa. By now, the Steel reinforcing bar of grade 500MPa is widely used in constructing reinforced concrete structures in Bangladesh. Grade 600 steel is being aligned to the track of RC construction since Bangladesh Standards and Testing Institution (BSTI) has introduced grade 600 reinforcing steel in their standard BDS6935-21. Vacillation, the arbitrariness of the users, over the agreement of higher-grade steel with concrete of lower bound strength makes it difficult to cash the gain from using steel of higher grades in RCC. Bangladesh National Building Code (BNBC-2020) permits concrete compressive strength (f'c) of 17MPa for low-rise buildings up to 4-storied (Part-VI, Sec-5.5.4). In BNBC-2020, concrete compressive strength value, a minimum of 20MPa in general, other than severe to extreme exposure conditions and 21MPa in the seismic design category, SDC - D has been mentioned (Part-VI, Sec-8.1.7 & 8.3.3.3) respectively.

The compatibility of concrete strength with high-strength reinforcing steel is related to numerous design parameters (i.e., member capacity, bond strength, confinement demand, serviceability requirement, etc.). Several building codes including ACI 318-19 have introduced higher strength reinforcement in seismic design and opened the window of using the updated provisions in engineering practice. It is important in the sense of resource utilization, leading to possible measures for environmental sustainability, economy, and encompassment of developing technology.

Different building codes related to the use of higher-strength reinforcing steel based on different parameters including seismic application have been studied. The latest research findings and recommendations have been reviewed. A combination of different concrete grades with reinforcement grades of 400, 500 & 600 have been compared to quantify the strength compatibility of lower-bound concrete strengths with higher grades of reinforcement. A parametric study based on an analytical approach has provided comprehensive insight into the effect of concrete grade paired with high-strength reinforcement. However, the correlation of concrete grade with specific reinforcement grade is vested in the best engineering judgment, existing knowledge, and provisions of relevant building code(s).

The findings include the performance reliability of high-strength steel reinforcement with different concrete grades and potential sensitivity in aspects mostly related to serviceability and behavior against seismic load. As a whole, high-strength reinforcement has been found to be reliable in terms of use in RC design with different ranges of concrete grades (including lower bound values) maintaining updated building code provisions.

Keyword: High strength, Steel reinforcement, Concrete, Grade, Strength, Compatibility

1 Introduction

High-strength steel reinforcement refers to steel materials designed to resist high tensile and compressive stresses within reinforced concrete structures. This reinforcement is engineered to have superior mechanical properties compared to conventional mild steel, making it essential for modern construction projects. The use of high-strength reinforcement in construction has evolved significantly over the past century, driven by advancements in material science, construction techniques, and the growing demand for efficient, durable, and cost-effective infrastructure. To address the issue, building codes have been updating continuously with different aspects related to high strength reinforcement. Several research work on high strength reinforcement both experimental and analytical has been performed around the globe and the findings have been published in prominent journals to provide guidance towards design practitioners.

1.2 Historical background of using high-strength reinforcement

During the late 20th century, high-strength reinforcing bars with yield strengths of 600–800 MPa were developed to meet the demands of taller buildings, longer bridges, and larger infrastructure projects. The development of epoxy-coated, stainless steel, and other corrosion-resistant reinforcements addressed durability issues in aggressive environments. High-strength reinforcement began to play a role in seismic-resistant design, where ductility and energy dissipation were critical. Codes increasingly incorporated guidelines for using high-strength reinforcement effectively. Modern high-strength reinforcements now achieve yield strengths exceeding 1000 MPa. Such materials are used in demanding applications like high-rise buildings, long-span bridges, and offshore structures. High-strength reinforcement contributes to sustainability by reducing the volume of steel and concrete required, leading to lower carbon footprints in construction. Modern structural codes now incorporate performance-based approaches, allowing for the optimized use of high-strength reinforcement in terms of strength, ductility, and durability.

1.3 Purpose and Scope

Basic purpose of this study is to literature review on use of high strength steel reinforcement in Reinforced Concrete (RC) building design. In current edition of building code being practiced is BNBC 2020 that has significant coherence with the design basics of ACI 318. There is significant modification in current version of ACI

1

318 (19) with respect to the upper limits of rebar yield strength considering seismic performance. Besides ACI, there are several building codes that incorporated advanced reinforcing material with higher grades and enhanced properties. A focus on comparison among basic parameters in different codes are intended to discuss. Not confining the study within codes and standards, research works on performance of high strength reinforcement and concrete compatibility based on seismic performance are also included for the purpose of review. A parametric exercise through analytical approach will be further worked on to compare the existing theoretical approaches and experimental coherence. Though the importance can't be ignored of physical test work but it has been kept out of the scope of this study work due to time and resource constraint. Finally, a conclusive remarks and recommendation is intended to draw on using high strength reinforcing steel and concrete compatibility issue.

2 Literature review

Reinforced Concrete (RC) is a widely applied construction material for building structures in developing Bangladesh. Carbon mild steel bars are mostly used as reinforcement in RC structures. Due to the vast development of the manufacturing industry in our country, the steel rebar grade has been improved in terms of high yield strength (fy) starting from 400MPa up to 600MPa. For further discussion, reinforcing bar yield strength below 420MPa can be considered as normal strength and beyond 500MPa can be considered high strength. Limitation is found with the concrete quality in terms of compressive strength (f'c) in the majority of the cases. Compressive strength (f'c) of 20~35MPa is the general concrete grade (with stone aggregates) being used for common RC design and construction practice in our country. In addition to that, brick chips are often used for concrete production which results in low compressive strength. For intermediate moment frames (IMF), the Bangladesh National Building Code (BNBC-2020) allows a minimum design compressive strength of 17MPa for buildings below 4-storied with a maximum 550MPa yield strength of reinforcing bars while for special moment frame (SMF) the minimum design compressive strength is 21MPa for concrete with a maximum 420MPa yield strength of reinforcing bars [1]. This combination of lowerbound concrete strength with high-strength reinforcing steel leaves questions on sound engineering practice in terms of considering strain compatibility, bond stress at steel concrete interface, allowable crack width of concrete, shrinkage, creep, fatigue, development length requirement etc.

Experimental research works have been performed to understand the behavior of high strength steel in RC members to achieve desired performance level. From experimental work of R. Ahsan [2], use of high strength reinforcement exhibited satisfactory performance in terms of flexural capacity, axial capacity, sustaining higher load cycles, lateral load capacity etc. H. Tavallali, A. Lepage, J. M. Rautenberg, and S. Pujol [3] also found good flexural performance comparable to conventional reinforcement grade but resulted higher crack width for higher grade steel. Naturally, higher grade steel (fy \geq 550MPa) can undergo higher strain therefore the RC section is considered compression controlled where steel tensile strain (ϵ_t) is below 0.004 and considered tension controlled when steel tensile strain (ϵ_t) is above 0.008 [4, 5, 6] whereas this limit is $\epsilon_t \leq 0.002$ for compression controlled and $\epsilon_t \geq 0.005$ for tension controlled in case of normal strength steel (fy \leq 400MPa). RC frame with high strength steel reinforcement can produce comparable drift capacity compared to that of normal strength steel reinforcement whereas, even higher lateral drift capacity can be achieved due to higher strain capacity of high strength steel [7, 8, 9] compared to normal strength steel reinforcement which is a significant

property necessary for ductile earthquake resistant structural design. But, ductility and structural performance of RC frame also depends on concrete properties namely compressive strength, modulus of rupture, bond capacity etc. In addition to that serviceability of RC structure is related to concrete cracking. Lower strength of concrete yields more cracks and wider crack widths than higher strength concrete with high strength reinforcing steel [10]. High strength steel reinforcement causes higher crack widths in concrete due to higher strain [11] and effective crack control can be achieved by using concrete with higher compressive strength, keeping lower tensile stress in steel, keeping smaller gaps in tensile steel placement, provide higher compression steel and lower tensile steel [12, 13]. Cracking of concrete can adversely affect ductility, cyclic load resistance, energy dissipation capacity, frame stiffness reduction etc. and specially uses of steel microfiber reinforcement in concrete [14], closer confinements [15, 16] can be effective to enhance ductility and cyclic load resistance by arresting concrete cracks. In case of compression members like columns and piers high stress ratio [17] and very low longitudinal reinforcement ratio [18] is not desirable for ductile framing to dissipate seismic energy and can cause brittle type failure of members. High strength steel reinforced flexural member can even undergo lower ductility as per findings of few experiments [19] as well. A minimum concrete compressive strength of 28 MPa (cylinder strength) was recommended for using with 500 MPa rebar [20] and 60 MPa concrete (cube strength) was recommended for using with 630 MPa rebar [17] considering strain compatibility, bond strength and development length requirements. As per ACI 318-19 the requirement of minimum concrete compressive strength for special structural wall with 690 MPa reinforcement is 35 MPa [21]. Therefore, compatibility of concrete has been emphasized with respect to the strength of steel reinforcement in many documents including building codes. This compatibility is related to factors like bond strength, development length, strain limit, crack width, ductility, deflection, stress level at service load, flexural stiffness, cyclic load resistance etc.

3 Material characteristics

This chapter discusses the desirable material properties of High Strength Reinforcement (HSR). The chemical composition according to different specification is also discussed. In addition, limitation of concrete and steel reinforcement grades are also discussed according to different code provisions. HSR typically has a yield strength of 500 MPa or higher (e.g., 600 MPa, 700 MPa). High-strength reinforcement must retain adequate ductility to ensure energy absorption during seismic or dynamic loading. The stress-strain curve of HSR is steeper, which can affect the design and detailing of reinforced concrete building.

3.1 Use of High-Strength Reinforcement in RC Design

After incorporation of higher graded reinforcement considering seismic provisions in different design codes, the production of high-strength reinforcement is increasing worldwide. In United States, Grade 80 reinforcement are frequently manufactured in the recent days. ASTM A615 (ASTM, 2009a) and ASTM A706 (ASTM, 2009b) both provides guideline of Grade 80. ASTM A615 rebars are generally called carbon steel bars and ASTM 706 are called low-alloy steel. ASTM A1035 has guidelines of Grade 100 and Grade 120 reinforcement. ASTM A1035 (ASTM, 2011) are called low-Carbon, chromium, steel bars. ACI 439.6R-19 has complete guideline with provisions and design examples of using grade 100. ICC ESR-2107 also offers design guidelines for using ASTM A1035 steel with a yield strength of up to 100 ksi in special purpose structural applications.

The high-strength reinforcing bar types developed in Japan include the following: (1) USD685A and USD685B, both with a yield strength of 100 ksi, designed for use as reinforcement in beams and columns that are expected to yield; (2) USD980, with a yield strength of 142 ksi, intended for beams and columns that are not expected to yield; (3) USD785, with a yield strength of 114 ksi; and (4) USD1275, with a yield strength of 185 ksi, designed for use as transverse reinforcement. Although these new reinforcement types have not yet been included in the Japanese Industrial Standard (JIS), but accepted by the Ministry of Construction as part of the New RC Construction Standard.

However, Grade 500 reinforcement is only produced in New Zealand, Australia, and China commercially.

3.2 Availability of High-Strength Reinforcement in Bangladesh

The inclusion of high-strength reinforcement in construction industry is not long ago. Grade 600 are the latest available high strength steel in Bangladesh. BDS ISO 6935-2:2021 has specification of producing both B600C-R and B600D-R. In BNBC 2020, for non-prestressed RC design, there is mention of maximum reinforcement yield strength to be 550 MPa (80 ksi) for design against flexural and axial loads in Intermediate Moment Frame, 420 MPa (60 ksi) for shear design, and 700 MPa for confinement design.

3.3 Comparison of Reinforcement Properties as per standards

Current practice of steel manufacturing process in Bangladesh is based on BDS ISO 6935-2:2021 which is somewhat comparable to the specification of ASTM A615. A comparison between different specifications of reinforcement standards being practiced and recognized under BNBC (i.e., ASTM A615, ASTM A706, and BDS ISO 6935-2:2021) for maximum grades of rebar is presented as follows.

Table 1: Comparison of required material properties of reinforcing bars of maximum grade allowed according to different standards

Parameter Considered	Standard			Comments
	ASTM	ASTM	BDS-ISO	
	A615-22	A706-22a	6935-2:2021a	
Highest Rebar grade	690 [100]	690 [100]	700 [101]	^a considering highest
allowed, MPa [ksi]				ductility class (D) of this
Min. Yield strength, fy	690 [100]	690 [100]	700 [101]	standard.
Min. Tensile strength,	790 [115]	805 [117]	875 [127]	^b Varies depending on bar
fu				diameter.
Min. elongation %	6-7 ^b	10	10	^c Only major elements are
Chemical Composition ^c	-	C ≤ 0.30	C ≤ 0.30	mentioned.
(%)		$Si \le 0.50$	$Si \leq 0.55$	^d This value is 1.25 for
		$Mn \le 1.50$	$Mn \le 1.50$	rebar Grade 420 &
min. (fu / fy) required	1.10	1.17 ^d	1.25	550MPa.

3.4 Material Grade & properties applicable as per Building Codes

The ACI 318 (19) code has been updated enhancing upper limit of reinforcement grade compared to that is mentioned in current version of BNBC (2020). Therefore, we're going to try understand the requirements mentioned for higher rebar grades with reference to ACI 318-19. ASTM A615, A706 and A1035 rebar specifications are incorporated in ACI 318-19 according to application limitation in terms of seismic performance requirement. In addition, BDS-ISO 6935-2:2021 also has the provision of reinforcement grade as high as 700MPa with

different ductility criteria. The applicable reinforcement and concrete grade as per ACI 318-19 for different seismic applications is discussed as follows.

Table 2: Comparison of applicable reinforcement grade as per ACI 318-19 for different seismic applications (limited ASTM standards for deformed bars have been considered)

Usage	A	Application Application Maximum value yield strength, f _y design calculatio Mpa (psi)		Applicable ASTM standard	
Flexure; axial	Special Special moment frames		550 (80000)	A 706[2]	
force; and shrinkage and	seismic systems	Special structural walls [1]	690 (100000)	A706 ^[2]	
temperature	Other		690 (100000) [3][4]	A615, A706, A1035	
Lateral support of	Special se	eismic systems	690 (100000)	A615, A706, A1035	
longitudinal bars; or concrete	Spirals		690 (100000)	A615, A706, A1035	
confinement	Other		550 (80000)	A615, A706	
	Special seismic	Special moment frames [8]	550 (80000)	A 615 A 706	
	systems [7]	Special structural walls [9]	690 (100000)	A615, A706	
Shear	Spirals		420 (60000)	A615, A706	
	Shear fric	tion	420 (60000)	A615, A706	
	Stirrups, t	ies, hoops	420 (60000)	A615, A706, A1035	
			550 (80000)	Not permitted	
Torsion	Longitudinal and transverse		420 (60000)	A615, A706	
Anchor	Special seismic systems		550 (80000)	A706 ^[2]	
reinforcement	Other		550 (80000)	A615, A706	
Regions designed	Longitudi	nal ties	550 (80000)		
using strut-and-tie method	<u> </u>		420 (60000)	A615, A706	

^[1] All components of special structural walls, including coupling beams and wall piers.

^[2] ASTM 615 Grade 60 shall be permitted if, $fu/fy \ge 1.25$ and other ductility requirements are satisfied.

^[3] In slabs and beams not part of a special seismic system, are permitted under certain conditions.

^[4] Longitudinal reinforcement with fy > 550 MPa is not permitted for intermediate moment frames and ordinary moment frames resisting earthquake demands E.

^[7] This application also includes shear reinforcement with a maximum value of 550 Mpa for fy or fyt permitted for design calculations for diaphragms and foundations for load combinations including earthquake forces if part of a building with a special seismic system.

^[8] Shear reinforcement in this application includes stirrups, ties, hoops, and spirals in special moment frames.

^[9] Shear reinforcement in this application includes all transverse reinforcement in special structural walls, coupling beams, and wall piers. Diagonal bars in coupling beams shall comply with ASTM A706 or Footnote [2].

Table 3: Comparison of applicable concrete grade as per ACI 318-19 for different seismic applications

Application	Minimum f'c, MPa (psi)
Foundations for structures assigned to SDC A, B, or C and for foundations for Residential and Utility use and occupancy classification with stud-bearing wall construction two stories or less assigned to SDC D, E, and F	17 (2500)
Foundations for structures assigned to SDC D, E, or F other than Residential and Utility use and occupancy classification with stud-bearing wall construction two stories or less	21 (3000)
Special moment frames, Special structural walls with Grade 60 or 80 reinforcement	21 (3000)
Special structural walls with Grade 100 reinforcement	34 (5000)
Precast-non prestressed driven piles, Drilled shafts	27 (4000)
Precast-prestressed driven piles	34 (5000)

Material grade reference concerning seismic applications from some other building codes can be compared with local code provision to understand the design being practiced worldwide as a whole. Therefore, a general material grade comparison for RC building design goes as follows;

Table 4: Material grade comparison specified in different building codes for RC building design considering seismic application (only longitudinal reinforcement considered here)

Reference Building Code	min. f'c MPa (psi)	max. fy		max. fy MPa (psi)		•		Remarks
Code	wir a (psi)	Others	SMF					
BNBC 2020	21 (3000)	550 (80000)	420 (60000)	f'c=17MPa is allowed for IMF up to 4-stories				
ACI 318-19	21 (3000)	690 (10000)	550 (80000)	TWIT up to 4-stories				
NZS 3101.2:2006	20 (2900)	500 (72500)						
Eurocode 8	20 (2900)	600 (87000)						
AS 3600:2018	20 (2900)	500 (7	(2500)					
IS 456: 2000	20 (2900)	500 (7	(2500)					
TS 500	20 (2900)	420 (60000)		Values taken from Turkish earthquake code requirements				
CSA A23.3-04	20 (2900)	500 (72500)						

IMF – Intermediate Moment Frame, SMF – Special Moment Frame

It can be said that use of high strength reinforcement (i.e., Grade $500 \sim 600 MPa$) in earthquake resistant building design has been started in some of the building codes with some application limitations. These limitations are often imposed due to absence of sufficient and reliable experimental data. The basic expected property of high strength reinforcement is ductility of reinforcement and strain compatibility with concrete.

3.5 Comparison of Reinforcement Properties Available in Bangladesh

Mechanical properties of reinforcing bars of grade 500MPa and 600MPa were checked and compared by sample collection from different mills. A comparison of different rebar grades with respect to BDS ISO 6935-21 has been showed below.

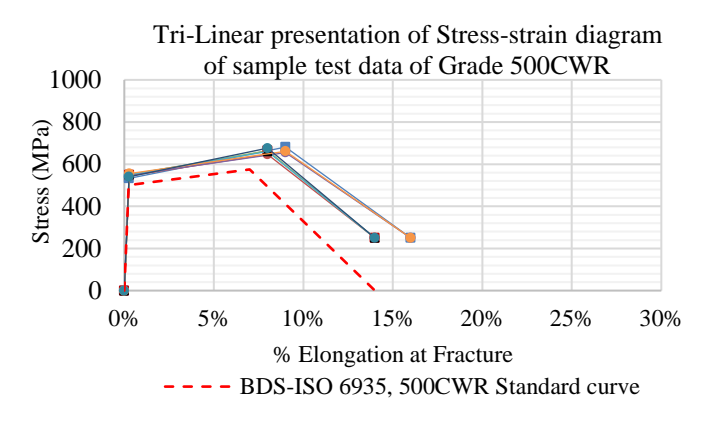


Figure 1: Tri-linear presentation of Stress-strain diagram of Grade 500CWR Rebar

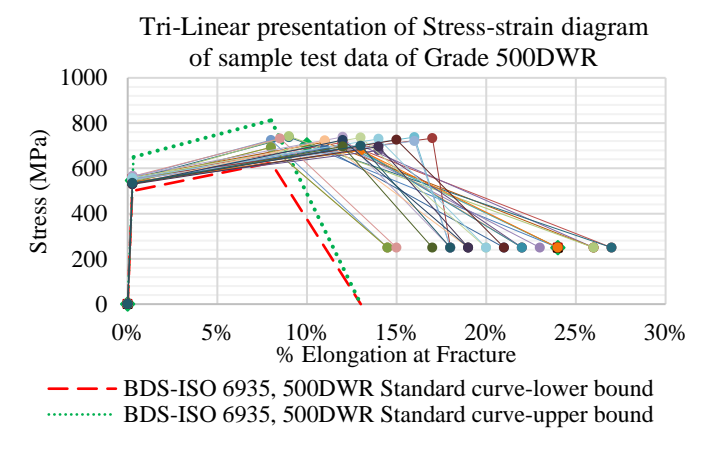


Figure 2:Tri-linear presentation of Stress-strain diagram of Grade 500DWR Rebar

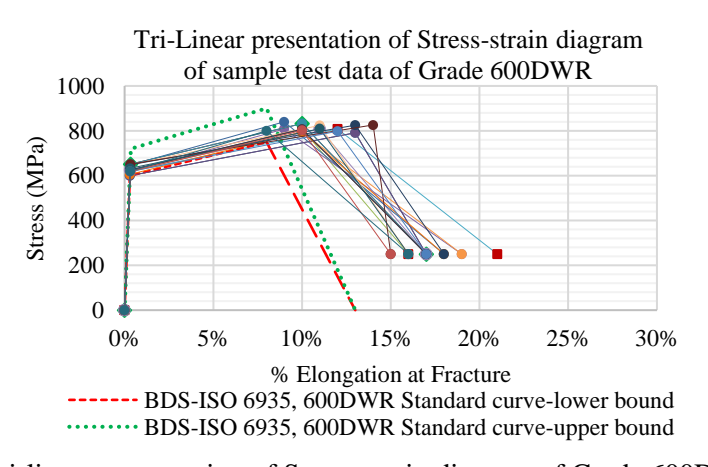


Figure 3:Tri-linear presentation of Stress-strain diagram of Grade 600DWR Rebar

The mechanical properties and ductility largely depend on the chemical composition of reinforcing steel bars. In addition, a common rebar production technique includes thermal quenching in local practice. Therefore, for seismic application, chemical composition shall be maintained to achieve mechanical as well as ductility and fatigue tolerance according to material standards and building code.

3.6 Role of stress-strain relationship in structural behavior

High-strength reinforcement has generally a lack of well-defined yield point and yield plateau (i.e., ASTM A1035). Their strength gradually increases over a yield point. A typical stress-strain curve of ASTM A1035 reinforcement has been shown in Figure 4. However, high-strength reinforcement could also produce with distinct yield plateau such as USD685A of Japan, as shown in Figure 5. USD685A are commonly used in Japan.

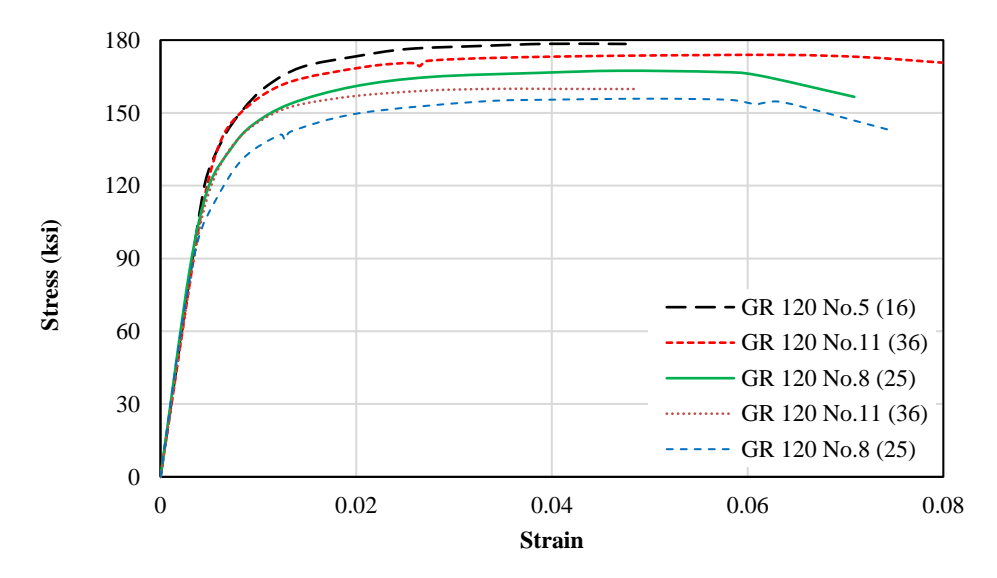


Figure 4: Stress-strain curve for ASTM A1035 Grade 100 and Grade 120 reinforcement (Wiss Janney Elstner Associates, Inc., Copyright 2008)

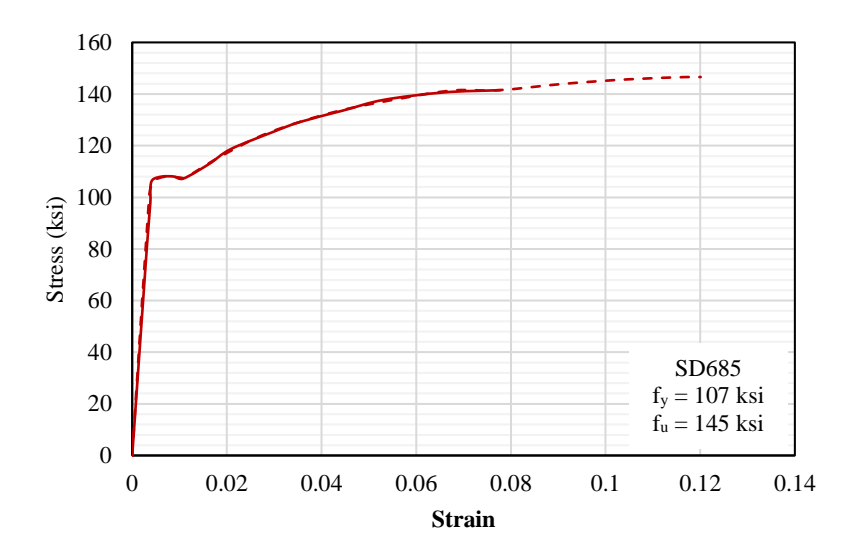


Figure 5: Stress-strain curve for USD685A reinforcement (Ousalem et al., 2009)

The behavior of the stress-strain curve of any reinforcement has an important role in the performance under lateral example. For instance, reinforcement with a higher ratio of tensile strength to yield strength (T/Y) (i.e., 1.25 for A706 steel) is better at spreading plastic deformation in areas where the steel is yielding compared to reinforcement with a lower ratio (i.e., T/Y= 1.10). This spread of plasticity leads to longer plastic hinge zones and potentially more flexibility in the structure. Another advantage of a higher T/Y ratio is that it helps maintain or even increase the strength of a structural member after the spalling of the outer concrete. Spalling affects shallower members more because the removed cover makes up a larger portion of the total depth. If the T/Y ratio is high enough, the member's strength can be preserved due to the steel's strain hardening after spalling occurs.

3.7 Required minimum compressive strength of concrete

There is not limit in the codes for compatible strength of concrete for high-strength reinforcement. However, different literatures suggested the use of high strength concrete with high-strength reinforcement that is advantageous to reduce the requirement of development length.

According to NIST (2014)'s manual of "Use of High-Strength Reinforcement in Earthquake-Resistant Concrete Structures", using high-strength concrete in flexural members of the same size and reinforcement improves their deformation capacity. Between two beams with the same design but different concrete strengths, the one with higher strength concrete will have a shallower neutral axis, slightly higher peak moment strength, more curvature, higher tensile strain in the bars, and higher hinge rotation.

Table 5: Permissible limit of compressive strength of concrete according to ACI 318-19

Design Code	Application	Minimum f'c, MPa (psi)	Maximum f'c, MPa (psi)
	General	17 (2500)	N/A
	Foundations for structures assigned to SDC A, B, or C	17 (2500)	N/A
	Foundations for Residential and Utility use and occupancy classification with stud bearing wall construction two stories or less assigned to SDC D, E and F	17 (2500)	N/A
ACI 318-19	Foundations for structures assigned to SDC D, E, or F other than Residential and Utility use and occupancy classification with stud bearing wall construction two stories or less	21 (3000)	N/A
	Special moment frames, Special structural walls with Grade 60 or 80 reinforcement	21 (3000)	34 (5000) for lightweight concrete
	Special structural walls with Grade 100 reinforcement	34 (5000)	N/A
	Precast-non prestressed driven piles Drilled shafts	27 (4000)	N/A
	Precast-prestressed driven piles	34 (5000)	N/A

ACI 318-19 specified maximum permissible compressive strength of concrete to be 34 MPa (5000psi) for special moment frames, special structural walls with Grade 60 (420MPa) or 80 (550MPa) reinforcement.

4 Technical aspects of using high-strength reinforcement

Since High Strength Reinforcement has higher tensile strength that allows designers to use smaller bar diameters or fewer bars. This can lead to reduced congestion in heavily reinforced members. Higher stresses in reinforcement can lead to larger crack widths. Enhanced crack control measures, such as closer spacing of bars may be necessary. Adequate anchorage lengths are critical as the bond stress between steel and concrete increases with the higher stress in the bar. Mechanical splices or couplers are useful to overcome the difficulties of traditional lapping. The performance of HSR under high-temperature scenarios (e.g., fire exposure) must be carefully evaluated as its properties can degrade more significantly than traditional reinforcement. The use of HSR in seismic regions requires special considerations for ductility and energy dissipation to ensure the structure can withstand cyclic loading without brittle failure.

4.1 Design Considerations

The effect of HSR in design of RC members compared to that of regular grade (up to grade 420MPa) reinforcement has been discussed in terms of structural capacity and serviceability criteria. Here, all references have been taken according to ACI 318-19.

4.1.1 Flexural Capacity of Beam

Following simply supported beam has been considered to compare the flexural capacity to be designed with different grade (400, 500 & 600MPa) of reinforcing bars.

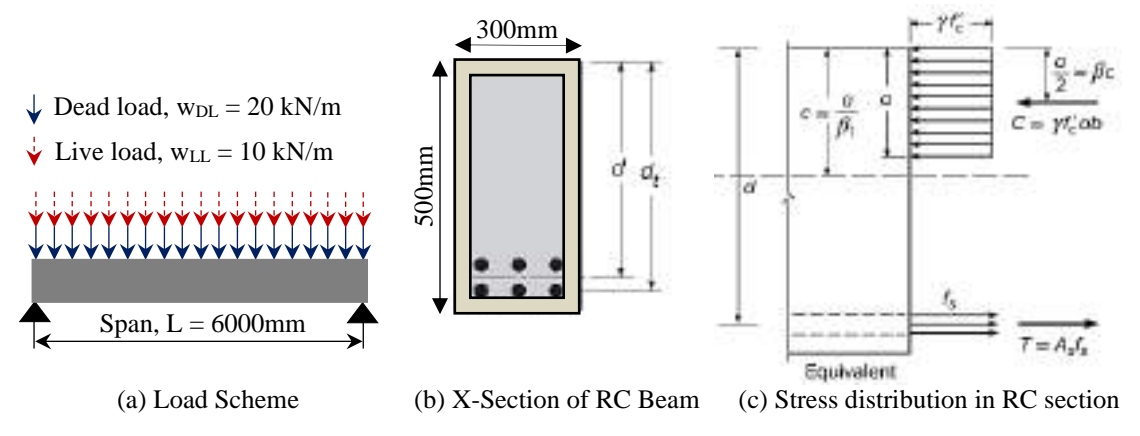


Figure 6: Span length, Loading and RC member detail for Flexural capacity comparison

Design data; Ultimate Load, $w_u = 1.2w_{DL} + 1.6w_{LL} = 1.2*20 + 1.6*10 = 40 \text{ kN/m}$

Design moment, $M_u = w_u L^2/8 = 40*6^2/8 = 180 \text{ kN-m}$

Rebar closest to the tension face, $d_t = 440 \text{ mm}$

Effective depth of beam tension bar, d = 417 mm

Width of beam, $b_w = 300 \text{ mm}$

Height of beam, h = 500 mm

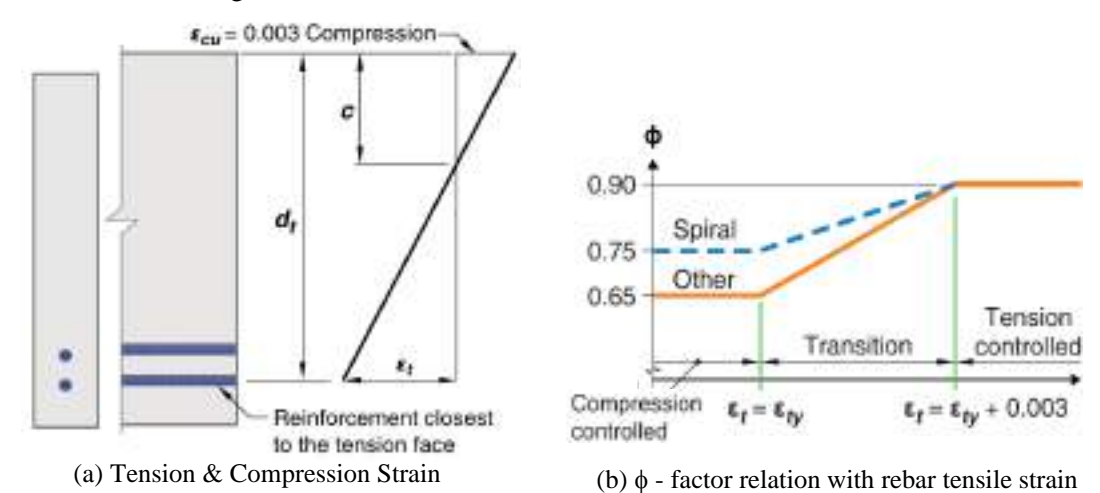


Figure 7: Strain limit states and relation to Strength reduction factor, φ (ACI 318-19)

Using; Concrete design compressive strength = f'_c (MPa)

Elastic modulus of concrete = $E_c = 4700 \sqrt{f'_c}$ (MPa)

Elastic modulus of reinforcing bar = E_s (MPa)

Modular ratio = n

Reinforcement yield strength = fy (MPa)

Rebar yield strain = $\varepsilon_{ty} = f_y/E_s$

Concrete ultimate compressive strain = $\varepsilon_{cu} = 0.003$

Balanced reinforcement ratio = $\rho_b = 0.85 \beta_1 (f' \circ / f_y) * \epsilon_{cu} / (\epsilon_{cu} + \epsilon_{ty})$

Minimum reinforcement ratio = $\rho_{s,min}$ = greater of $[0.25\sqrt{(f'_c)/f_y}, 1.4/f_y]$

Factor relating depth of equivalent rectangular compressive stress block to neutral axis depth, $\beta_1 = 0.85 - 0.007143 (f'_c - 28)$ and $0.65 \le \beta_1 \le 0.85$ [BNBC-2020]

To ensure tension bar yielding before concrete crushing, $\varepsilon_t \ge \varepsilon_{ty} + \varepsilon_{cu}$ is required.

Table 6: Material Properties for various concrete grades

f'c (MPa)	$E_c = 4700 \sqrt{f'_c} \text{ (MPa)}$	E _s (MPa)	$n = E_s/E_c$	β_1
20.0	21019.0	200000.0	9.52	0.85
30.0	25743.0	200000.0	7.77	0.84
40.0	29725.4	200000.0	6.73	0.76

Table 7: Flexural Capacity of Beam section using f'c = 20MPa

fy (MPa)	ϵ_{ty}	ε _{cu}	ρь	A _s (mm ²)	a (mm)	ε _t	M _n (kN- m)	ф	φM _n (kN- m)	$egin{array}{c} A_{s,fy}/\ A_{s,400} \end{array}$
400	0.0020	0.0030	0.0217	1378	108.1	0.0074	200	0.90	180	1.00
500	0.0025	0.0030	0.0158	1102	108.1	0.0074	200	0.90	180	0.80
600	0.0030	0.0030	0.0120	919	108.1	0.0074	200	0.90	180	0.67

Table 8: Flexural Capacity of Beam section using f'c = 30MPa

fy (MPa)	ϵ_{ty}	ε _{cu}	ρ _b	A _s (mm ²)	a (mm)	$\epsilon_{ m t}$	M _n (kN- m)	ф	φM _n (kN- m)	$egin{array}{c} A_{s,fy}/\ A_{s,400} \end{array}$
400	0.0020	0.0030	0.0320	1306	68.3	0.0132	200	0.90	180	1.00
500	0.0025	0.0030	0.0232	1045	68.3	0.0132	200	0.90	180	0.80
600	0.0030	0.0030	0.0178	871	68.2	0.0131	200	0.90	180	0.67

Table 9: Flexural Capacity of Beam section using f'c = 40MPa

fy (MPa)	ϵ_{ty}	ε _{cu}	ρь	A _s (mm ²)	a (mm)	ε _t	M _n (kN- m)	ф	$\begin{array}{c} \phi M_n \\ (kN-\\ m) \end{array}$	$A_{s,fy}/$ $A_{s,400}$
400	0.0020	0.0030	0.0390	1276	50.0	0.0172	200	0.90	180	1.00
500	0.0025	0.0030	0.0283	1021	50.0	0.0172	200	0.90	180	0.80
600	0.0030	0.0030	0.0217	851	50.1	0.0172	200	0.90	180	0.67

Therefore, it's clearly found that flexural capacity of an under reinforced beam remains same if the $A_s f_y$ remains constant. It means, the required rebar area linearly decreases with increase of reinforcement yield strength. But minimum flexural reinforcement ratio $\rho_{s,min}$ has to be maintained.

Low-strength of concrete compressive strength has no limitation to be used with high strength reinforcement for design against flexural demand. Issues related to bond stress, splicing and development length for the strength combination of concrete and reinforcement has to be met as per the code requirements to attain full flexural capacity.

4.1.2 Deflection characteristics of beam

The deflection of a Reinforced Concrete (RC) beam is a critical parameter in structural design, as it directly impacts the serviceability of the structure. Higher elastic modulus (E_c) values result in stiffer beams with less deflection. Adequate and appropriately placed steel reinforcement

minimizes excessive deflections. Moreover, cracks in concrete reduce stiffness, leading to increased deflection. Long-term effects like creep and shrinkage of concrete increase deflection over time. The simply supported beam sample used for flexural capacity comparison (Figure 7: Strain limit states and relation to Strength reduction factor, ϕ (ACI 318-19)Figure 7) will also be used for deflection comparison as follows. Compression reinforcement has been neglected for calculation.

Using; Concrete modulus of rupture = $f_r = 0.62\sqrt{f'_c}$ (MPa)

Gross moment of Inertia (Uncracked section) = I_g

Cracking Moment of Inertia = I_{cr}

Distance of extreme tension face from neutral axis at cracking = $Y_t = h/2 = 250$ mm

Cracking Moment = $M_{cr} = f_r I_g / Y_t$

Service Load Moment = $M_a = w_{(DL+LL)}L^2/8 = 30*6^2/8 = 135 \text{ kN-m}$

Effective Moment of Inertia = $I_{eff} = I_{cr}/[1-(2/3)M_{cr}/M_a)^2(1-I_{cr}/I_g)]$

Midspan deflection of simply supported beam, $\Delta = 5 \text{wL}^4/(384 E_c I_{eff})$

Distance from extreme compression fiber to neutral axis = c (mm) (Figure 7)

Considering immediate deflection, the following tables are presented.

Table 10: Deflection of Beam section using f'c = 20MPa

fy (MPa)	f _r (MPa)	M _{cr} (kN-m)	A _s (mm ²)	$\rho_s = A_s/b_w d$	c (mm)	I _{cr} (mm ⁴)	$I_{\rm eff}$ (mm^4)	Δ (mm)	$\Delta_{ m ,fy}/\ \Delta_{ m ,400}$
400	2.77	35	1378	0.0110	157	1.44x10 ⁹	1.46x10 ⁹	16.5	1.00
500	2.77	35	1102	0.0088	144	1.22x10 ⁹	1.24x10 ⁹	19.4	1.18
600	2.77	35	919	0.0073	134	1.06x10 ⁹	$1.08x10^9$	22.3	1.35

Table 11: Deflection of Beam section using f'c = 30MPa

fy (MPa)	f _r (MPa)	M _{cr} (kN-m)	A_s (mm^2)	$\rho_s = A_s/b_w d$	c (mm)	I _{cr} (mm ⁴)	I _{eff} (mm ⁴)	Δ (mm)	$\Delta_{ m ,fy}/\ \Delta_{ m ,400}$
400	3.40	42	1306	0.0104	142	1.19x10 ⁹	1.22x10 ⁹	16.1	1.00
500	3.40	42	1045	0.0084	130	1.22x10 ⁹	1.24x10 ⁹	19.1	1.19
600	3.40	42	871	0.0070	120	1.06×10^9	1.08×10^9	22.0	1.37

Table 12: Deflection of Beam section using f'c = 40MPa

fy (MPa)	f _r (MPa)	M _{cr} (kN-m)	A _s (mm ²)	$\rho_s = A_s/b_w d$	c (mm)	I _{cr} (mm ⁴)	$\begin{array}{c} I_{\rm eff} \\ (mm^4) \end{array}$	Δ (mm)	$\Delta_{ m ,fy}/\ \Delta_{ m ,400}$
400	3.92	49	1276	0.0102	133	1.04×10^9	1.09x10 ⁹	15.7	1.00
500	3.92	49	1021	0.0082	121	0.88×10^9	0.92×10^9	18.6	1.18
600	3.92	49	851	0.0068	112	0.76×10^9	0.79×10^9	21.5	1.37

The deflection is found to be higher (Table 10Table 11, Table 12) with higher grade reinforcement since the reinforcement quantity is reduced for flexural capacity design. Reinforcement quantity has a major role in section stiffness but its tensile strength. Another observation is that the use of higher-grade concrete is also helpful in reducing deflection but with minor effects. Deflection can also be controlled by increasing the depth of the beam. The following table is presented to compare the depth increase required to keep the same deflection found with grade 400MPa reinforcement. The target deflection limit has been considered, L/360 = 6000/360 = 16.67mm.

Table 13: Beam depth demand for target deflection control with different graded reinforcement

fy (MPa)	f'_c = 20 MPa & Δ=16.5mm			f' _c =30	MPa & Δ:	=16.1mm	f' _c =40 MPa & Δ=15.7mm		
(2.22.3)	A _s (mm ²)	Reqd. h (mm)	$h_{fy}/h_{,400}$	A _s (mm ²)	Reqd. h (mm)	$h_{fy}/\ h_{,400}$	A _s (mm ²)	Reqd. h (mm)	h _{fy} / h _{,400}
400	1378	500	1.00	1306	500	1.00	1276	500	1.00
500	1102	790	1.58	1045	730	1.46	1021	690	1.38
600	919	890	1.78	871	815	1.63	851	770	1.54

From (Table 13), the beam depth demand ratio $(h_{,fy}/h_{,400})$ is higher for lower-grade concrete. In addition, an increase of beam depth for deflection control and reducing reinforcement ratio may not be a practical option considering architectural limitations, increase of concrete volume, formwork, and overall economy.

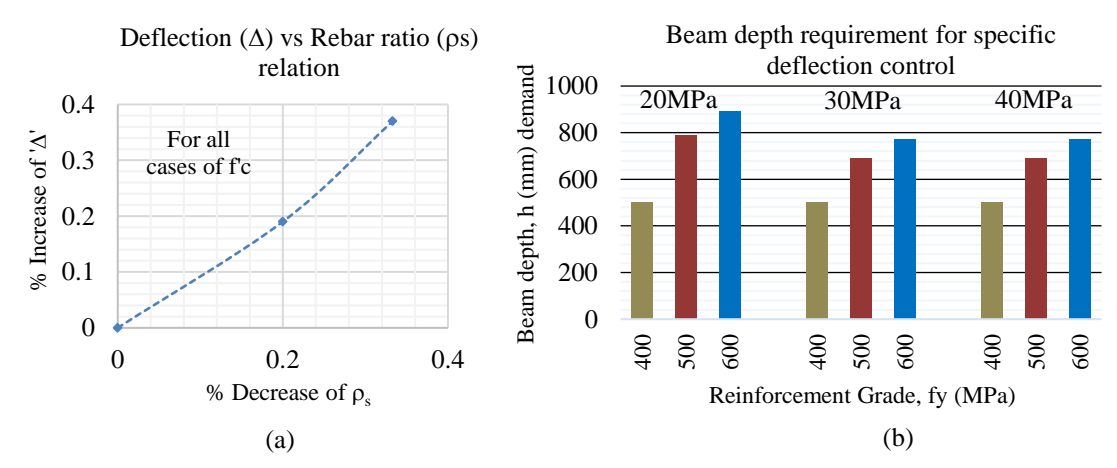


Figure 8: Relation of Beam Deflection with Reinforcement ratio, Beam depth & Concrete grade

Comparing Figure 8, as the beam deflection directly depends on section stiffness, it is eminent that the adjustment of rebar quantity is easier and more practical compared to beam depth adjustment to ensure required stiffness of the beam section to keep desired level of deflection.

Member deflection is sensitive to quantity of longitudinal reinforcement rather it's strength. Use of higher strength concrete is relatively better for deflection control, but lower strength concrete can also be used with high strength reinforcement and still the deflection limit criteria can be achieved by optimization of reinforcing steel quantity and section depth.

4.1.3 Flexural Crack Width

Among various causes of crack in RC members, the reinforcement stress level has direct effect on flexural crack formation. In comparison, high-strength rebar typically forms fewer but wider cracks in concrete, which could affect the bond between the concrete and the reinforcement. Poor bond strength reduces the ability of the structure to transfer forces, affecting structural integrity. Besides the flexure or shear stresses, cracks in concrete also may occur due to shrinkage, evaporation of moisture from concrete, chemical attack, rebar corrosion etc. Cracks can facilitate the ingress of water, chlorides, and other corrosive agents, accelerate the corrosion of reinforcement. Despite the fact that crack width is not the only factor behind durability, it may be a serviceability criterion due to aesthetic or functional requirement. Excessive cracking can lead to deflection or vibrations affecting usability. Therefore, allowable crack width is an important parameter for the use of High Strength Reinforcement in reinforced concrete. Various experiment based empirical approaches are available to assess concrete cracking due to flexure but all of them don't give a very close result for same condition. Most formulas forecast the maximum probable crack width, which typically signifies that approximately 90% of the crack widths in the flexural member are below the determined value.

Some guided values for reasonable flexural crack width limit under service load has been proposed based on exposure condition in ACI 224R-19 [22] as follows. These general guidelines for design have been proposed to use in conjunction with sound engineering judgement.

Table 14: Guideline for reasonable flexural crack width under service load as per ACI 224R-01

Exposure Condition	Limiting Crack width, mm (inch)
Dry air or protective membrane	0.41 (0.016)
Humidity, moist air, soil	0.30 (0.012)
Deicing chemicals	0.18 (0.007)
Seawater and seawater spray, wetting and drying	0.15 (0.006)
Water-retaining structure	0.10 (0.004)

Table 15: Recommended maximum surface crack width at serviceability limit state as per NZS 3101:2006 [23]

Surface and Exposure Environment	Limiting Crack width for specified serviceability limit state, mm (inch)
Protected by damp proof membrane, interior environment	0.40 (0.016)
in contact with non-aggressive soil, inland above ground, repeated wetting and drying, above ground at Coastal frontage, in contact of fresh water, permanently submerged in sea water etc.	0.30 (0.012)
Tidal spray/splash	0.20 (0.008)

Table 16: Recommended values of maximum crack width limit as per Eurocode 2 (EN 1992-1-1) [24]

Exposure Condition	Limiting Crack width, mm (inch)
Dry or permanently wet exposure	0.4 (0.016)
Wet, cyclic wet and dry, exposed to airborne salt, permanently submerged in sea water, tidal splash and spray	0.30 (0.012)

To control crack at concrete surface several calculation methods have been described in building codes. Few of the code references for determining crack width has been presented as follows.

ACI:

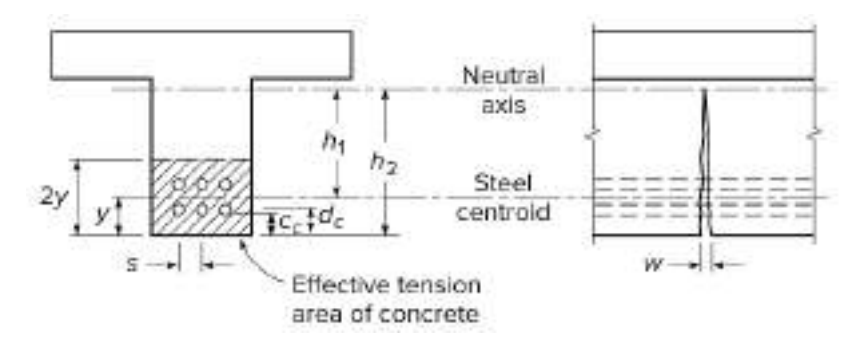


Figure 9: Geometrical basis of Crack width in flexural member [25]

ACI 318-95 provided following equation to determine design crack width.

$$\begin{split} W_{max} &= 0.011 \beta f_s \sqrt[3]{d_c A_o} * 10^{-3} mm \text{ [Metric unit],} \\ &= 0.076 \beta f_s \sqrt[3]{d_c A_o} * 10^{-3} inch \text{ [Imperial unit]} \end{split}$$

Where,

 $\beta = \frac{h2}{h1}$ is the ratio of the distance between the neutral axis and extreme tension face to the distance between the neutral axis and centroid of reinforcing steel.

 A_0 = the area of concrete surrounding each reinforcing bar = A_e/n_b ,

 A_e = the effective area of concrete in tension = 2yb,

 n_b = the number of tension reinforcing bars.

y = the distance measured from the centroid of tensile steel to the extreme tensioned fiber.

However, the code limits the value of $f_s \sqrt[3]{d_c A_o}$ to 3064.5, 2539.2, and 1700 N/mm, corresponding to a limiting crack width of 0.41, 0.33, and 0.20 mm for interior exposure, exterior exposure, and very aggressive exposure or designed to be watertight.

Later, ACI introduced changes to the crack rules in which a maximum bar spacing, rather than a crack width is prescribed. ACI 318-05, and ACI 318-08 proposed the following equation for crack control:

Rebar spacing,
$$s_{max}$$
 (mm) = $380 \left(\frac{280}{f_s}\right) - 2.5c_c \le 300 \left(\frac{280}{f_s}\right)$

where,

 c_c = least distance from the surface of reinforcement to the tension face(mm);

 f_s = rebar stress at tension face due to service load moment. ACI permits the use of f_s = 0.67 f_y . However, ACI 318-19 does not specify a crack width limit, acknowledging that crack widths vary widely and are difficult to predict.

Eurocode 2:

Eurocode 1992-1-1:2004 proposed the following equation for calculating crack width.

$$w_k = s_{r,max}(\varepsilon_{sm} - \varepsilon_{cm})$$

where, $S_{r,max} = \text{maximum crack spacing}$; $S_{r,max} = 3.4c + \frac{0.425k_1k_2\varphi}{\rho_{eff}}$

c = concrete clear cover,

 $k_1 = 0.8$ for high bond reinforcing bars, 1.6 for plain reinforcing bars,

 $\phi =$ average bar diameter (mm);

 $k_2 = 0.5$ for sections subjected to pure bending and 1.0 for sections subjected to pure axial tension.

 ϵ_{sm} = the mean strain in the reinforcement under the relevant combination of loads, including the effect of imposed deformations and taking into account the effects of tension stiffening.

 ε_{cm} = mean strain in the concrete between cracks.

Indian Standard (IS):

IS 456:2000 proposed equation to calculate design crack width due to tension due to bending [26]. The strain in the tension reinforcement is limited to 0.8 fy/E_s .

$$W_{\alpha} = \frac{3a_{cr}\epsilon_m}{1 + \frac{2(a_{cr} - C_{min})}{h - x}} \label{eq:wave_eq}$$

where, a_{cr} = distance from the point considered to the surface of the nearest longitudinal bar; C_{min} = minimum cover to the longitudinal bar;

 $\epsilon_{m} = \quad \text{ average steel strain at the level considered; } \epsilon_{m} = \epsilon_{1} - \frac{b(h-x)(a-x)}{3E_{s}A_{s}(d-x)}$

h= overall depth of the member;

x= depth of the neutral axis.

A_s= area of tension reinforcement;

b = width of the section at the centroid of the tension steel;

 ε_1 = strain at the level considered, calculated ignoring the stiffening of the concrete in the tension zone;

a = distance from the compression face to the point at which the crack width is being calculated;

d = effective depth of beam

New Zealand Standard (NZS):

The reinforcement is supposed to be distributed in case of flexural and axial force resistance either by maintaining maximum rebar spacing or controlling crack width limit [23]. As per NZS 3101.1:2006, maximum rebar spacing is allowed,

$$s_{\text{max}} (mm) = \left(\frac{90000}{f_s}\right) - 2.5c_c \le \left(\frac{70000}{f_s}\right)$$

Design service crack width limit,

$$W_{\text{max}} = 2.0\beta' \frac{f_{\text{s,ch}}}{E_{\text{s}}} g_{\text{s}} \text{ (mm)}$$

Where, $f_{s,ch}$ = change in the stress in the reinforcement = f_s - 0.5 $f_{s,c}$

 $f_{s,c}$ = the stress in the reinforcement when the stress in the concrete alongside the reinforcement is zero prior to crack formation.

 g_s = the distance from the center of the nearest reinforcing bar to the surface of the concrete

$$\beta' = \quad \frac{(y-kd)}{(d-kd)}$$

kd = depth of the neutral axis

y = the distance from the extreme compression fiber to the tension face.

d = distance of the tension bar from the extreme compression fiber

Comparison of crack width in various building codes for different serviceability limit states

Equations specified in various building codes for crack width calculation are basically empirical ones that are derived from experimental results. Various factors (i.e. member geometry, rebar arrangement, steel tensile stress level, etc.) have been considered in those equations in different approaches. As a result, considerable variation has been observed in crack width calculation by using those equations for the same section configuration.

A theoretical analysis has been conducted to compare the crack width requirements of different grades of rebar and service load conditions. The beam specimen shown in Figure 10 has been considered to determine the crack width limit for 400, 500, and 600 MPa rebars.

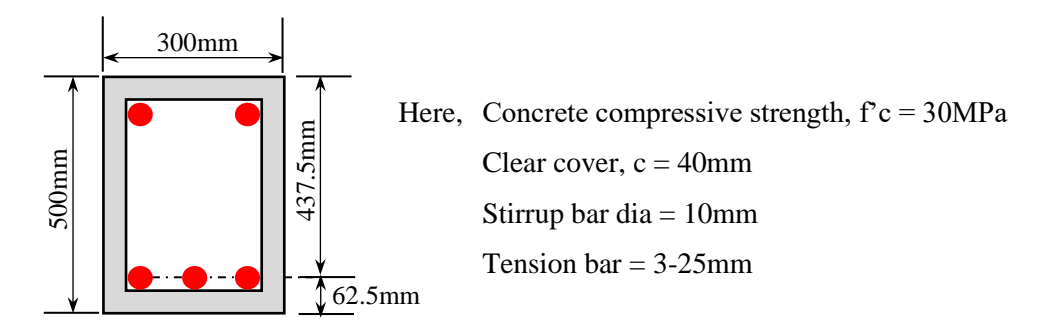


Figure 10:Beam section used for crack width analysis

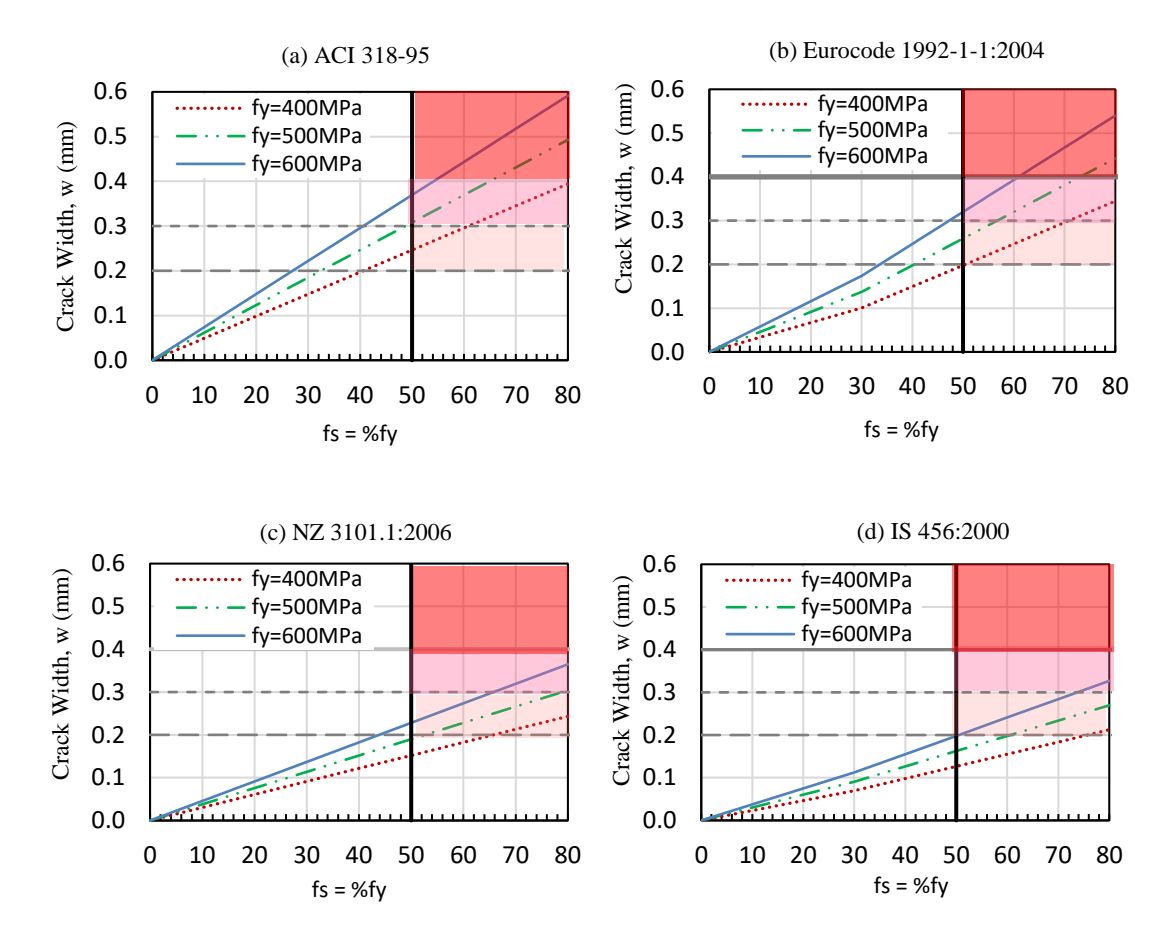


Figure 11: Comparison of crack width at various serviceability limit state according to (a) ACI 318-95 (b) Eurocode 1992-1-1:2004 (c) NZ 3101.1:2006 (d) IS 456:2000

Considering functional requirement, durability and aesthetic reasons, typically for RC members maximum crack width of 0.40mm for interior exposure, 0.30mm for members in earth exposure and 0.20mm for saline exposure is to be maintained. For crack width calculation, ACI 318 has allowed to use f_s =67% of f_y as service level load stress. Considering different service load stress level, a comparative study for different reinforcement grades (fy=400, 500 & 600MPa) has been performed and presented in Table 17.

Table 17: Comparison of Crack width compliance for different stress level of various yield strength of Reinforcement based on formula shown with ACI (clear cover=40mm)

Rebar	f_s	= 0.67% c	of f _y		$f_s = 0.50\% \text{ of } f_y$				$f_s = 0.40\% \text{ of } f_y$		
Yield		Crack Limit (mm)									
Strength, f _y (MPa)	0.40	0.30	0.20		0.40	0.30	0.20		0.40	0.30	0.20
400	$\sqrt{}$	×	×		\checkmark	\checkmark	×		\checkmark	$\sqrt{}$	$\sqrt{}$
500	×	×	×		$\sqrt{}$	×	×		$\sqrt{}$	$\sqrt{}$	×
600	×	×	×		\checkmark	×	×		~	$\sqrt{}$	×
Here, ×	= Crac	= Crack limit not complied, ✓ = Crack limit Complied									

This phenomenon of rebar stress level to comply crack width limit can also be described as follows;

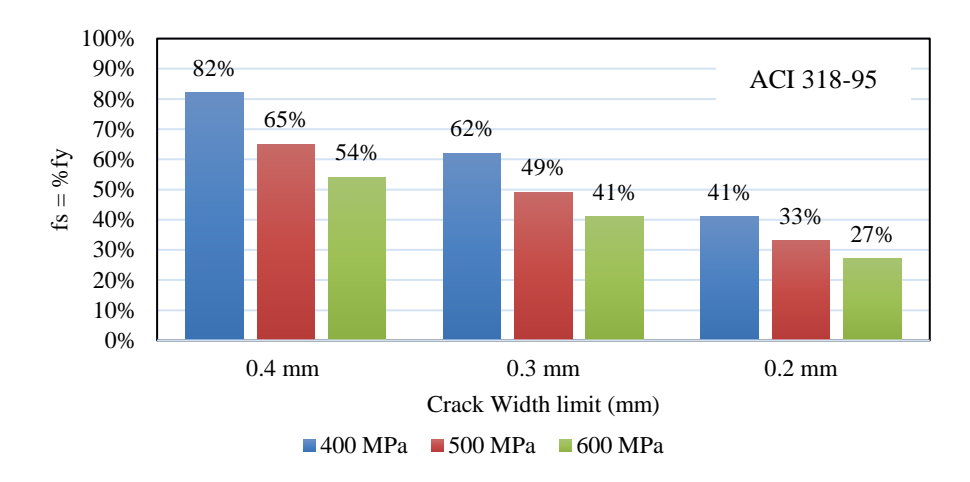


Figure 12: Maximum allowable serviceability stress limit (f_s=%f_y) for various rebar grade at different crack width based on exposure condition (as per ACI 318-95)

Maximum rebar spacing and serviceability stress condition

Based on ACI 318-19 criteria, Rebar spacing, s_{max} (mm) = $380 \left(\frac{280}{f_s}\right) - 2.5c_c \le 300 \left(\frac{280}{f_s}\right)$ is used for crack control. The permissible rebar spacing decreases with increase of stress level. The service stress level limit is somewhat independent of reinforcement yield value. Therefore, adjustment of bar spacing and maintaining stress level is actually an important criterion to comply flexural member design with high strength reinforcement. Figure 15 shows that for 600MPa rebar the maximum spacing at 50%, 60%, 70% & 80% stress level is 255mm, 196mm, 153mm & 122mm respectively.

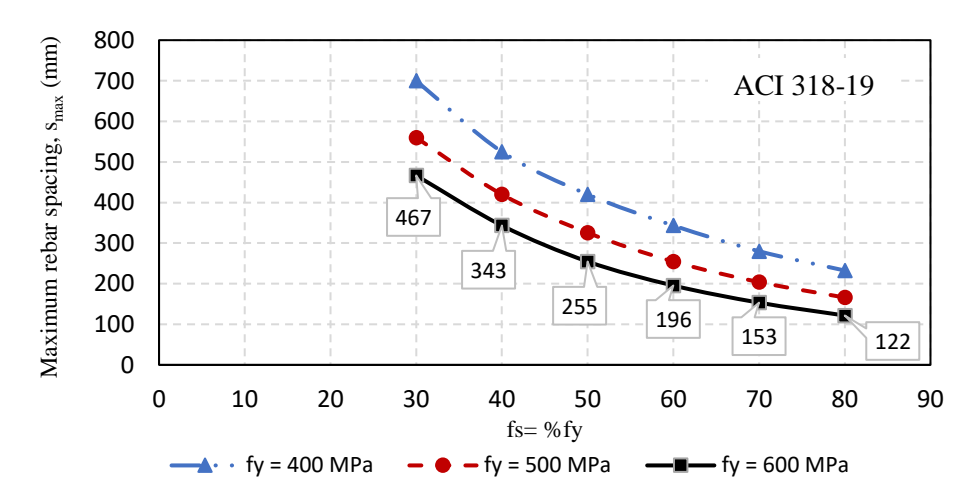


Figure 13: Maximum rebar spacing required for crack control at serviceability limit state

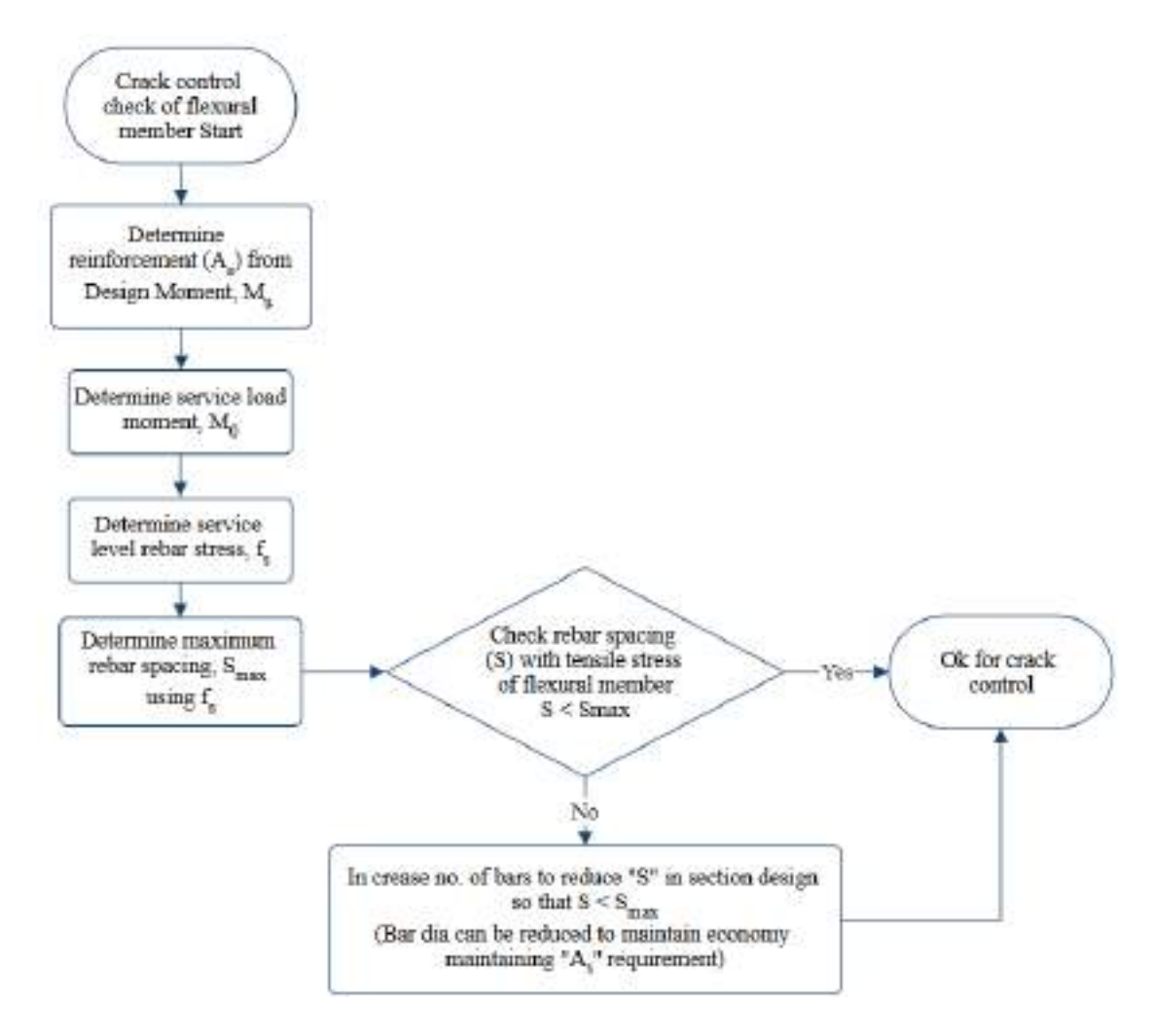
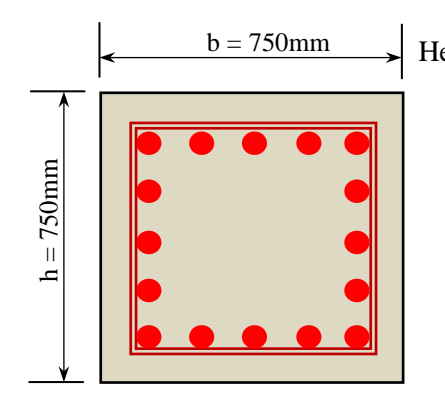


Figure 14: Flow diagram for checking rebar spacing limit for crack control

Concrete grade has no significant role in terms of crack control whereas, level of rebar tensile stress is the significant parameter for this issue. Since, higher strength reinforcement remains at higher stress level at service load condition, attention is required to keep the stress level within limit to comply the serviceability requirement and ensure durability.

4.1.4 Column capacity (axial load-moment interaction)

Referring to ACI 318-19 for compression capacity calculation of RC member, the value of reinforcement yield strength (f_v) in compression is limited to 550MPa despite the actual yield strength (f_y) may be of higher value. This is because of the strain compatibility issue between steel reinforcement and concrete in compression. Higher grade steel has higher strain capacity at yield stress level and the concrete capacity is likely to be reached at its ultimate strain limit before rebar compressive yield stress is exceeded. Based on this theory, a comparison for certain column section has been made as follows.



Here, Concrete compressive strength, f'c = 20MPa, 40MPa Clear cover, c = 40mm

Stirrup bar dia = 10mm

6750kN

Axial capacity, $P_{n-max} = 0.80(0.85f_c' [A_c - A_{st}] + f_y A_{st})$ Reinforcement ratio, ρ_s :

Reinforcement yield strength, f_v 400MPa 500MPa 600MPa 2.4% 2.0% 3.0% $\rho_{s} \\$

6750kN

6750kN

Figure 15: Column section used for nominal capacity analysis

 $A_s f_y$

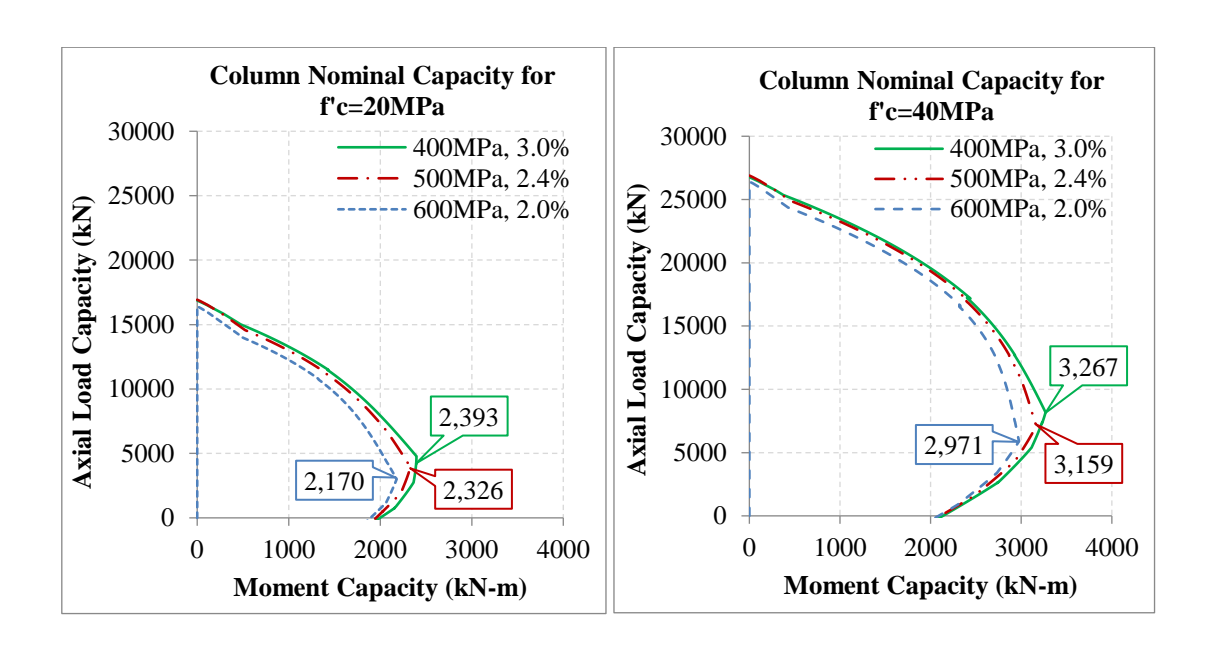


Figure 16: Comparison of Column nominal capacity using Different Rebar grade and using constant "Asfv"

Figure 16 shows that, for column the nominal moment capacity decreases with increase of rebar grade in presence of axial compression with constant $A_s f_y$.

Table 18: Trend of Column nominal capacity increase for Different Rebar grade and increasing concrete compressive strength, f_c

f _y (MPa)			400 MPa	500 MPa	600 MPa	
$\rho_s = A_s/bh \ (\%)$			3.0%	2.4%	2.0%	
$A_s f_y$			6750 kN	6750 kN	6750 kN	
Nominal Maximum Moment capacity,	$f_c = 20MPa$	M _{n-max,20}	2393 kN-m	2326 kN-m	2170 kN-m	
M_{n-max}	$f'_c = 40MPa$	$M_{n\text{-max},40}$	3267 kN-m	3159 kN-m	2971 kN-m	
Moment Capacity rat	io, $M_{n-max,40}/M_{n-n}$	nax,20	1.36	1.36	1.36	
Nominal Maximum Axial capacity,	$f_c = 20MPa$	P _{n-max,20}	16900 kN	16900 kN	16400 kN	
P _{n-max}	$f'_c = 40MPa$	P _{n-max,40}	26800 kN	26800 kN	26400 kN	
Axial Capacity ratio,	$\overline{P_{n\text{-}max,40}/P_{n\text{-}max,20}}$		1.59	1.59	1.61	

From Table 18 we see the nominal moment capacity is roughly 3% less for 500MPa reinforcement compared to 400MPa reinforcement whereas this capacity reduction is around 9% in case of 600MPa reinforcement compared to 400Mpa reinforcement with constant $A_s f_y$. In case of nominal axial capacity, using 400MPa and 500MPa has same maximum capacity but it gradually decreases for higher grades compared to 400MPa reinforcement with increase of load eccentricity (moment). But maximum axial capacity is found roughly 3% less for 600MPa grade rebar compared to the 400MPa and 500MPa with constant $A_s f_y$. This variation of maximum axial capacity is due to the fact that we can't take $f_y > 550$ MPa for compression despite the rebar grade was taken to be 600MPa grade due to the limitation of concrete compressive strain at ultimate load. Both the variation of moment capacity and axial capacity for higher grade reinforcement is insignificant compared to savings in rebar volume and workmanship.

Irrespective of rebar grade, higher concrete compressive strength is desirable to achieve higher column capacity with same section size and reinforcement. But low strength concrete can also be used with higher grade reinforcement to meet capacity demand providing adequate member size and reinforcement.

4.1.5 Confinement requirement for Column

Confinement refers to the lateral support provided to concrete by reinforcement. Conventional transverse steel reinforcement (in the form of rectangular hoops or spirals) significantly enhances the ductility and ultimate capacity of reinforced concrete (RC) columns by confining the internal concrete and longitudinal reinforcement. The confinement is closely associated with the ductility, energy dissipation, and effective stiffness of RC columns which is the primary performance indicator of earthquakeresistant structure. So, the confinement issue is directly related to the seismic capacity of the associated member and structural performance as a whole.

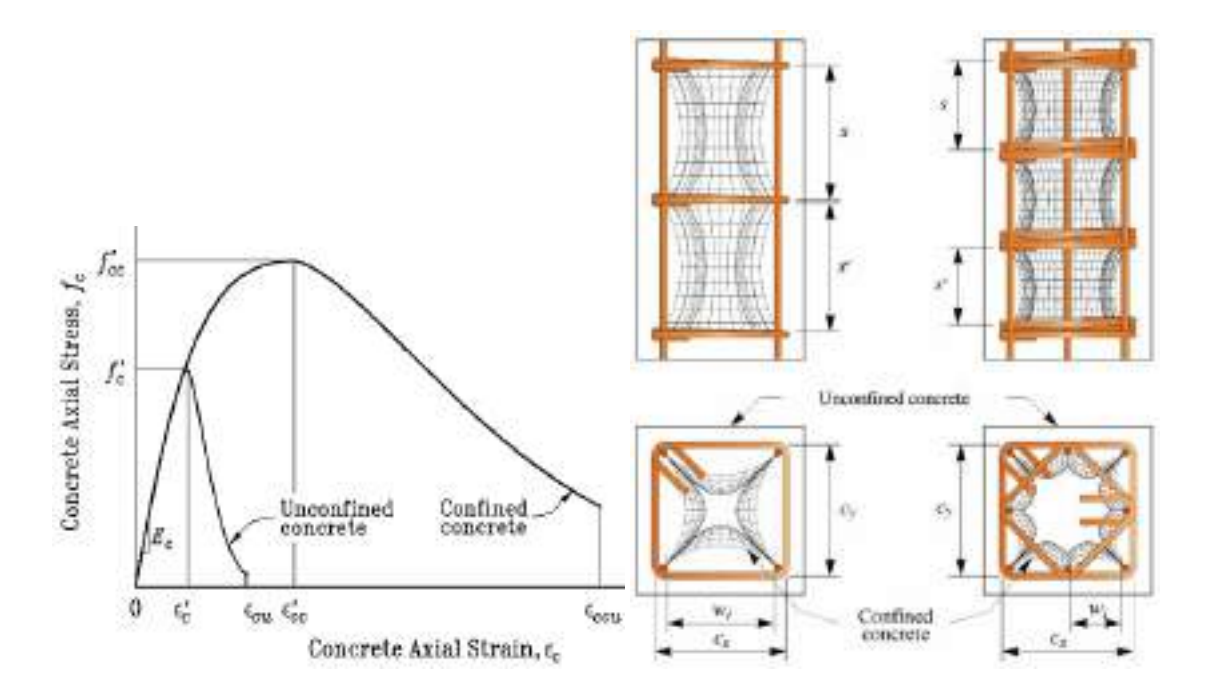


Figure 17: Effect of Confinement on concrete capacity [27]

In high-strength reinforcement performance for reinforced concrete (RC) building design, the confinement requirement is crucial because it directly impacts both the strength and ductility of concrete structures. Therefore, an analytical study has been performed to assess confinement requirement for high-strength reinforced concrete member for different concrete and rebar grades according to different design codes.

BNBC 2020

BNBC 2020 refers to consider confinement ratio for axial members in special moment frame (SMF). For rectilinear hoops,

$$A_{sh} = \max of \left[0.3 \left(\frac{sh_c f_c'}{f_{yt}} \right) \left(\frac{A_g}{A_{ch}} - 1 \right) \text{ and } 0.09 \left(\frac{sh_c f_c'}{f_{yt}} \right)$$

Where,

 A_{sh} = Total cross-sectional area of transverse reinforcement (including cross ties) within spacing and perpendicular to dimension h_c (mm²)

s = Spacing of transverse reinforcement measured along longitudinal axis of the structural member (mm)

 h_c = Cross-sectional dimension of column core measured to the outside edge of the transverse reinforcement composing area A_{sh} center to center of confining reinforcement (mm)

f'c = Specified compressive strength of concrete (MPa)

 f_{yt} = Specified yield strength of transverse reinforcement (MPa)

 $A_g = Gross area of section (mm²)$

 A_{ch} = Cross-sectional area of a structural member measured out to out of transverse reinforcement (mm²)

ACI 318-19

Similar to BNBC 2020, ACI 318-19 refers to consider confinement ratio for axial members in special moment frame (SMF). In addition, effect of axial load ratio has been incorporated in this updated version of ACI code.

Table 19: Transverse reinforcement for columns of SMF

Transverse reinforcement	Conditions	Applicable expressions				
A _{sh} /sh _c for rectilinear hoop	$\begin{aligned} P_u &\leq 0.3 A_g f_c \text{ and} \\ f_c^* &\leq 70 MPa \end{aligned}$	Greater of (a) and (b)	(a) $0.3 \left(\frac{A_g}{A_{ch}} - 1\right) \left(\frac{f'_c}{f_{yt}}\right)$			
	$\begin{aligned} P_u &> 0.3 A_g f^*_c \text{ and} \\ f^*_c &> 70 MPa \end{aligned}$	Greater of (a), (b) and (c)	(b) $0.09 \left(\frac{f_c'}{f_{yt}}\right)$			
			(c) $0.2k_f k_n \left(\frac{P_u}{f_{yt}A_{ch}}\right)$			

Here, concrete strength factor, $k_f = (f'_c/175+0.6) \ge 1.0$,

Confinement effectiveness factor, $k_n = n_l/(n_l-2)$,

 n_l is the number of longitudinal bars or bar bundles around the perimeter of a column core with rectilinear hoops that are laterally supported by the corner of hoops or by seismic hooks.

In addition, spacing of transverse reinforcement shall not exceed any of the dimensions mentioned as follows;

- (a) One-fourth of the minimum column dimension
- (b) For Grade 60, 6db of the smallest longitudinal bar
- (c) For Grade 80, 5db of the smallest longitudinal bar
- (d) s_0 , as calculated by: $s_0 = 100 + \left(\frac{350 h_x}{3}\right)$ here, h_x = maximum center-to-center spacing of longitudinal

bars laterally supported by corners of crossties or hoop legs around the perimeter of a column (mm)

Eurocode 8:

Eurocode 1998-1-1:2004 refers to consider confinement ratio for axial members both in medium (DCM) and high ductility (DCH) class comparable to IMF and SMF respectively as mentioned in ACI [28].

$$\alpha \omega_{\text{wd}} \ge 30 \mu_{\varphi} v_{\text{d}} \cdot \varepsilon_{\text{sy,d}} \cdot \frac{b_{\text{c}}}{b_{\text{o}}} - 0,035$$

where

 ω_{wd} is the mechanical volumetric ratio of confining hoops within the critical regions

$$\omega_{\text{wd}} = \frac{\text{volume of confining hoops}}{\text{volume of concrete core}} \cdot \frac{f_{\text{yd}}}{f_{\text{cd}}};$$

 μ_{ϕ} is the required value of the curvature ductility factor;

 v_d is the normalised design axial force ($v_d = N_{Ed}/A_c f_{cd}$);

 $\varepsilon_{\text{sy,d}}$ is the design value of tension steel strain at yield;

 h_c is the gross cross-sectional depth (parallel to the horizontal direction in which the value of μ_{ϕ} used in (6)P of this subclause applies);

 h_0 is the depth of confined core (to the centreline of the hoops);

 b_c is the gross cross-sectional width;

b_o is the width of confined core (to the centreline of the hoops);

 α is the confinement effectiveness factor, equal to $\alpha = \alpha_n \cdot \alpha_s$, with:

a) For rectangular cross-sections:

$$\alpha_{n} = 1 - \sum_{n} b_{i}^{2} / 6b_{o}h_{o}$$

$$\alpha_s = (1 - s/2b_o)(1 - s/2h_o)$$

is the total number of longitudinal bars laterally engaged by hoops or cross ties;
 and

b_i is the distance between consecutive engaged bars (see Figure 5.7; also for b_a, h_a, s).

fed design value of concrete compressive strength

 f_{ctm} mean value of tensile strength of concrete

 $f_{\rm vd}$ design value of yield strength of steel

NZS 3101-2006:

New Zealand building code refers confinement issues considering longitudinal reinforcement ratio, axial stress ratio, concrete compressive strength and transverse reinforcement yield strength as follows;

$$A_{sh} = \frac{(1.3 - \rho_t m)s_h h^* A_g}{3.3} \frac{f_s^*}{A_o} \frac{f_s^*}{f_{y1}} \frac{N_o^*}{\phi f_c A_g} - 0.006 s_h h^*$$

A_{sh} total effective area of hoop bars and supplementary cross-ties in the direction under consideration within spacing s_h, mm²

As gross area of section, mm2

A_c area of concrete core of section measured to outside of peripheral spiral or hoop, mm²

f'_c specified compressive strength of concrete, MPa

 fy lower characteristic yield strength of non-prestressed reinforcement or the yield strength of structural steel casing, MPa

f_{yt} lower characteristic yield strength of spiral, hoop, stirrup-tie or supplementary cross-tie reinforcement, MPa

h" dimension of concrete core of rectangular section, measured perpendicular to the direction of the hoop bars, measured to the outside of the peripheral hoop, mm

N° design axial load derived from overstrength considerations (capacity design), N

s_h centre-to-centre spacing of hoop sets, mm

 $m = t/(0.85 t_0^2)$

 ρ_1 ratio of non-prestressed longitudinal column reinforcement = A_x/A_y

Where the value of p.m used in the equation shall not be taken greater than 0.4.

For comparative study on confinement ratio A_{sh}/sh_c , three column sections have been considered (Figure 18). Other properties and dimensions have been shown in Table 20.

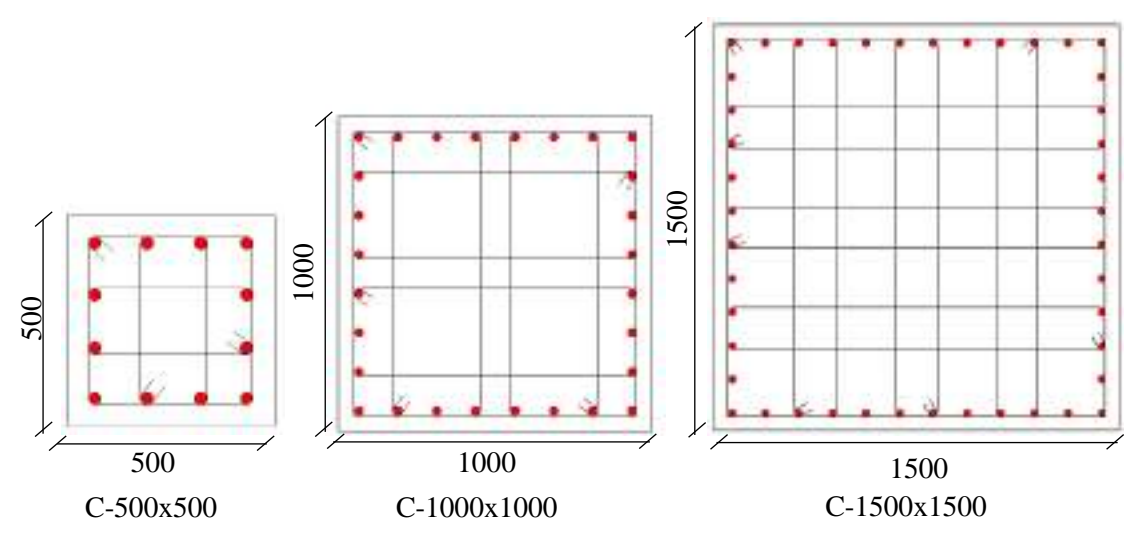


Figure 18: of column specimens for confinement calculation

Table 20: Properties of analytical specimens for confinement calculation

Properties Specimen	C-500x500	C-1000x1000	C-1500x1500
f'c (MPa)	20~60	20~60	20~60
f _{yt} (MPa)	400~600	400~600	400~600
E _s (MPa)	200000	200000	200000
Spacing, s (mm)	100	100	100
Clear cover, c (mm)	40	40	40
Transverse bar dia (mm)	12	12	12
Axial stress ratio, $\frac{P_u}{A_g f'_c}$	0.40	0.40	0.40
No. of confinement bar	4	6	8

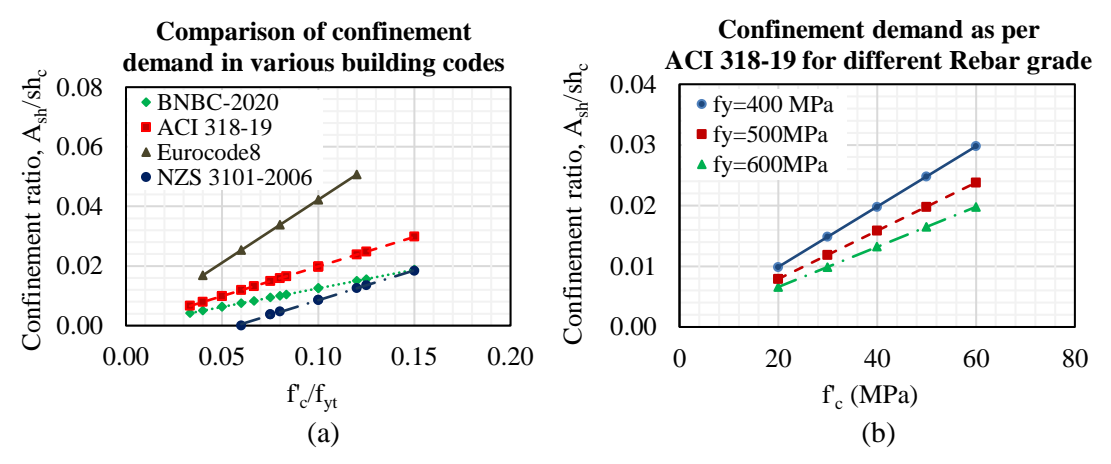


Figure 19: Comparison of confinement requirement (a) according to different building codes, (b) variation with respect to f'c for different rebar grade according to ACI 318-19

The confinement ratio vs concrete compressive strength-to-rebar yield ratio plot has indicated an increasing trend for all design codes, as shown in Figure 23(a). For axial stress ratio above 0.3 the confinement demand is higher according to ACI 318-19 compared to BNBC 2020. The confinement demand is most stringent according to Eurocode though. Moreover, it is observed that the requirement of confinement ratio increases with the increase of compressive strength of concrete if yield strength of transverse bar kept the same.

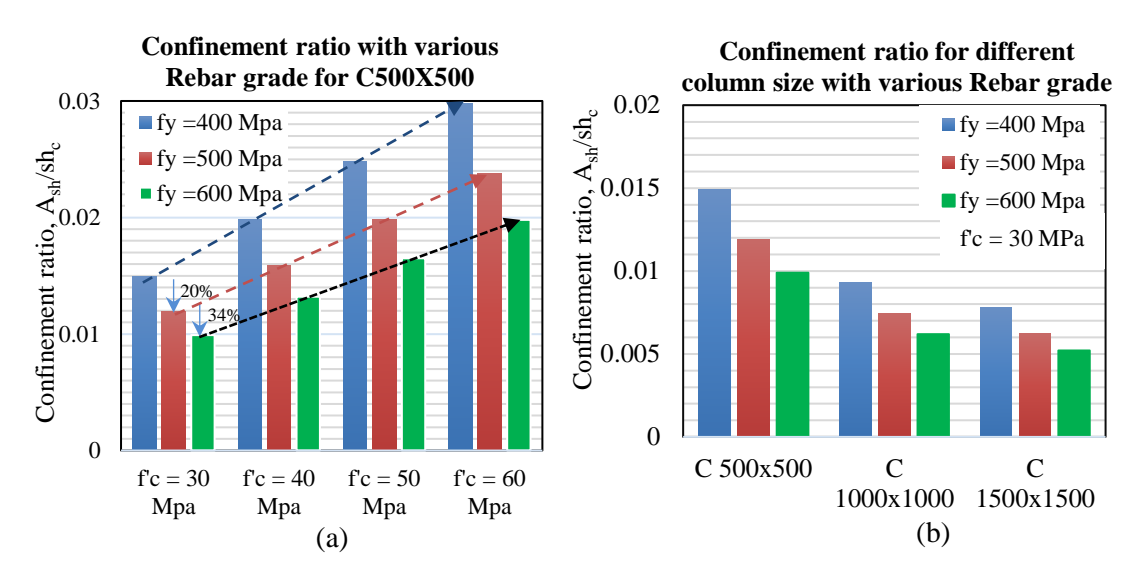


Figure 20: Comparison of confinement ratio according to ACI 318-19 with different rebar grade (a) for various concrete grade with C-500x500 (b) for various column size with f'c = 30MPa

Increasing the yield strength of rebar (f_y) reduces the required of confinement ratio but use of higher strength concrete increases the confinement demand (Figure 20). From Figure 20(a), we find a reduction of confinement demand by 20% and 34% using 500MPa and 600MPa rebar respectively compared to that is required by using 400MPa rebar.

Lower grade concrete requires lower confinement demand leading to easier rebar placement opportunity. But when the higher-grade concrete is in use considering other factors, higher grade reinforcement is better in terms of meeting confinement demand with least possible rebar congestion within RC section.

4.1.6 Bond and Development Length Demand

Development of straight deformed bars in tension

For tensioned reinforcing bars, two forms of bond failure have been identified. The first form is the direct pullout of the bar, which happens when there is adequate confinement provided by the surrounding concrete. This situation could be anticipated when smaller diameter bars are

utilized with sufficiently large distances for concrete cover and bar spacing. The second form of failure involves the splitting of the concrete along the bar when the cover, confinement, or spacing of the bar fails to withstand the lateral tension in the concrete resulting from the wedging effect of the bar deformations. Considering this bond phenomena, building codes have suggested sufficient length of development to transfer stress at reinforcement-concrete interface. There's significant modification in development length value for straight deformed bar in tension if compared between BNBC 2020 and ACI 318-19.

BNBC 2020 refers,

Development length for straight deformed bar in tension,

$$l_d(mm) = (\frac{f_y}{1.1\lambda\sqrt{f_c'}}\frac{\psi_t\psi_e\psi_s}{(\frac{c_b+k_{tr}}{d_b})})d_b \geq 300mm \qquad \qquad [\text{Metric unit}] \qquad \text{here}, \\ \frac{c_b+k_{tr}}{d_b} \leq 2.5, \\ \psi_t\psi_e \leq 1.7$$

Where,

 ψ_t = 1.3 Where horizontal reinforcement is placed such that more than 300 mm of fresh concrete is cast below the development length or splice.

= 1.0 for all other cases.

 $\psi_e = 1.5$ For epoxy-coated bars with cover less than $3d_b$, or clear spacing less than $6d_b$.

= 1.2 For all other epoxy-coated bars.

= 1.0 For uncoated and zinc-coated (galvanized) reinforcement.

 $\psi_s = 0.8$ For 19 mm diameter and smaller bars.

= 1.0 For 20 mm diameter and larger bars.

 λ = 0.75 Where lightweight concrete is used

= 1.0 Where normal weight concrete is used.

This l_d can also be multiplied by a reduction factor of $[\frac{A_{s,required}}{A_{s,required}}]$.

ACI 318-19 refers,

Development length for straight deformed bar in tension,

$$l_{\rm d}(\rm mm) = (\frac{f_y}{1.1\lambda\sqrt{f_c'}} \frac{\psi_t\psi_e\psi_s\psi_g}{(\frac{c_b+k_{tr}}{d_b})})d_b \geq 300 \rm mm \qquad [Metric unit] \quad here, \frac{c_b+k_{tr}}{d_b} \leq 2.5, \psi_t\psi_e \leq 1.7$$

Comparing the equations between BNBC 2020 and ACI 318-19, we find and additional factor to consider yield strength grade of reinforcement, that is ψ_g .

 ψ_g = 1.00 For Grade 420MPa or 275MPa

= 1.15 For Grade 550MPa

= 1.30 For Grade 700MPa

Therefore, an analytical study has been performed as follows to compare this modification.

For analytical study, material properties are used according to Table 21. Development length in tension has been calculated using formula of previously mentioned equations.

Table 21: Material properties used for analytical study of development length for straight bar

Parameters	Corresponding value
Design compressive strength of Concrete, f'c	30~70 MPa
Design yield strength of longitudinal bars, f_y	400~600 MPa
Modulus of Elasticity of Rebar, Es	200000 MPa
Bar diameter, d_b	25 mm

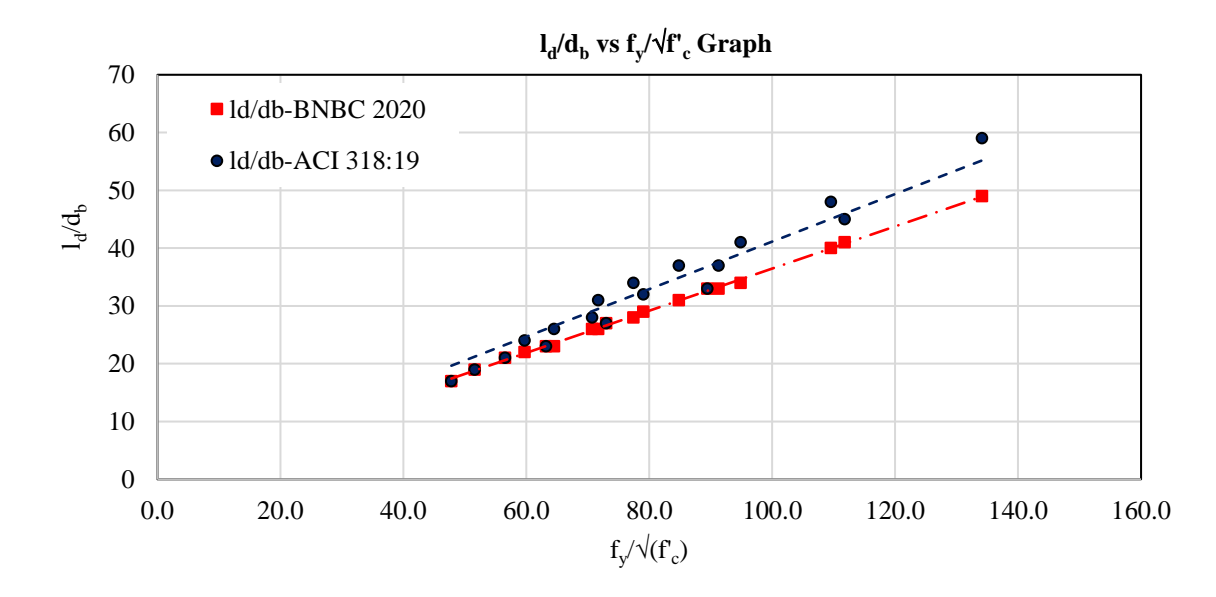


Figure 21: Development length of straight deformed bar, l_d requirement for different grade of concrete and rebars

It is found from Figure 21 that the development length of straight deformed bar is higher according to ACI 318-19 than that is according to BNBC 2020 for rebar grade higher than 420MPa. Moreover, Figure 22 exhibits that the development length is about 10% and 20% higher according to ACI 318-19 than that is according to BNBC 2020 for rebar grade 500MPa and 600MPa respectively, whereas this length is unchanged for rebar grade 420MPa and lower.

Comparison of Development length requirement according to BNBC 2020 and ACI 318-19

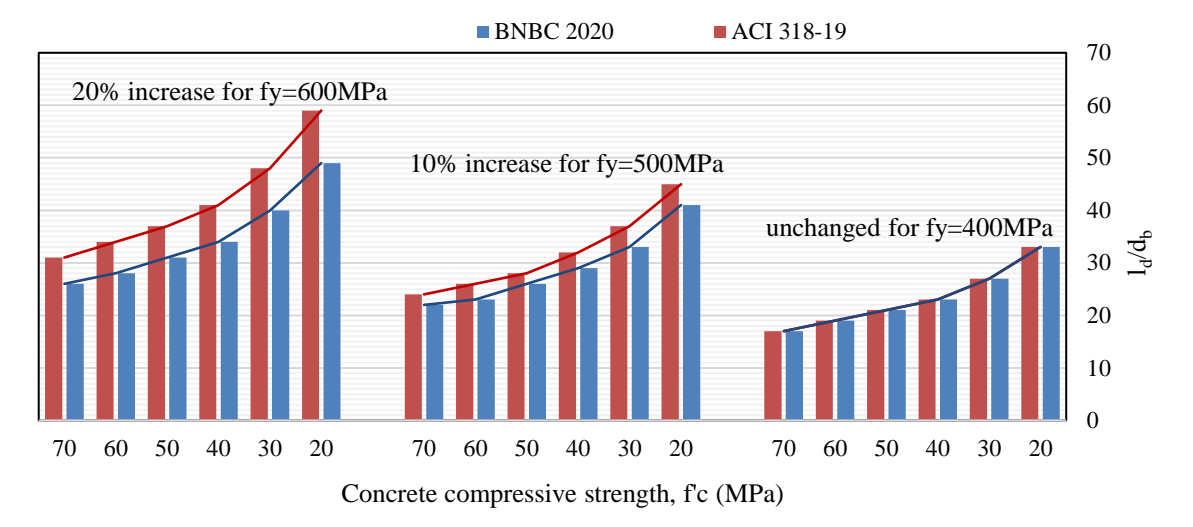


Figure 22: Comparison of Development length requirement according to BNBC 2020 and ACI 318-19

Development of standard hook in tension

In case of flexural reinforcement development within end column, standard hooks or mechanical anchor arrangement are used to reduce the length which can alternatively reduce the requirement of column dimension along the beam considered. In different building codes the advantage of standard hook geometry has been incorporated in terms of allowing reduced bar length of development compared to straight bar.

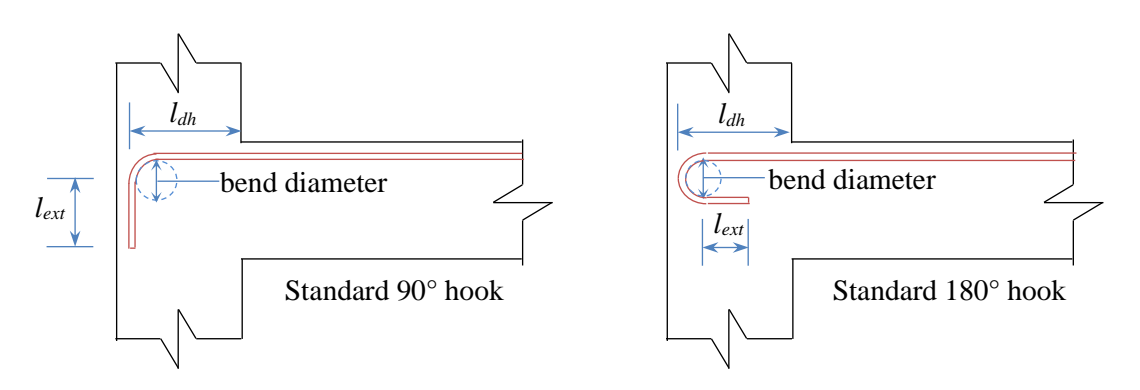


Figure 23: Standard hook geometry for bar development in tension

BNBC 2020 refers,

Development length for hooked bar in tension,
$$l_{dh}(mm) = \frac{0.24\psi_e f_y d_b}{\lambda \sqrt{f_c'}}$$
 [Metric unit]

where, ψ_e shall be taken as 1.2 for epoxy-coated reinforcement, and λ taken as 0.75 for lightweight concrete. For other cases, ψ_e and λ shall be taken as 1.0. This l_{dh} can also be multiplied by a reduction factor of $\left[\frac{A_{s,required}}{A_{s,provided}}\right]$.

ACI 318-19 has provided modified form of the equation from previous edition for calculating hooked development length. Development length terminating in a standard hook, l_{dh} (in mm) for deformed bars in tension shall be calculated according as follows.

$$l_{dh}(mm) = \left(\frac{f_y \psi_e \psi_r \psi_o \psi_c}{23\lambda \sqrt{f_c'}}\right) d_b^{1.5} \ge 8d_b \text{ and } 150\text{mm [Metric unit]}$$

Where,

 ψ_e = 1.2 For epoxy-coated bars or zinc and epoxy dual coated reinforcement.

= 1.0 For uncoated and zinc-coated (galvanized) reinforcement.

 $\psi_r = 1.0 \text{ For 35mm dia bar with } A_{th} \geq 0.4 A_{hs} \text{ or hoops spacing } s \geq 6 d_b.$

= 1.6 For all other cases.

 $\psi_0=1.0$ For 35mm and smaller diameter hooked bars: (1) Terminating inside column core with side cover normal to plane of hook ≥ 65 mm, or (2) With side cover normal to plane of hook $\geq 6d_b$.

= 1.25 For other cases.

 $\psi_c = (f'c/100+0.6)$ For f'c < 40 MPa.

= 1.0 For f'c \geq 40 MPa.

 $\lambda = 0.75$ Where lightweight concrete is used

= 1.0 Where normal weight concrete is used.

NZS 3101.1:2006 suggested development length in tension for yield strength of rebar limited to 500 MPa and concrete compressive strength is limited to 70MPa.

$$l_{dh}(mm) = 0.24\alpha_1\alpha_2\alpha_b \frac{f_y d_b}{\sqrt{f'_c}} \ge 8d_b$$
 [Metric unit]

Where,

 $\alpha_1 = 0.7$ for 32mm bar or smaller with side cover normal to the plane of the hook \geq 60mm, and cover on the tail extension of 90° hooks \geq 40mm.

= 1.0 for all other cases.

 $\alpha_2=0.8$ where confined by closed stirrups or hoops spaced at 6db or less and which satisfy the relationship $A_{tr}/s \geq A_b/1000$.

= 1.0 for all other cases.

$$\alpha_b = \left[\frac{A_{s,required}}{A_{s,provided}}\right]$$

A_{tr} = smaller of area of transverse reinforcement within a spacing "s" crossing plane of splitting normal to concrete surface containing extreme tension fibers, or total area of transverse reinforcement normal to the layer of bars within a spacing "s", divided by number of longitudinal bars in the layer through which a potential plan of splitting would pass (mm²)

 A_b = area of individual bar (mm²)

s = maximum spacing of transverse reinforcement (mm).

For analytical study, material properties have been used according to Table 22. Development length for hooked bar in tension is calculated using formula of previously mentioned equations.

Table 22: Material properties used for analytical study of development length for hooked bar

Parameters	Corresponding value
Design compressive strength of Concrete, f'c	30~70 MPa
Design yield strength of longitudinal bars, $f_{\boldsymbol{y}}$	400~600 MPa
Modulus of Elasticity of Rebar, Es	200000 MPa
Bar diameter, d _b	25 mm

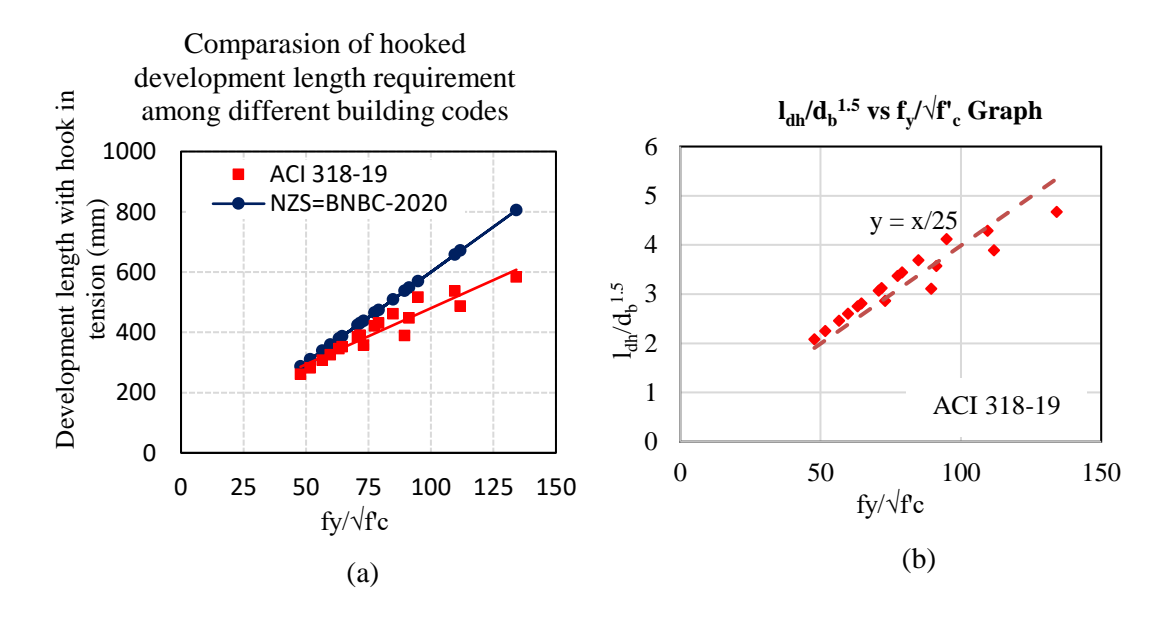


Figure 24: Hooked Development length, l_{dh} requirement for different grade of concrete and rebars

Figure 24 has showed an increasing trend has found form the plot of development length with hook in tension vs $f_y/\sqrt{f'_c}$. The NZS 3101.1:2006 and BNBC 2020 showed same values of

development length in tension. However, there is a reduction in development length requirement by ACI 318-19 compared to BNBC-2020. From Figure 24(b) a simplified equation can be generated for quick assessment of hooked development length calculation for λ , ψ_e , ψ_r , ψ_0 as 1.0.

The equation can be written as,
$$l_{dh}(mm) = \left(\frac{f_y}{25\sqrt{f'_c}}\right) d_b^{1.5}$$
 [Metric unit]

Moreover, Figure 25 shows that for 500MPa and 600MPa rebar the hooked development length demand is 25% and 50% higher respectively than that is required for 400MPa rebar. Whereas, the development length demand reduces with increase of concrete compressive strength.

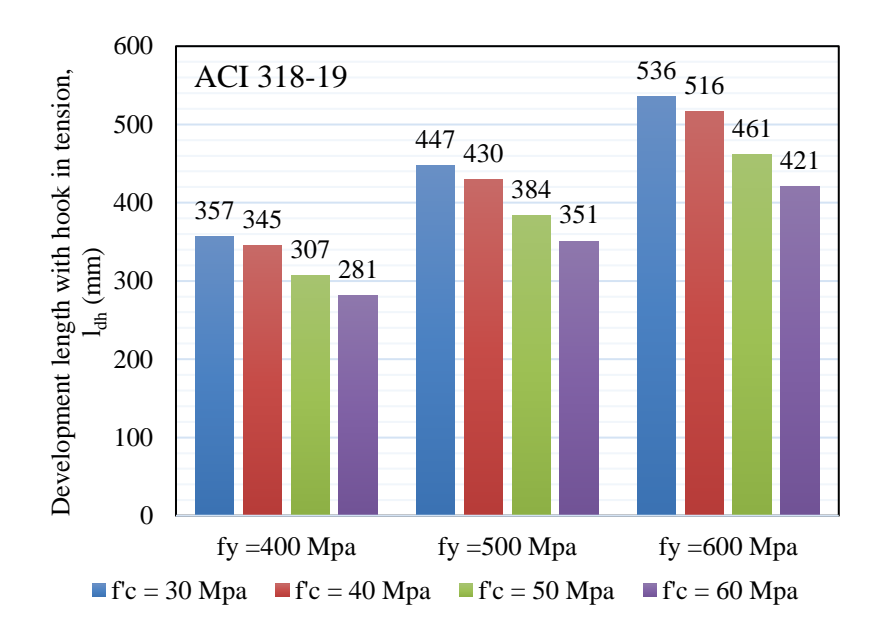


Figure 25: Hooked Development length, l_{dh} requirement for different grade rebars by varying concrete's grade according to ACI 318-19 with 25mm dia bar.

Development of headed deformed bar in tension

Headed anchors refer to reinforcing bars that have mechanical or forged heads at one or both ends are intended to provide anchorage in tension or compression zones, substituting traditional hooked bars or straight development lengths. Usually, circular, rectangular, or square speed heads are utilized with sufficient bearing area. This approach eliminates long hooks or overlapping lengths, lessening rebar congestion in crucial areas such as beam-column joints or pile caps. It offers anchorage through bearing stress at the head, minimizing dependence on bond strength along the bar. It improves performance in seismic zones, especially in confined spaces where standard anchorage may not operate effectively. It simplifies installation and

decreases mistakes during construction. To guarantee successful load transfer in confined regions. Load transfer occurs through both bearing stress at the head against concrete and through bond strength along the bar's deformed surface. The minimum net bearing area must be at least 4 times the bar cross-sectional area. Proper confinement is necessary if used in tension areas. Reinforcement surrounding the headed bar is essential to prevent splitting or cone failures.

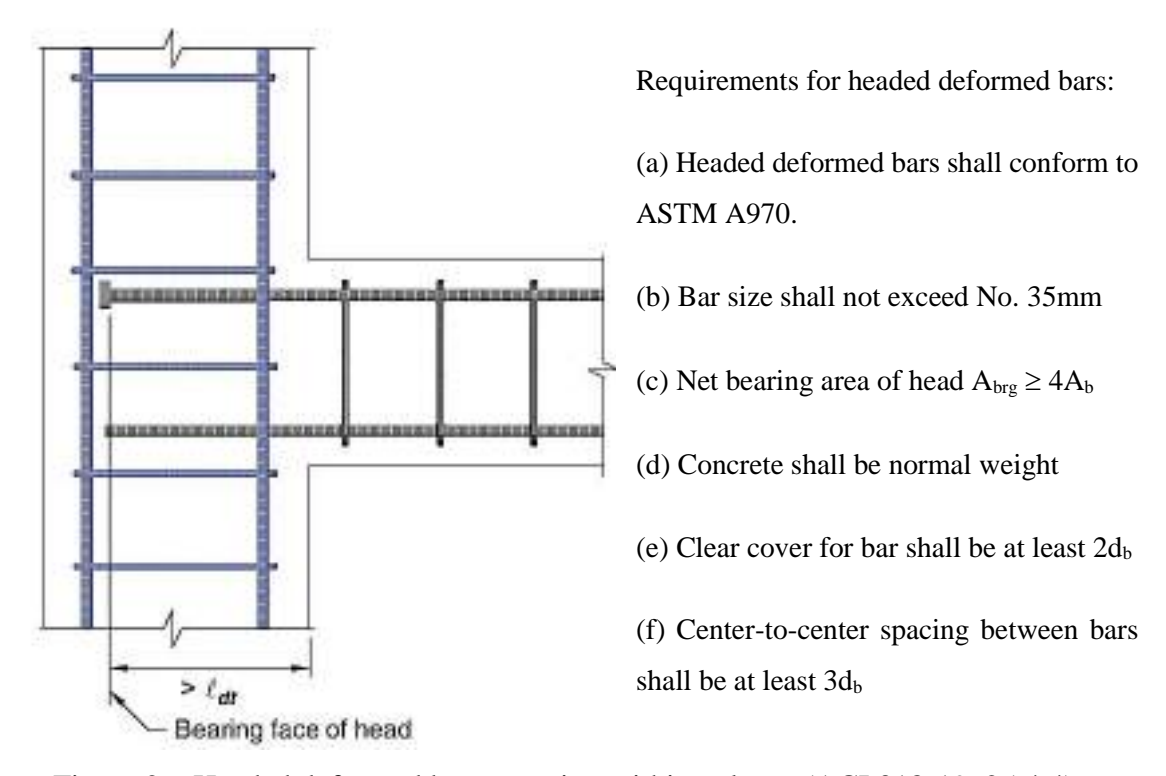


Figure 26: Headed deformed bar extension within column (ACI 318-19, 25.4.4)

ACI 318-19 has provided formula for headed deformed bar development in as follows.

$$l_{dt}(mm) = \left(\frac{f_y \psi_e \psi_p \psi_o \psi_c}{31\lambda \sqrt{f'_c}}\right) d_b^{1.5} \ge 8d_b \text{ and } 150\text{mm [Metric unit]}$$

Where, $\psi_r = 1.0$ For 35mm dia bar with $A_{tt} \ge 0.3 A_{hs}$ or hoops spacing, $s \ge 6 d_b$. = 1.6 For all other cases.

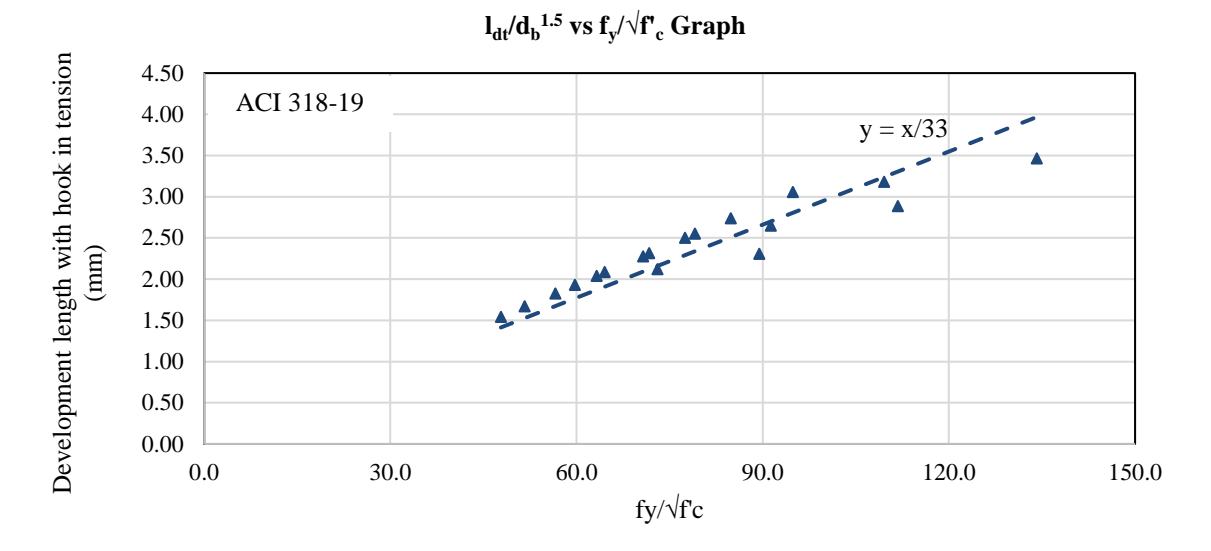


Figure 27: Headed bar Development length, l_{dt} requirement for different grade of concrete and rebars

From Figure 27, a simplified equation can be generated for quick assessment of hooked development length calculation for λ , ψ_e , ψ_p , ψ_0 as 1.0.

The equation can be written as,
$$l_{dt}(mm) = \left(\frac{f_y}{33\sqrt{f'_c}}\right) d_b^{1.5}$$
 [Metric unit]

Comparing Figure 24(b) and Figure 27, it's observed that the development length can be reduced by more than 30% by using headed deformed bars replacing hooked bar.

In addition to the structural load consideration and stability requirement, the development length has a major role to fix the dimension of columns where beam is discontinued at ends. A comparison based on typical beam-column end joint detailing has been made to attain the minimum column dimensions that can ensure full tensile stress transfer as per rebar yield capacity.

With reference to Figure 28, the following values have been considered for column size demand calculation.

Concrete clear cover, c = 40mm

Transverse bar dia, $d_1 = 10$ mm

Longitudinal bar dia, $d_2 = 10$ mm

Gap between bars, g = y = z = 25mm

L_{dh} & L_{dt} are development length of hooked and headed deformed bars respectively.

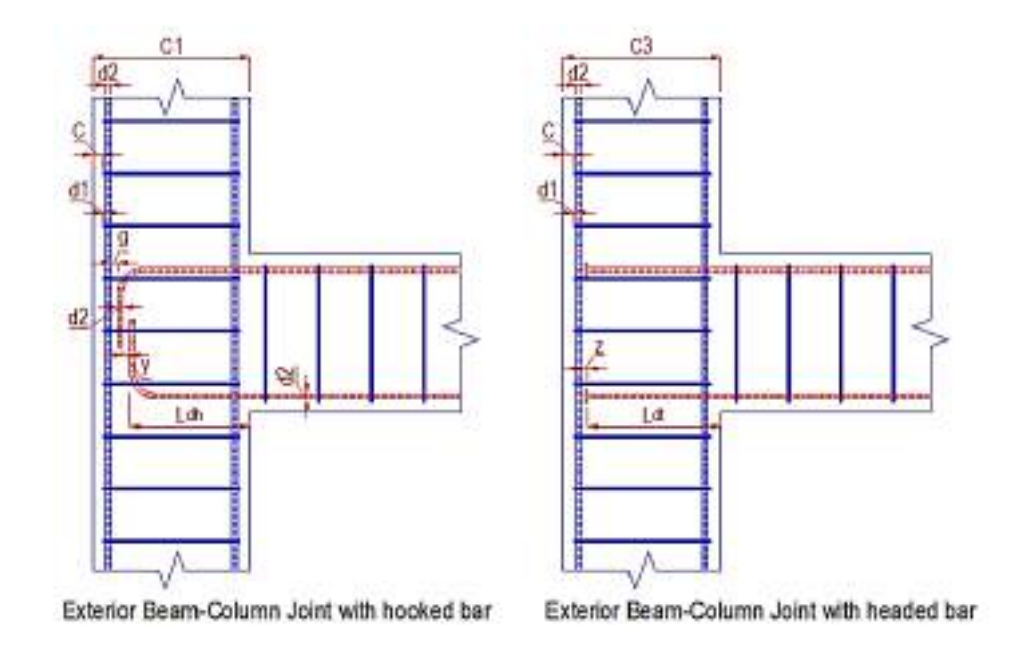


Figure 28: Typical end detailing of Beam-Column exterior joint

Table 23: Comparative end column dimensions for different combinations of concrete and rebar grades using hooked and headed deformed bar

SL	f_y	f'c	With	Min. required C	Remarks	
	(MPa)	(MPa)	Longitudinal	IMF (
			bar dia (mm)	C1 C2		
				(Hooked bar)	(Headed bar)	
1	400	20	16	331	241	acceptable
2	500	25	16	371	310	acceptable
3	550	30	16	383	319	acceptable
4	600	35	16	402	332	acceptable

Low strength concrete can be used but requires higher development length both for straight bars and hooked or headed bars. Use of high strength reinforcement also increases the development length demand significantly. Higher concrete compressive strength is suitable with high strength reinforcement considering development length demand. In addition, use of mechanical couplers replacing lap splices and headed type end anchorage replacing standard hooks are better compatible with high strength reinforcement that can potentially ensure improved bond development, reduced end column dimension, less rebar congestion, better capacity utilization of reinforcement etc.

5 Performance against lateral load

The main objective of seismic design is to ensure that structures can withstand sufficient inelastic deformations and effectively dissipate energy, thereby reducing damage and maintaining life safety during earthquakes. These elements can be assessed through the hysteretic response of structural components. In this subsection, various lateral behaviors in terms of lateral capacity, energy dissipation, ductility, and stiffness degradation of high-strength reinforced concrete members are examined.

5.1 Literature review of experimental works

Since this study was purely theoretical and not included with any experimental research, the basic resources were the academic papers and findings of other researchers' works. For this purpose, the research papers based on comparative performance analysis of RC members made with high-strength grade reinforcement and conventional graded reinforcement were considered exclusively. A few of the prominent works have been summarized as follows.

5.1.1 Behavior of Hysteresis loop due to cyclic load test

The behavior of RC frames, which consist of beams, columns, and joints in seismic load response, is a primary concern in design philosophy. One of the main challenges in using concrete elements reinforced with high-strength steel (f_y exceeding 550MPa) is the limited availability of experimental data. Therefore, the results of the cyclic load test of these structural members have been discussed. From the hysteresis loops, we can witness the inelastic characteristics and quantify the ability of energy dissipation of certain RC members and joints and therefore can compare the effect of reinforcement grade on the performance of RC frame under seismic load action.

Beam Test

This experimental study [3] investigates the feasibility of utilizing steel with f_y as high as 830MPa as the primary reinforcement in concrete elements by applying a cyclic loading protocol to beams and columns reinforced with ultrahigh-strength steel. The mechanical performance of these elements was compared to that of analogous elements reinforced with conventional steel.

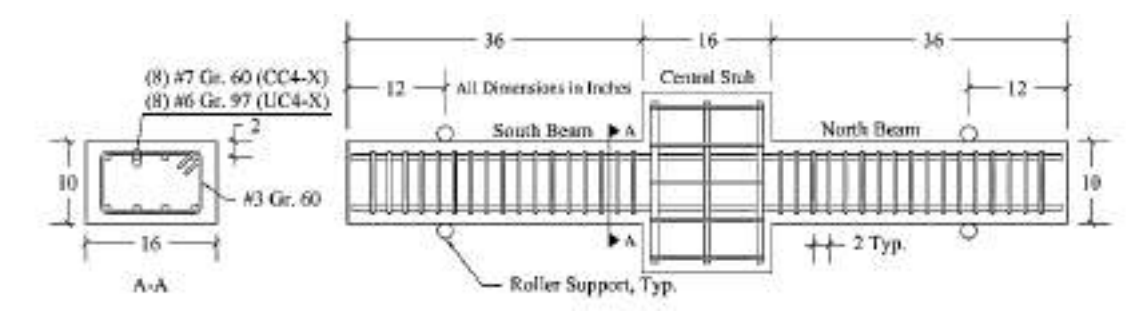


Figure 29: Reinforcement details and test set up for beam specimens [3]

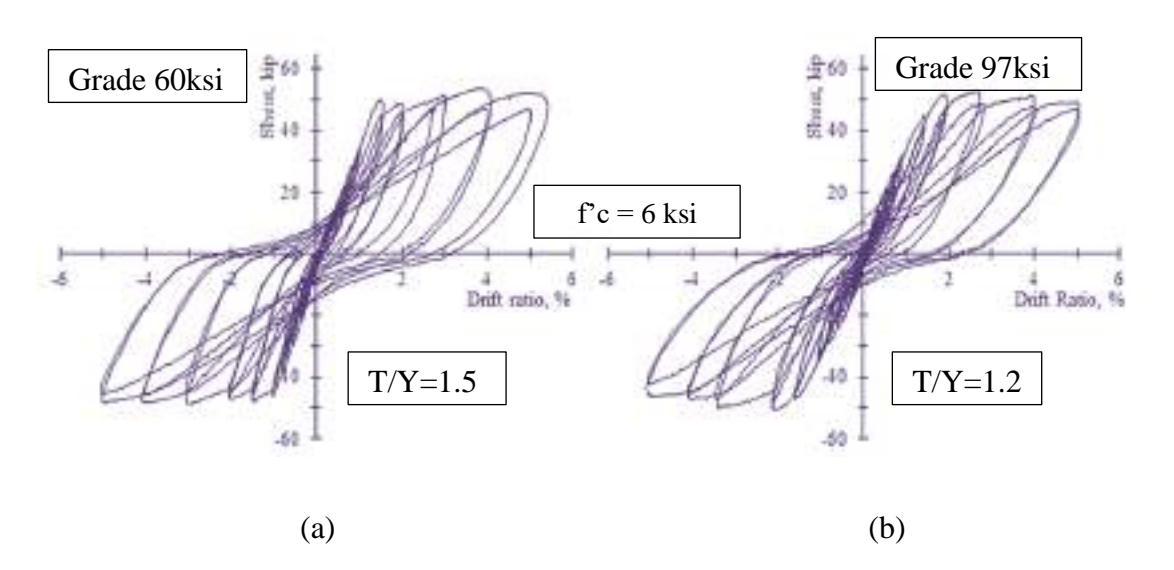


Figure 30: Measured shear versus drift ratio (a) Specimen with Grade 60 reinforcement; and (b) Specimen with Grade 97 reinforcement.

Findings are;

- I. Flexural strength and Drift capacity: Up to 5% drift limit the hysteretic response was well stable without dropping remarkable flexural strength and deformation capacity. This is significantly above the drift ratio requirements in the practical design of structures.
- II. Stiffness reduction: Both initial stiffness and unloading stiffness within 15 to 5% drift was 20% and 10% lower respectively with grade 830MPa steel compared to 415MPa steel since the reinforcement ratio was lower for higher grade. But the difference was reduced with increase of drift ratio.
- III. Crack width: Crack width is almost directly proportional to the designated yield strength of the longitudinal reinforcement. Higher grade steel forms higher crack widths. For RC beams where a significant portion of the necessary reinforcement results from seismic loads, crack widths arising from gravity loads should not be an issue in general unless it's a serviceability or functional requirement.

These indicate that high-strength reinforcement with $fy \ge 550$ MPa may be a feasible choice for RC construction resistant to earthquake forces.

Column Test

Column specimens underwent testing with a constant axial load and reverse cyclic lateral loading until there was a significant reduction in lateral load capacity [29].

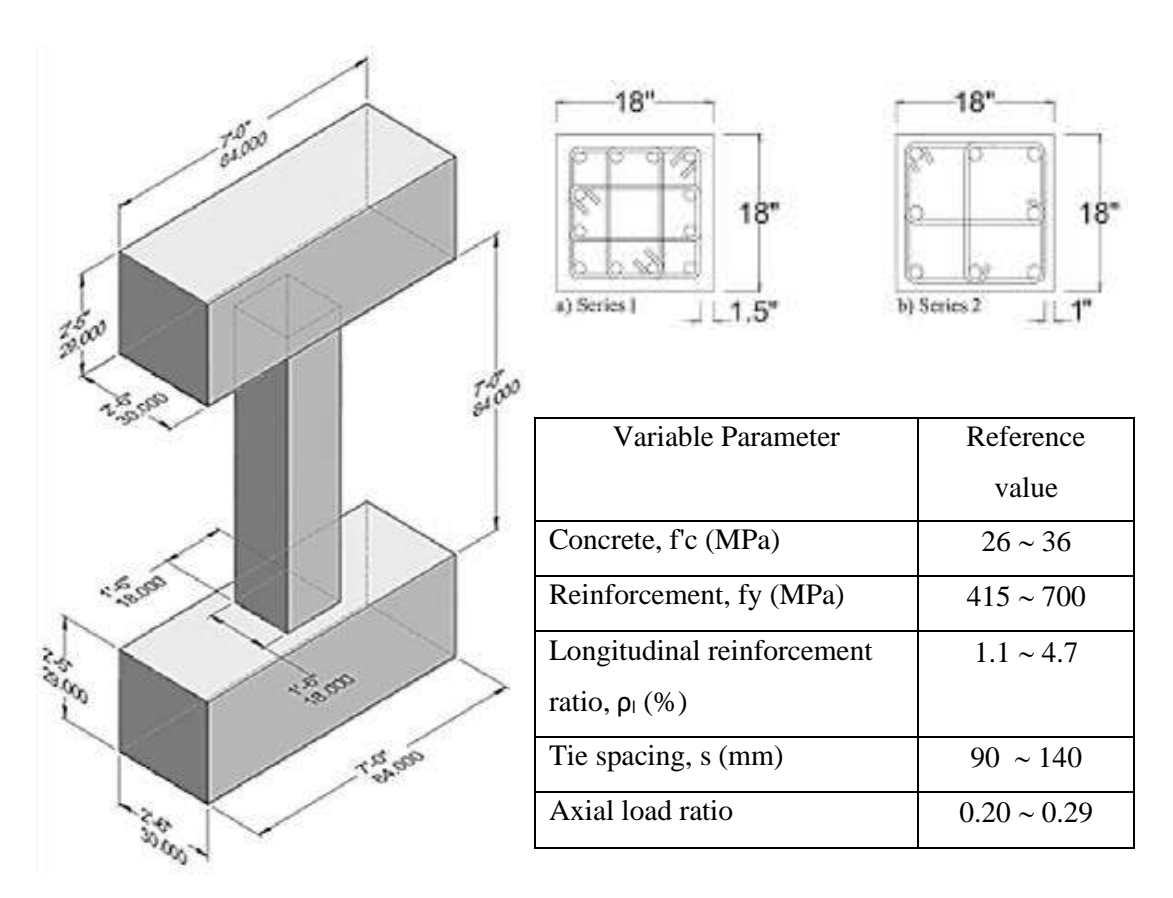


Figure 31: Test sample and experimental parameters for column capacity test [29]

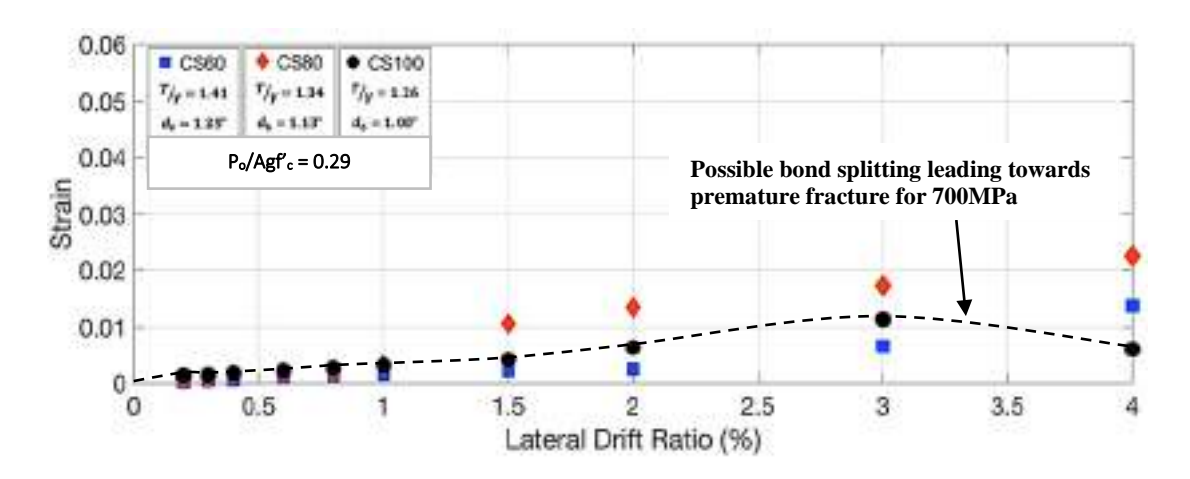


Figure 32: Tensile Strain vs Drift ratio for Reinforcement Grade 415, 550 and 700MPa [29]

Further extensive experiment-based research has been conducted with different variables using high strength reinforcement [30] and that can be described as follows.

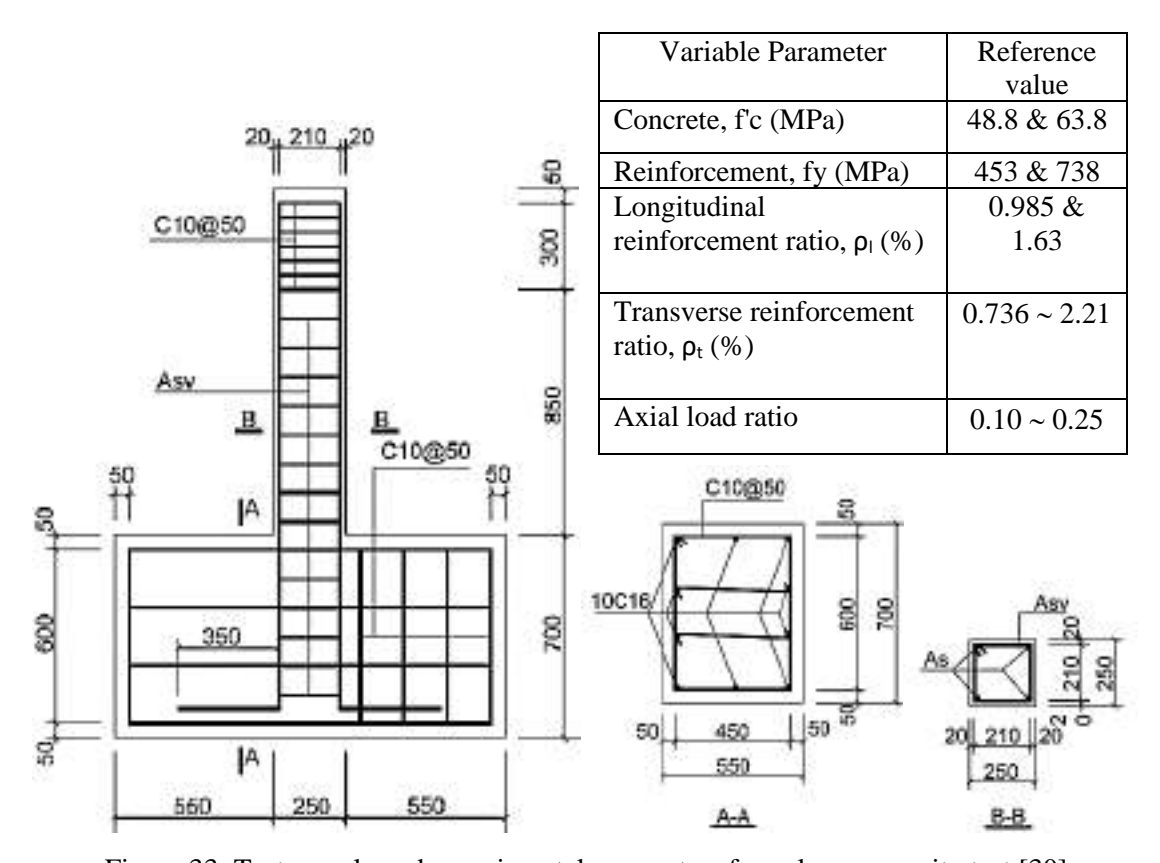


Figure 33: Test sample and experimental parameters for column capacity test [30]

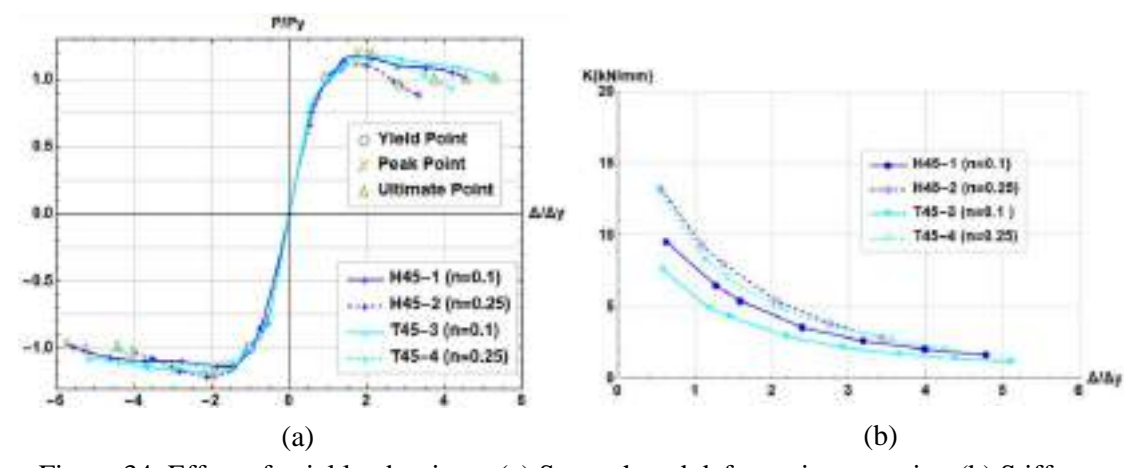


Figure 34: Effect of axial load ratio on (a) Strength and deformation capacity, (b) Stiffness degradation [30]

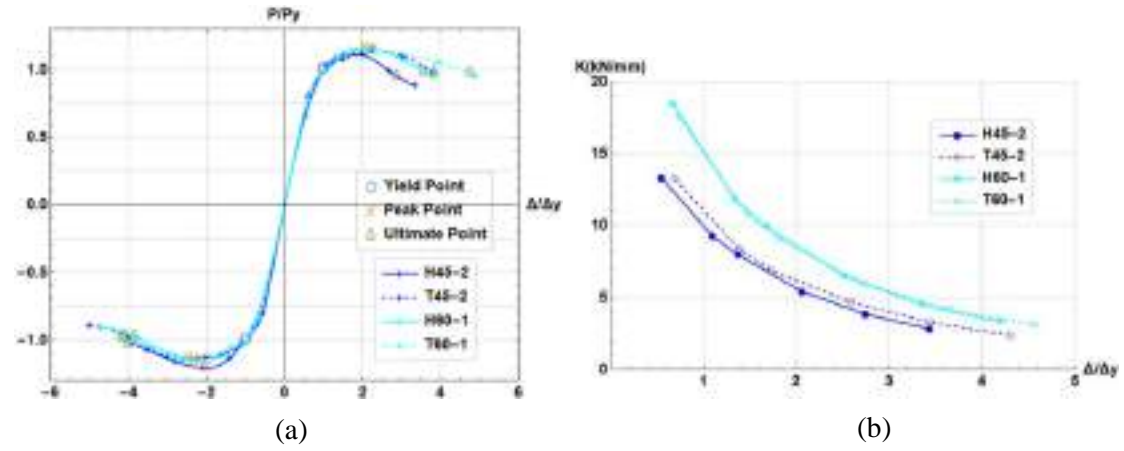


Figure 35: Effect of Equal Strength reinforcement replacement (constant $A_s f_y$) (a) Strength and deformation capacity, (b) Stiffness degradation [30]

Findings are;

- I. Drift capacity: All Column specimens demonstrated stable cyclic responses up to a drift ratio of 5.5%, which can be deemed adequate for collapse prevention at the Maximum Considered Earthquake (MCE) hazard level [29].
- II. Strain demand: Figure 32 shows that the longitudinal bars classified as grade 700MPa achieved their average yield strain by the conclusion of the initial cycle towards a drift ratio of 1.0%. Grade 550 MPa exhibits notably greater strains across all drift levels. In scenarios where high strain amplitudes are anticipated, higher strength bars might experience premature fracture due to bond splitting where high value of strain amplitudes are expected.
- III. Effect of axial load ratio: The lateral strength, energy dissipation capacity, and stiffness of specimens were initially higher for a higher load ratio, but the ductility and overall energy dissipation were significantly reduced, and the rate of stiffness degradation was also increased (Figure 34).
- IV. Effect of Equal Strength reinforcement replacement: The lateral strength of the concrete column specimen with 630MPa grade reinforcements saw a slight increase, the stiffness reduction was more gradual, and the ductility and energy dissipation capacity were lessened, the strength was marginally diminished but still satisfied the seismic design criteria (Figure 35).

Beam-Column Joint

Alavi-Dehkordi et al. (2019) [31] conducted an experimental study on the seismic performance of exterior beam-column joints with columns measuring 250×250 mm and beams measuring 300 mm deep by 250 mm wide.

Table 24: Properties of reference specimen for Beam-Column Joint experiment [31]

	Specimen ID	NS-30	RHS-30	NS-70	RHS-70
Material	f'c (MPa)	30	30	70	70
Properties	Longitudinal bar grade (MPa)	420	600	420	600
1	Hoops and cross-tie grade (MPa)	420	420	420	420
Beam	Top and bottom bar area ratio (%)	0.87	0.63	0.87	0.63
Column	Bar area ratio (%)	1.93	1.42	1.93	1.42
Column	Axial load ratio	0.080	0.080	0.036	0.036

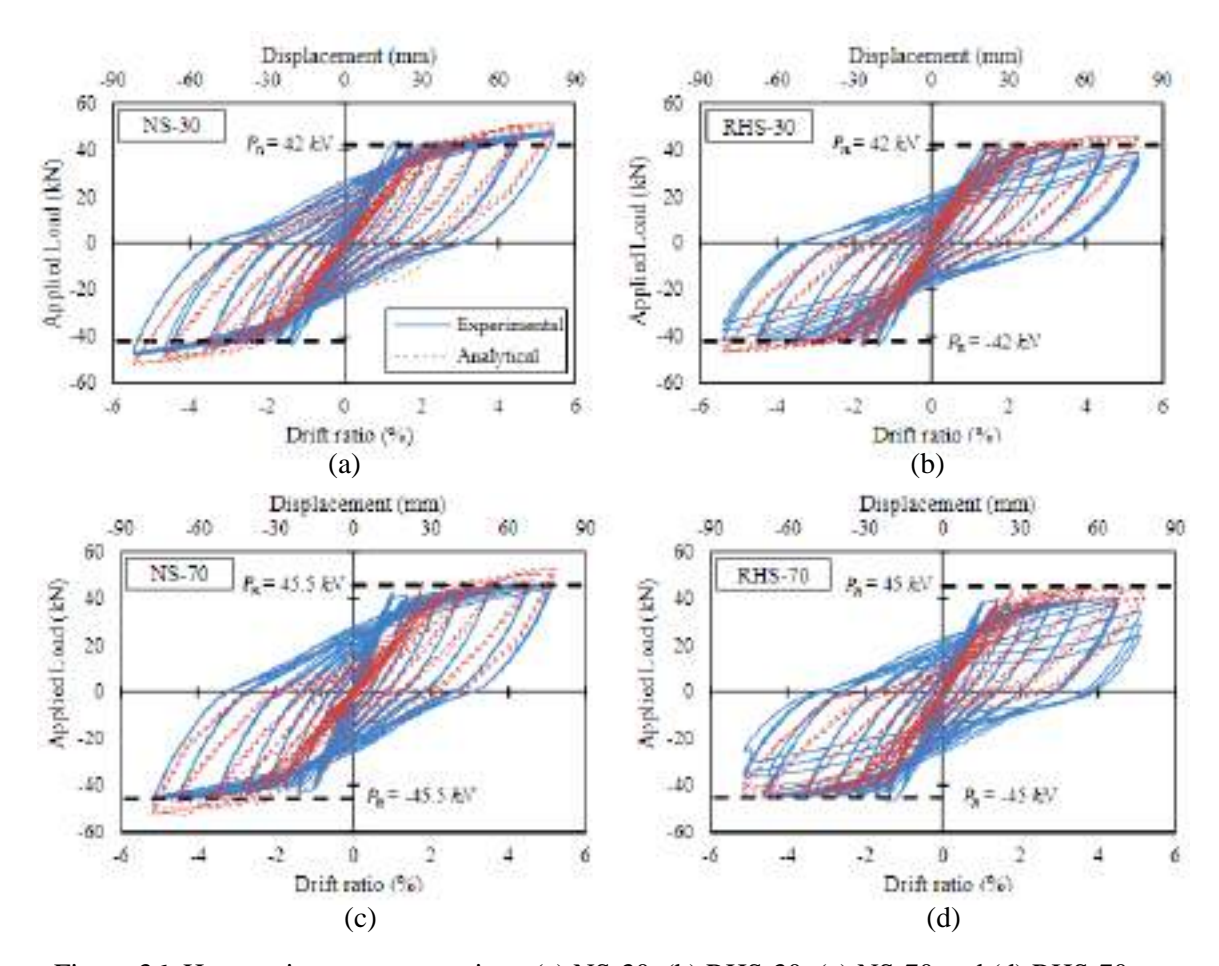


Figure 36: Hysteresis response specimen(a) NS-30, (b) RHS-30, (c) NS-70 and (d) RHS-70 [31]

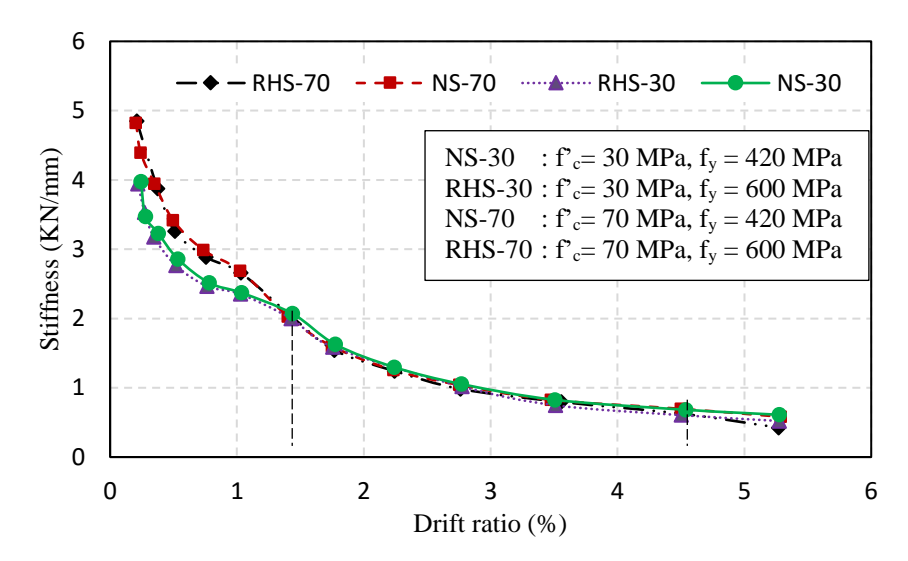


Figure 37: Stiffness degradation pattern for frame specimens [31]

Findings are;

- Ultimate capacity: Post yield strength retention slightly increased for specimens with Grade
 420MPa whereas the capacity remains unchanged for 600MPa specimens.
- II. Drift capacity: Deformation capacity is slightly higher for 420MPa specimens with respect to 600MPa. Still, all specimens demonstrated stable cyclic responses up to a drift ratio of 4.5%, which is good in terms of seismic design requirements.
- III. Energy dissipation: All specimens have shown more or less wide hysteretic cycles meaning good energy dissipation is possible for higher grade rebar of 600MPa.
- IV. Stiffness degradation: 600MPa grade specimens were found similar to 420MPa specimens, rather all specimens degraded consistently after 1.4% drift ratio.

5.2 Parametric Study on RC Frame

Non-linear static analysis is a popular method to find the lateral load resistance capacity of RC frames that can be compared with design earthquake force. Concerning our investigation, a parametric study with frame analyses corresponding to different rebar grades was performed to compare its possible effect on the lateral load capacity and ductility. The study was carried out utilizing finite element analysis (FEA) in ABAQUS [32]. Before that study, the employed finite element modeling technique was validated with the backbone curve of a reinforced concrete frame tested by Vecchio and Emara [33] and RC column specimen studied by Li et al. [8].

Philosophy of Member Capacity Analysis

The connection between the moment exerted on a specific beam section and the resulting curvature, encompassing the entire range of loading until failure, is crucial to the examination

of member ductility, comprehending the formation of plastic hinges, and considering the redistribution of elastic moments that takes place in the majority of reinforced concrete structures prior to failure. Utilizing the stress-strain relationships for steel and concrete, illustrated in idealized forms, alongside the standard assumptions concerning perfect bond and plane sections, it becomes feasible to compute the connection between moment and curvature for a standard under-reinforced concrete beam section, exposed to flexural cracking, as outlined below.

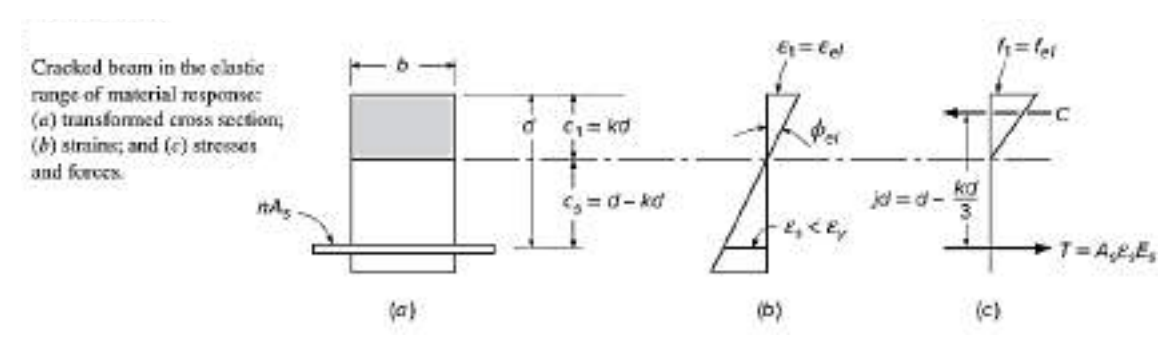


Figure 38: Stress-strain relationship in Flexural member section in uncracked section [25]

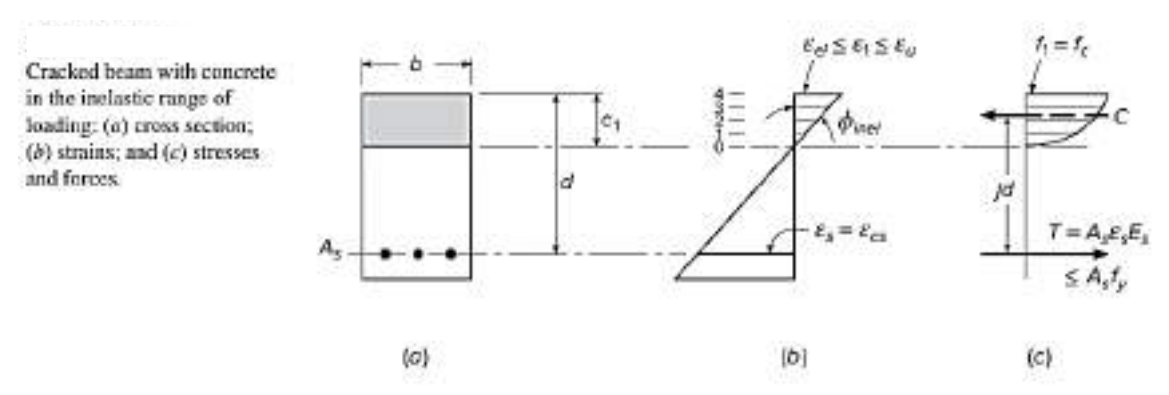


Figure 39: Stress-strain relationship in Flexural member in cracked section [25]

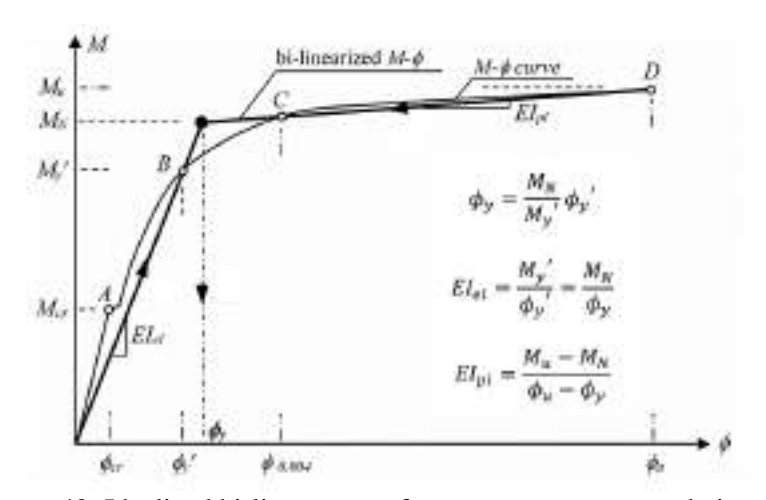


Figure 40: Idealized bi-linear curve for moment-curvature relationship

In case of column the axial load has significant effect on moment capacity of RC section. At pre-cracking stage, the initial stiffness is higher than in pure flexure because the axial load compresses the concrete, delaying the onset of cracking. Axial load and bending moments interact and at higher axial loads ductility reduces, causing a steeper initial slope and a quicker descent after the peak moment. The balance between axial load and moment dictates the failure mode. High axial load causes brittle failure due to crushing of concrete while low axial load ensures ductile failure due to steel yielding.

Modeling approach of materials

The Concrete Damage Plasticity (CDP) model has been utilized to represent the nonlinear and damaged characteristics of concrete. The CDP model effectively addresses the non-linearity in both tension and compression for plain concrete. The compression and tension curve employed in this research has been created as shown in Figure 41 based on the work of Carreira and Chu [34]. The splitting tensile strength of concrete is considered to be 0.62√f'c (MPa), with f'c representing the compressive strength of concrete (BNBC 2020). The bilinear steel model has been utilized for the modeling of reinforcement material properties (Figure 42). The elongation percentage of reinforcement has been established according to BDS ISO 6935-2-2021 for the highest ductility class (class-D, T/Y=1.25), and a modulus of elasticity of 200000 MPa has been considered to establish modeling parameters. Figure 43 shows a typical load-deformation curve and classification point of RC structural members [35]. A typical definition of ultimate drift is shown in Figure 44 [36].

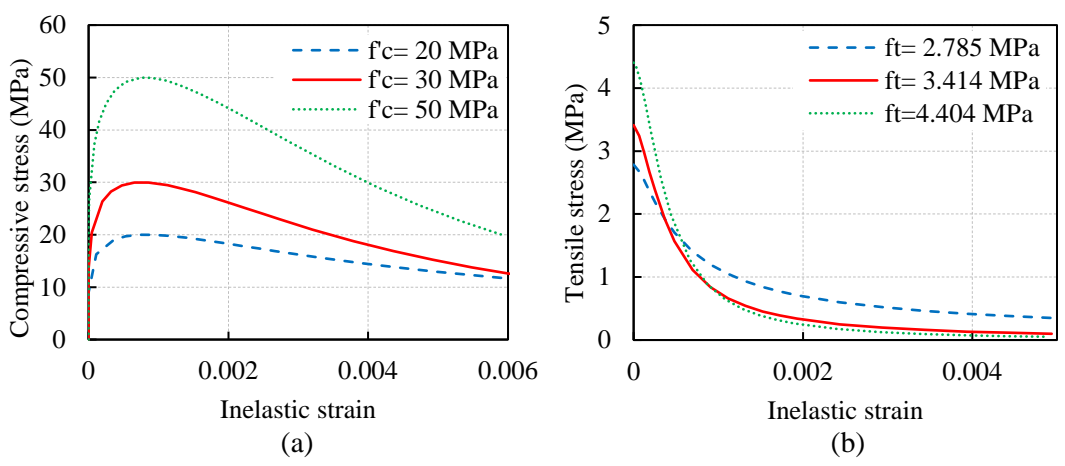


Figure 41: Concrete material properties used for Concrete Damage Plasticity (CDP) model [34] (a) compressive behavior (b) tensile behavior

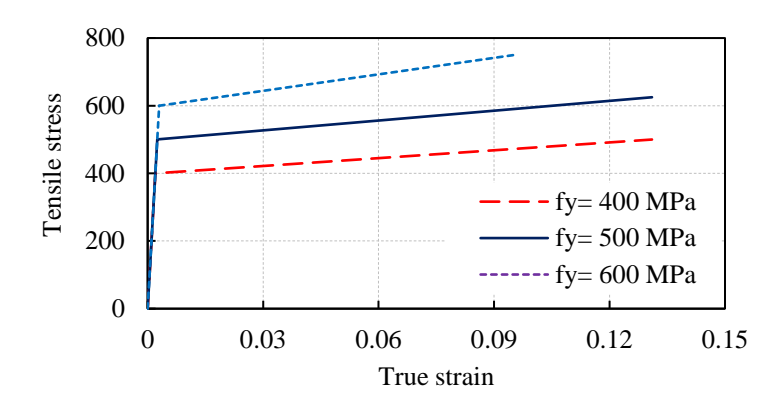


Figure 42: Bilinear steel model (for Class:D according to BDS-ISO 6935-2-2021)

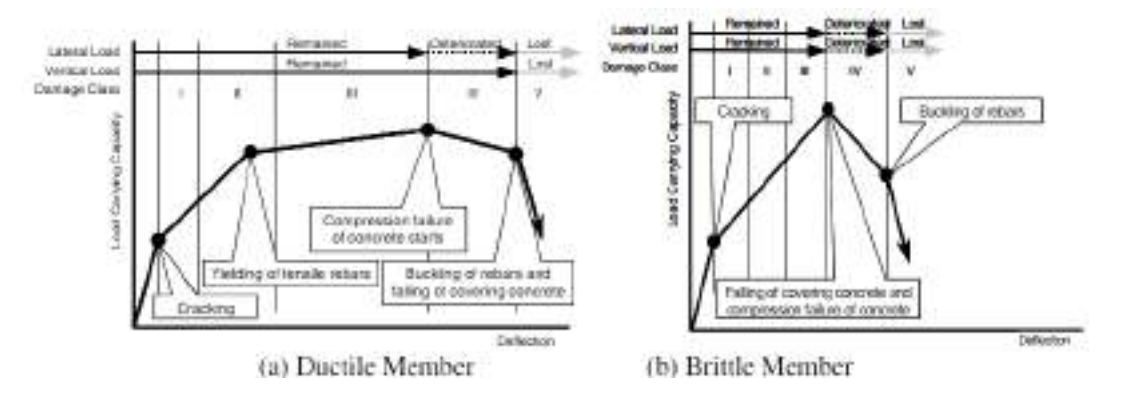


Figure 43: Typical load-deformation curve of RC structural members [35]

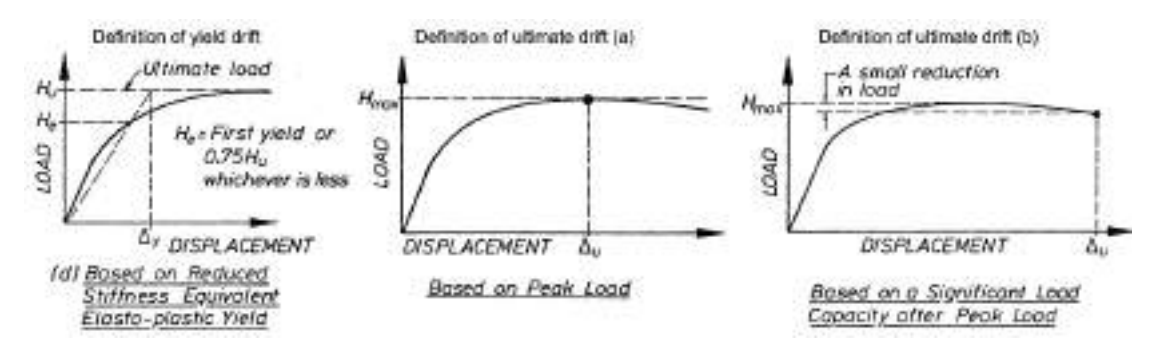


Figure 44: Definition of yield drift and ultimate drift [36]

Validation of Finite element modelling with experimental specimen

For validation of FEM, a RC frame specimen [33] has been selected. The test specimen with loading protocol used in the study has been shown in Figure 40. For element type for the concrete, eight-node linear brick element with reduced integration (C3D8R) has been used. A linear 3-D truss with 2-node (T3D2) has been used as an element type for modeling both longitudinal and transverse reinforcement type. The complete geometric modeling of the reference specimen is illustrated in Figure 41. The load and boundary conditions for the FEM have been established according to the experimental test setup depicted in Figure 3. A vertical

load of 700KN is distributed across the top cross-sectional area of the two columns as a pressure-type load. The reinforcements are integrated into the entire concrete region without taking into account any bond-slip relationship between the concrete and reinforcement for simplicity. Since this study focuses solely on positive loading, a displacement of 150 mm (equivalent to a 5% drift limit) is applied incrementally from left to right on the beam. Rather than applying the displacement to the outer face of the beam, a control point has been created using the MPC constraint (Abaqus, 2013) with a beam type, and all degrees of freedom of the beams have been fixed to that control point. The displacement or drift of the backbone curve must be monitored from the control point of the beam. The base of the stub is fixed using an ENCASTRE (Abaqus, 2013) boundary condition, in which all six degrees of freedom are assumed to be zero. The reaction of this base needs to be monitored to obtain the lateral load of the backbone curve. Similar FEM approach has been adopted for modelling beam column joint of Li et al [8].

Table 25: Material properties of reference experiments for FEM validation

Deference	f'c	Longitudi	nal reinforce	ement	Transverse reinforcement		
Reference	(MPa)	f _y (MPa)	f _u (MPa)	f_u/f_y	f _y (MPa)	f _u (MPa)	f _u /f _y
Vecchio and Emara [33]	30	418	596	1.43	454	640	1.41
Li et al. [8]	30.7	617	802	1.28	642	803	1.25

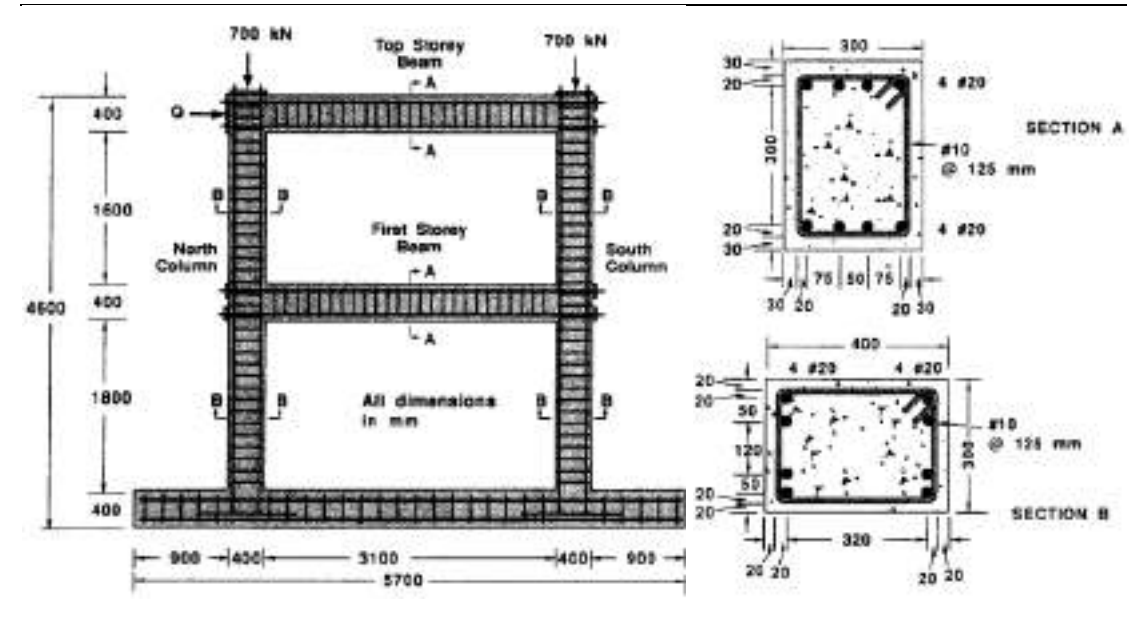


Figure 45: Details of Reference RC frame [33]

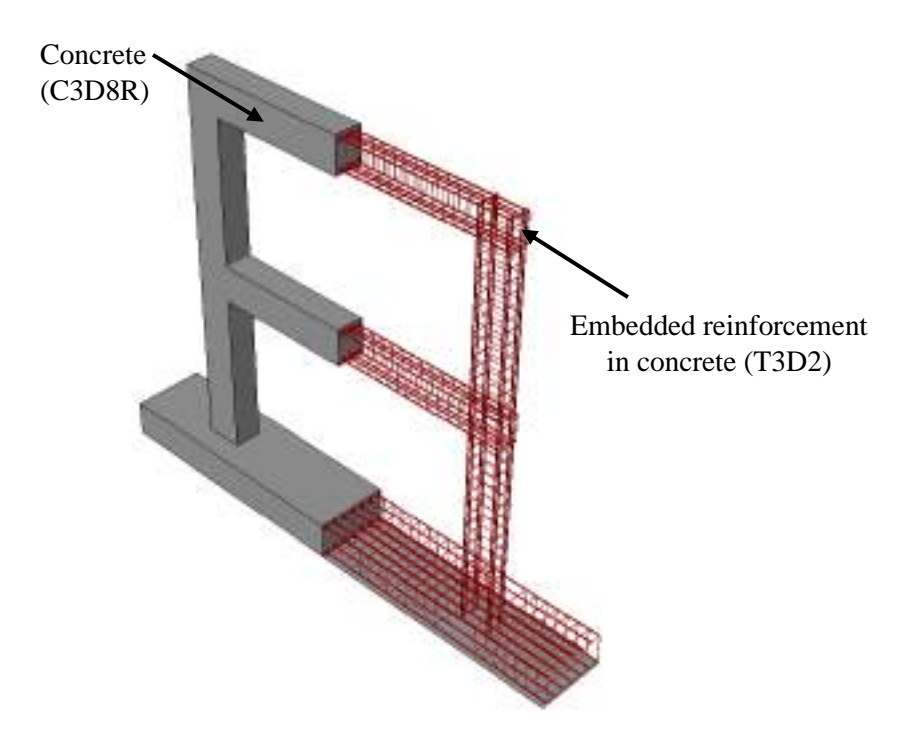


Figure 46: Geometric FE modelling of reference specimen in ABQUS

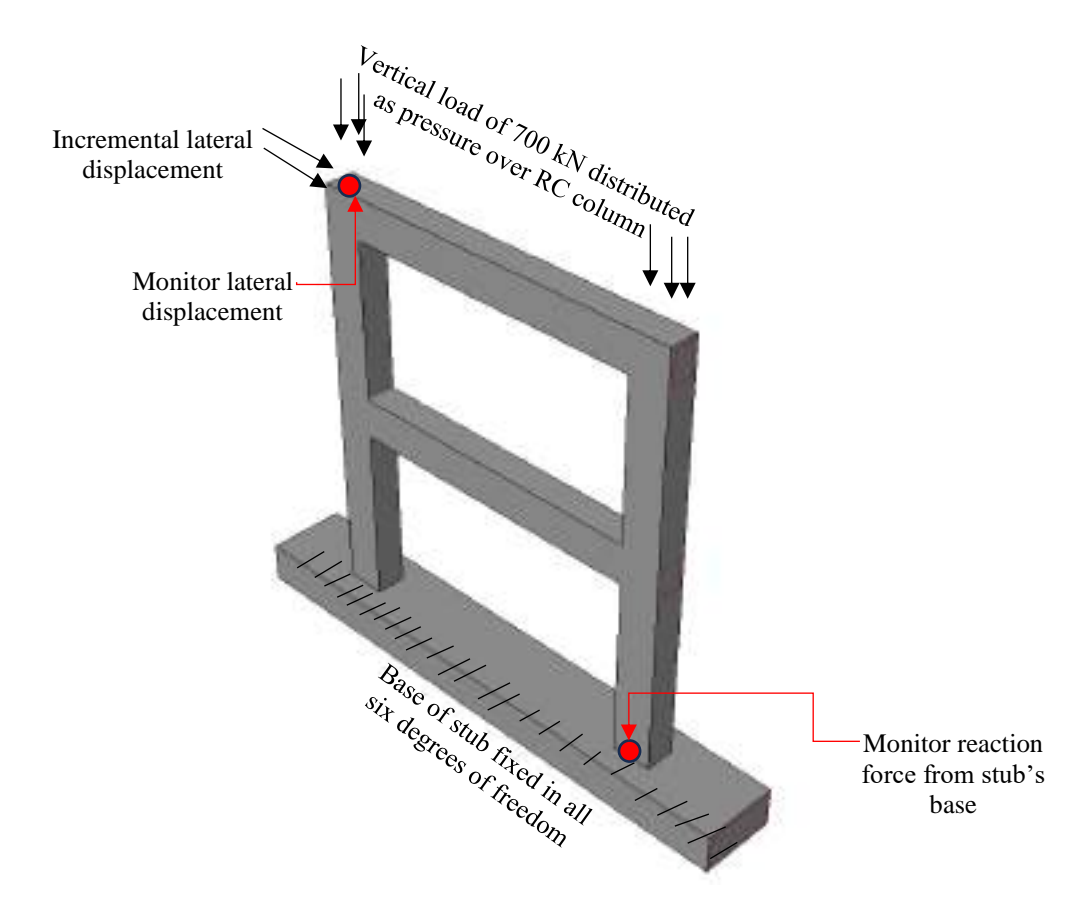


Figure 47: Load and boundary conditions of FEM according to reference RC specimen

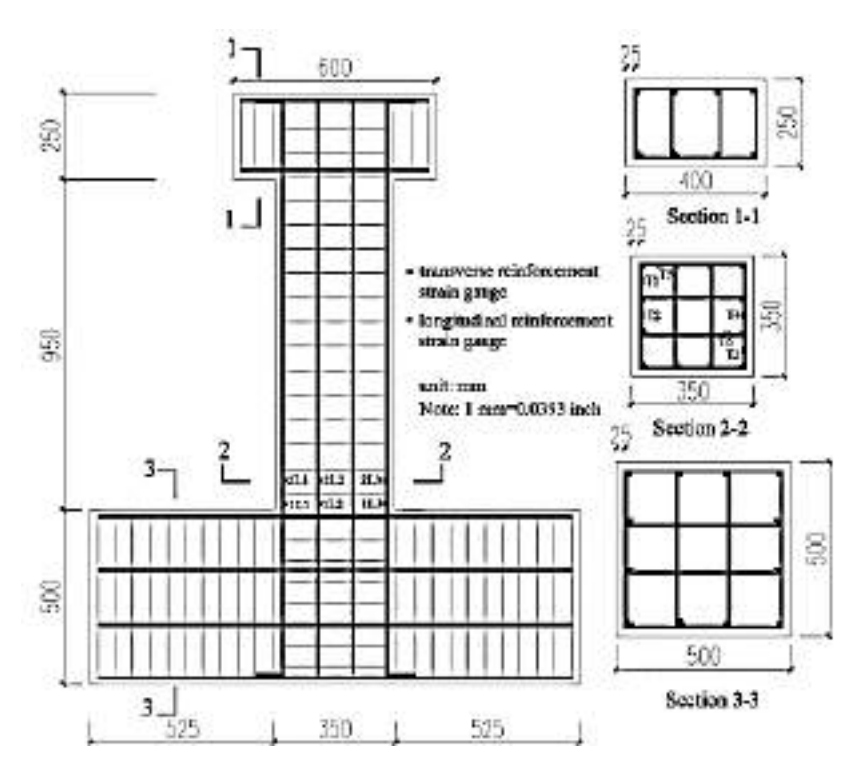


Figure 48: Details of reference RC column specimen [8] (all dimensions are in mm)

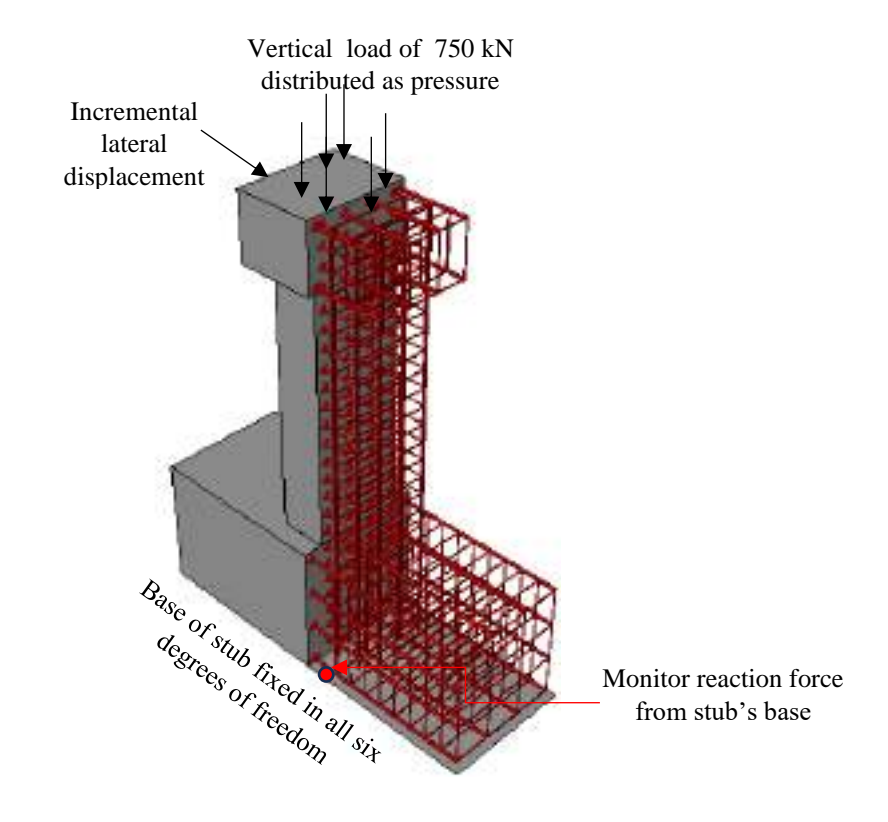


Figure 49: Finite element modeling of reference RC column in ABQUS

The illustration of the backbone curve from the experiment and FEM has been presented in Figure 50. It can be seen that the FEM mirrored the backbone curve from the experiment. Consequently, the FEM method could be adequate for conducting parametric analysis of comparable RC frames.

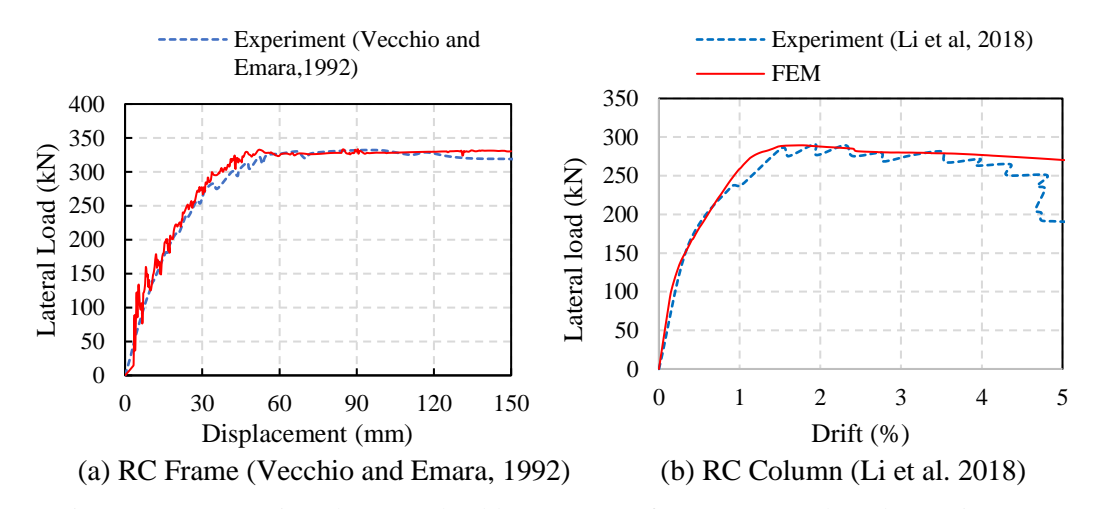


Figure 50: Comparison between backbone curve of FEM approach and experiment

Analytical specimen for parameteric study

For performing parametric study, a two dimensional two bay ,two storied RC frame has been considered. A schemic diagram of the frame has shown in Figure 51. The parametric study was performed by varying three different parameters (i.e., concrete grade, reinforcement grade, and axial load ratio), as shown in Table 2.

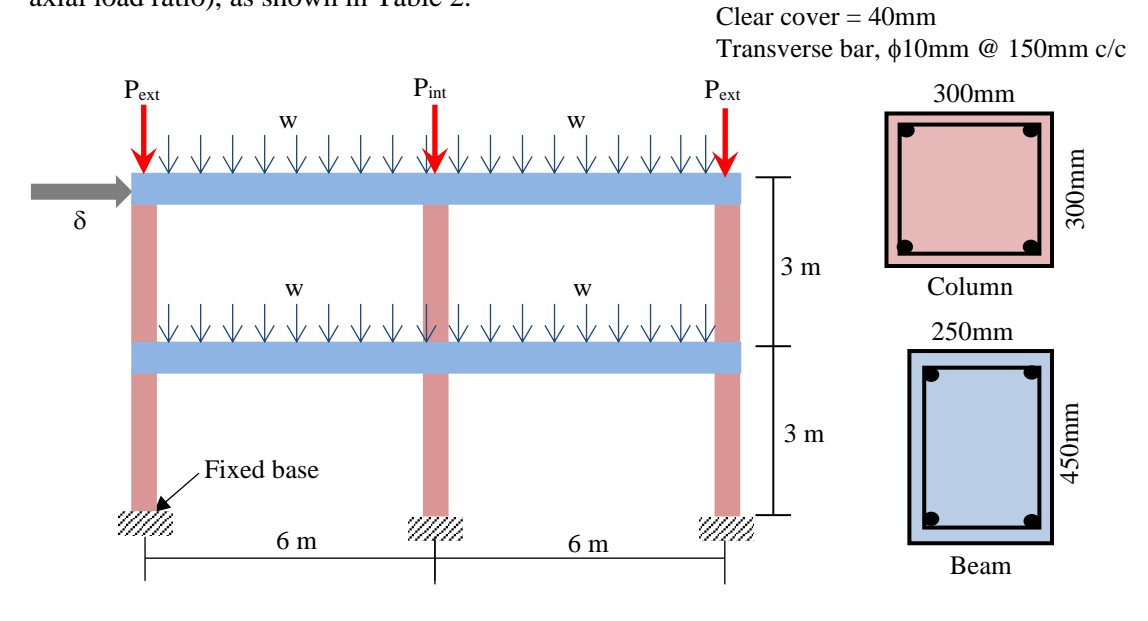


Figure 51: Schematic diagram of RC frame used for FEM parametric study

The parametric study has been performed by varying three different parameters (i.e., concrete grade, reinfircement grade and axial load ratio), as shown in Table 26.

where, fy = yield strength of reinforcement;

f'c = compressive strength of concrete;

P_{ext} = load on exterior column; P_{int} = load on interior column;

 ρ_s = steel ratio (%);

 A_s = area of total reinforcements in column;

 $A_{s,top}$ = area of top reinforcement in beam;

A_{s,bot} = area of bottom reinforcement in beam; w= distributed load on beam;

P/(Agf'c)=axial load ratio

Table 26: Variation of different parameters for FEM study

load ratio) (0.17) T		Car	1			D		I
fy	f'c	D. 4		lumn	A .	Α.	Beam		Pin
(MPa)	(MPa)	Pext (kN)	Pint (kN)	ρ _s (%)	A_s (mm^2)	$A_{s,top}$ (mm^2)	$A_{s,bot}$ (mm^2)	w (kN/m)	Ag
400				2.5	2250	563	375		0.1
500	20	90	180	2	1800	450	300	10	0.1
600				1.67	1500	375	250		
	riation of c				with fixed	Reinforce	ment yield	strength (60)0MPa
	20	30	60						
600	30	120	240	1.67	1500	375	250	25	0.2
	50	300	600						
	20	300	600						
600	30	525	1050	1.67	1500	375	250	25	0.5
	50	975	1950						
	compressiv	ve strengt	h (20, 30,		inforceme	nt yieid str	ength (600	MPa) for dif	
		30	60 240 1.67	<u> </u>				25	0.2
600	20	120		1.67	1500	375	250		0.3
		210	420						0.4
		300 120	600 240						0.3
		255	510	1					0.3
600	30	390	780	1.67	1500	375	250	25	0.4
		525	1050	<u> </u>					0.5
		300	600						0.2
		525	1050	1					0.3
600	50	750	1500	1.67	1500	375	250	25	0.4
		975	1950	1				2.5	0.2
Sat 1. W	riation of a			of concr	ate and avi	al load roti	on with fiv	ed Reinforc	
	ength (600N		ve suegu	i or concr	ete aliu axi	ai ioau iau	Oli With HX	teu Kennore	CIIICIII
	20	30	60						0.2
600	30	255	510	1.67	1500	375	250	25	0.3
000	40	575	1150	1.07	1500	313	230	23	0.4
	50	975	1950	1					0

The reference specimen is named according to this manner: $F_{f^c,fy,n}$ For instance, $F_{20,400,0.4}$ means the concrete's compressive strength of RC member is 20 MPa, yield strength of reinforcement is 400 MPa, axial load ratio is 0.4 and likewise for other cases.

Finite element modeling of RC frame

The finite element modeling technique outlined in the previous section has been utilized. The only variation from earlier modeling is that no stub has been taken into account. The primary function of the stub is to offer the RC frame a rigid foundation. In this parametric study, a fixed support (ENCASTRE) has been employed. The mesh size utilized for this study is 100 mm for concrete components while conducting mesh sensitivity analysis. In this analysis, the examination has been performed in two phases. In the initial phase, the load on the tops of each column and beam is applied, followed by a 5% (of 300mm story height) displacement applied incrementally to the RC frame. The second phase has commenced from the final increment of the first phase.

Results of parametric analysis

The results of parametric study have been evaluated with respect to lateral behavior such as backbone curve, stiffness degradation curve and damage pattern. Following symbols stands for,

 V_y = yield shear capacity (by following Park's model [37]);

 δ_y = yield drift (by following Park's model [26];

 V_{y-col} = yield shear capacity (at 1st yielding of column's reinforcement);

 $\delta_{y\text{-col}}$ = yield drift (at 1st yielding of column's reinforcement);

 V_m = maximum lateral capacity;

 $\delta_m\!=\!$ corresponding drift to maximum lateral capacity;

 $\frac{\delta_{\rm m}}{\delta_{\rm v}}$ = displacement ductility ratio (yield drift according to Park's model [37]);

 $\frac{\delta_m}{\delta_{y-col}}$ = displacement ductility ratio (yield drift as 1st yielding of column's reinforcement)

Effect of reinforcement grade pairing with low strength concrete (Set-1):

Table 27: Lateral behavior of analytical specimens varying rebar's grade

Specimen	At 75% of maximum lateral load		At 1st yielding of reinforcement of column		At maximum lateral capacity		$\frac{\delta_{\rm m}}{s}$	$\delta_{\rm m}$	$\frac{V_{\rm m}}{V_{\rm v}}$	$\frac{V_{m}}{V_{v-col}}$
Name	V _y (kN)	δ _y (%)	V _{y-col} (kN)	δy-col (%)	V _m (kN)	δ _m (%)	δ_{y}	δ_{y-col}	v _y	y-cor
F _{20,400,0.17}	86.87	0.97	96.27	0.99	115.83	1.94	2	1.96		1.20
$F_{20,500,0.17}$	87.86	1.21	102.35	1.33	117.14	2.31	1.9	1.74	1.33	1.14
$F_{20,600,0.17}$	87.43	1.40	108.01	1.79	116.57	2.71	1.94	1.52		1.08

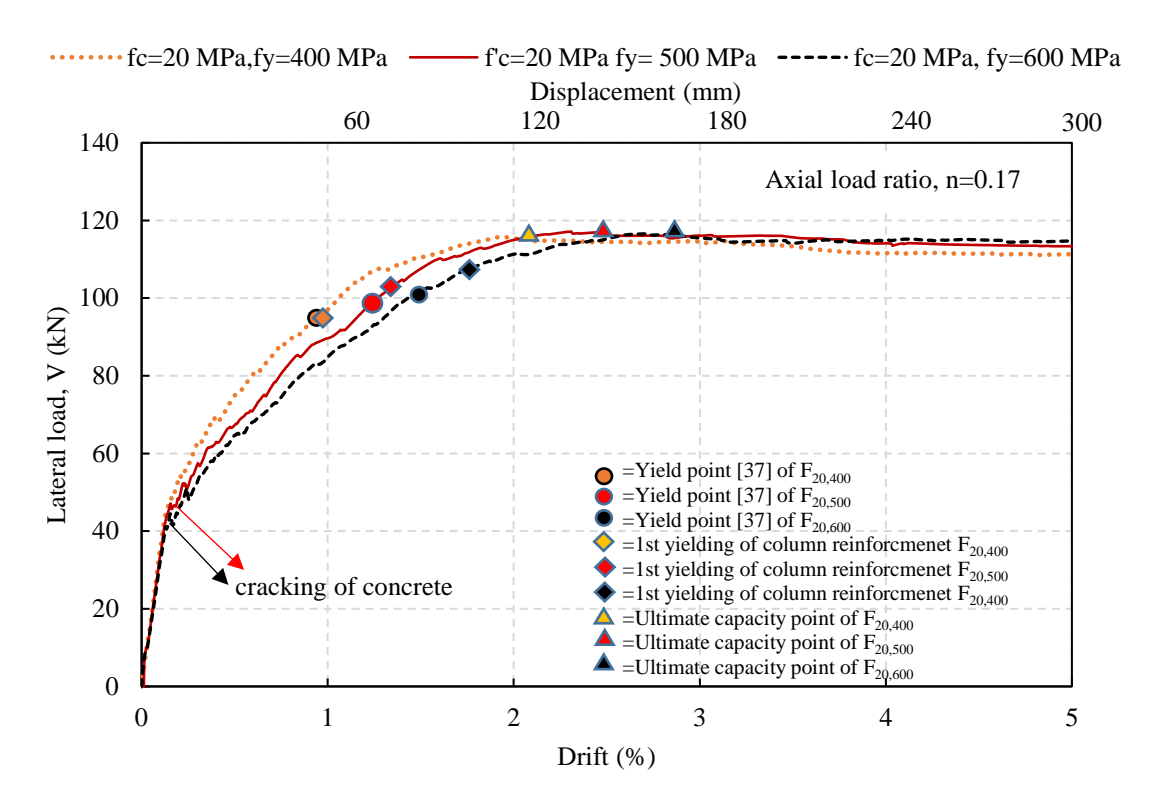


Figure 52: Backbone curve of analytical specimens varying rebar's grade

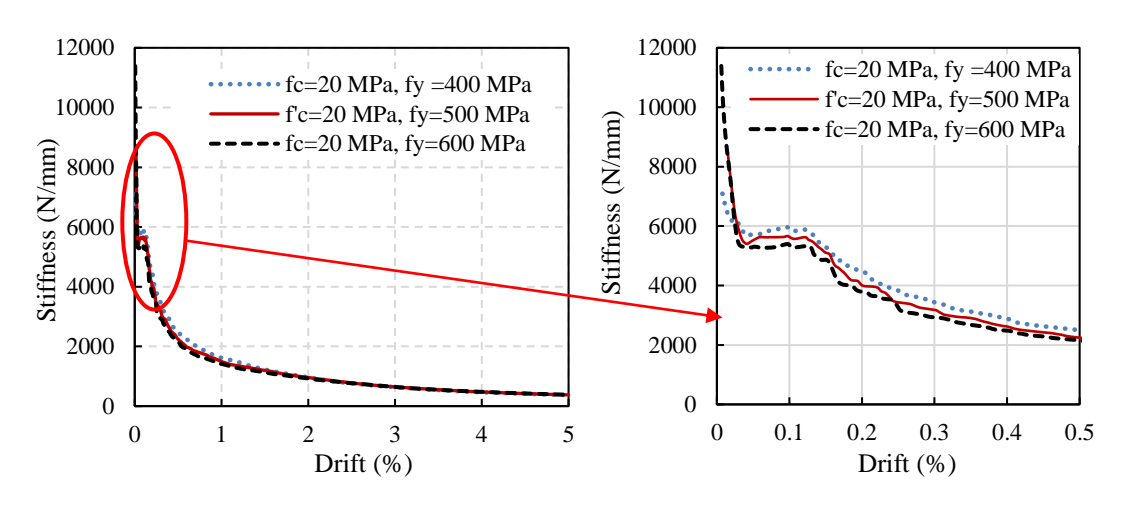


Figure 53: Stiffness degradation curve of analytical specimens varying rebar's grade

It is observed that the ultimate lateral capacity is comparable irrespective of rebar grade when $A_s f_y$ and axial load ratio remain constant. The drift value corresponds to yield level and ultimate capacity level increases with the increase of the reinforcement grade. However, the displacement ductility ratio decreased in specimens with higher reinforcement grade. Stiffness degradation is also comparable for all the specimens without showing any alarming behavior for high strength reinforcement and low strength concrete combination against lateral load application.

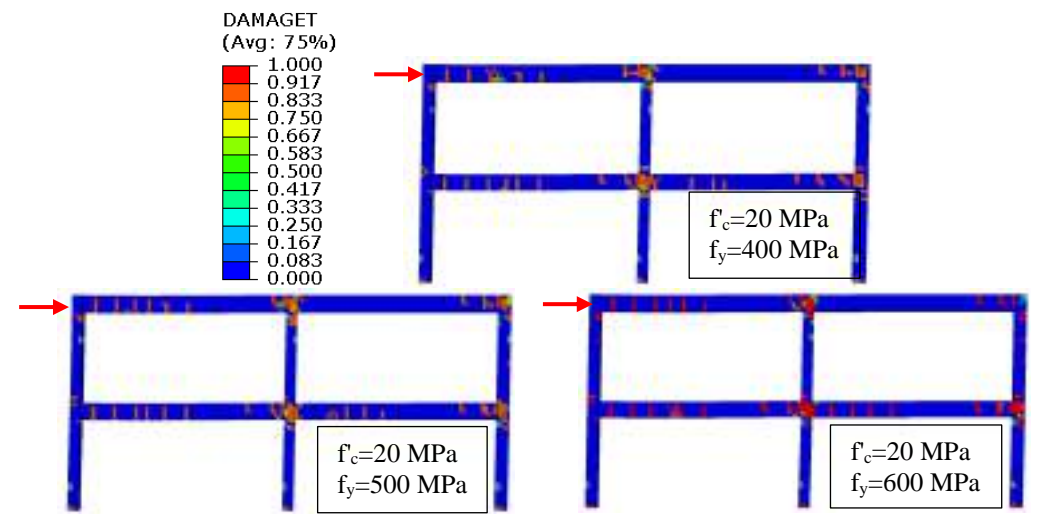


Figure 54: Damage of concrete due to tension for different specimens at 2% drift for Grade 400, 500 & 600MPa

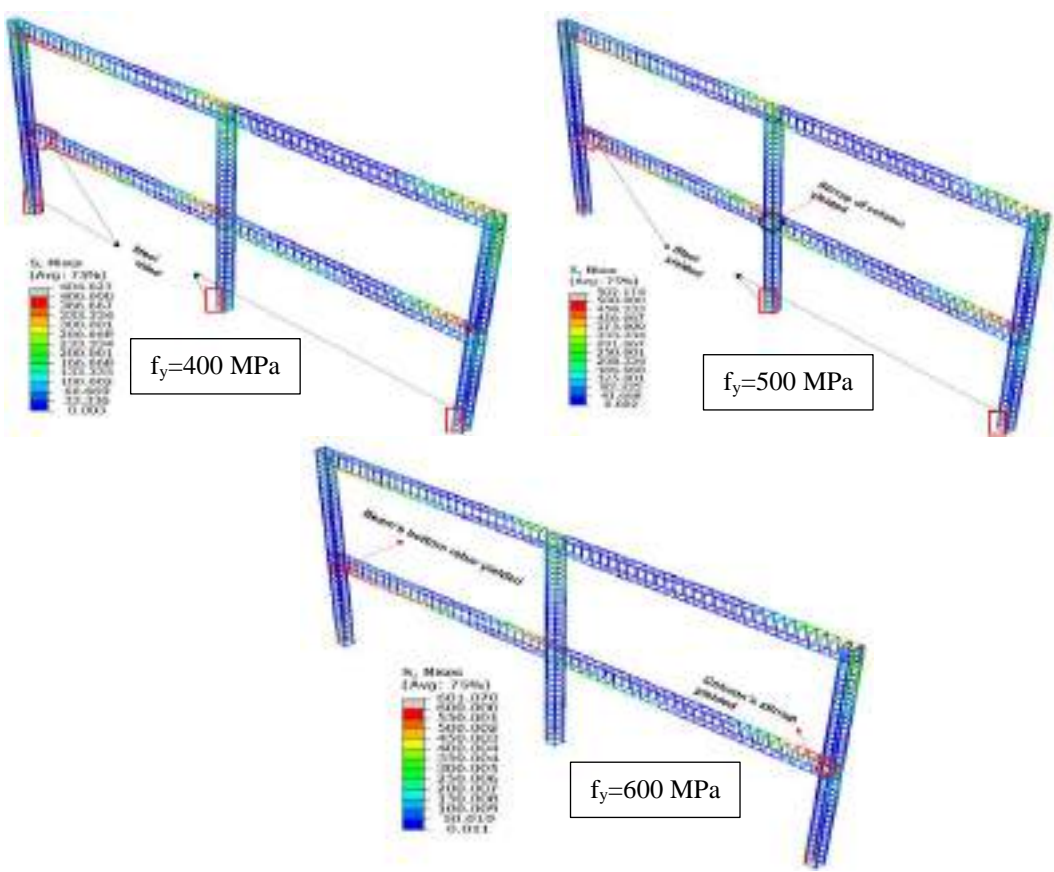


Figure 55: Stress level of reinforcement for different specimens at 2% drift for Grade 400, 500 & 600MPa

It is observed that critical members (i.e., column) have experienced higher tensile stress in reinforcement beyond yield limit with f'_c =20 MPa and f_y =400 MPa and 500MPa specimens, as longitudinal rebar of the base of all three columns yielded at 2% drift. But, in specimens with f_y =600 MPa, the longitudinal reinforcement of the column has not yielded at that drift.

However, transverse reinforcement of higher yield strength reinforcement of column under compression has yielded at joints, which indicates that high-strength reinforcements must be given special attention to joint detailing in terms of confinement requirements.

Effect of concrete grade pairing with high strength reinforcement (Set-2)

Table 28: Lateral behavior of analytical specimens varying concrete's grade

Specimen Name	At 75% of maximum lateral load		At 1st yielding of reinforcement of column		At maximum lateral capacity		$\frac{\delta_{\rm m}}{\epsilon}$	$\frac{\delta_{\rm m}}{\epsilon}$	$\frac{V_{\rm m}}{V_{\rm v}}$	$\frac{V_{\rm m}}{V_{\rm v-col}}$
	Vy	δ_{y}	V _{y-col}	δy-col	V _m	$\delta_{\rm m}$	δ_{y}	δ_{y-col}	v _y	y cor
	(kN)	(%)	(kN)	(%)	(kN)	(%)				
$F_{20,600,0.4}$	86.30	0.90	113.88	1.98	115.06	2.28	2.53	1.15		1.01
F _{30,600,0.4}	79.53	0.62	106.04	1.94	106.05	1.94	3.12	1.00	1.33	1.00
F _{40,600,0.4}	83.37	0.62	105.07	2.02	111.16	1.10	1.77	1.04		
F _{50,600,0.4}	86.96	0.63	*	*	115.94	1.16	1.84	*		*
* Means column reinforcement not yielded before attaining maximum load capacity.										

f'c=20 MPa ----- f'c=30 MPa - f'c= 40 MPa f'c=50 MPa 140 fy= 600 MPa, n=0.4 120 100 Lateral Load (kN) =Yield point- F_{20,600,0} 80 =Yield point- F_{30,600,0}. Yield point- F_{40,600,0.4} -40,600,0.4 -Yield point- F_{50,600,0.4} -1st yielding of column rebar- F_{20,600,0.4} 60 1st yielding of column rebar- F_{30,600,0.4} 40 =1st yielding of column rebar- F_{40,600,0.4} =1st yielding of column rebar- F_{50,600,0.4} =Maximum capacity- F_{20,600,0.4} =Maximum capacity- $F_{30,600,0.4}$ 20 =Maximum capacity- $F_{40,600,0.4}$ =Maximum capacity- F_{50,600,0}. 0 Drift (%)

Figure 56: Backbone curve of analytical specimens varying concrete's grade

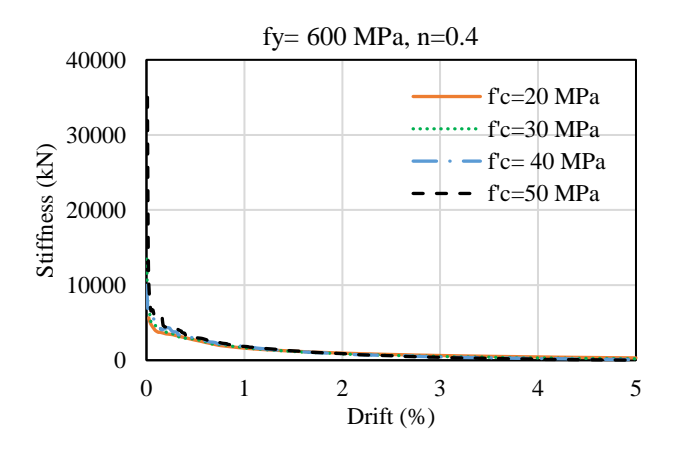


Figure 57: Stiffness degradation curve of analytical specimens varying concrete's grade

At constant axial load ratio, the maximum lateral load capacity is somewhat similar for different concrete grade but displacement ductility significantly lowers with increase of concrete grade due to higher tensile cracking both at beam and column. Stiffness degradation beyond 0.5% drift is found similar for all concrete grades.

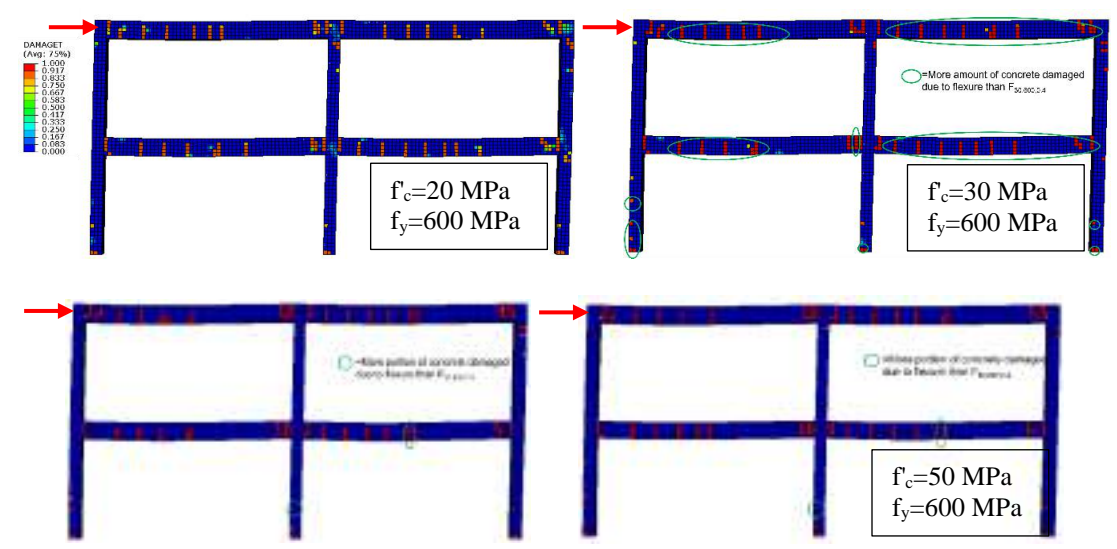


Figure 58: Damage of concrete due to tension for different specimens at 2% drift for Grade 20, 30 & 50MPa concrete

Higher grade concrete speciment undergoes higher cracking at same drift level leading to rapid capacity drop at relatively lower displacement level. For ductile frame behavior, control of this cracking is important which indicates the necessity of proper confinement design for compression members.

Effect of axial load ratio with high strength reinforcement (Set-3)

Table 29: Lateral behavior of analytical specimens varying axial stress ratio on column

Specimen Name	At 75% of maximum lateral load		At 1st yielding of reinforcement of column		At maximum lateral capacity		$\frac{\delta_{m}}{\delta_{y}}$	$\delta_{\rm m}$	$\frac{V_{\rm m}}{V_{\rm y}}$	$\frac{V_{\rm m}}{V_{\rm y-col}}$
	Vy	δ_{y}	$V_{y\text{-col}}$	$\delta_{y ext{-col}}$	V _m	δ_{m}	o_y	δ_{y-col}	v_{y}	· y=coi
	(kN)	(%)	(kN)	(%)	(kN)	(%)				
F _{20,600,0.2}	91.79	1.5	110.35	1.89	122.39	3.32	2.21	1.76		1.11
F _{20,600,0.3}	88.92	1.18	112.32	1.89	118.56	2.82	2.40	1.49	1.33	1.06
F _{20,600,0.4}	86.30	0.90	113.88	1.98	115.06	2.28	2.53	1.15		1.01
F _{20,600,0.5}	84.83	0.71	113.11	2.15	113.11	2.15	2.53	1.00		1.00
F _{30,600,0.2}	81.38	1.17	101.19	1.73	108.50	3.16	2.70	1.83		1.07
F _{30,600,0.3}	77.49	0.66	102.63	1.83	103.32	2.45	3.71	1.34		1.01
F _{30,600,0.4}	79.53	0.62	106.04	1.94	106.05	1.94	3.13	1.00		1.00
F _{30,600,0.5}	79.16	0.62	*	*	105.55	1.17	1.89	*		*
F _{50,600,0.2}	80.04	0.61	105.14	1.75	106.72	2.39	3.92	1.37		1.02
F _{50,600,0.3}	85.15	0.61	*	*	113.53	1.26	2.07	*		*
F _{50,600,0.4}	86.96	0.63	*	*	115.94	1.16	1.84	*		*
F _{50,600,0.5}	82.67	0.62	*	*	110.23	1.19	1.92	*		*
* Means column reinforcement not yielded before attaining maximum load capacity.										

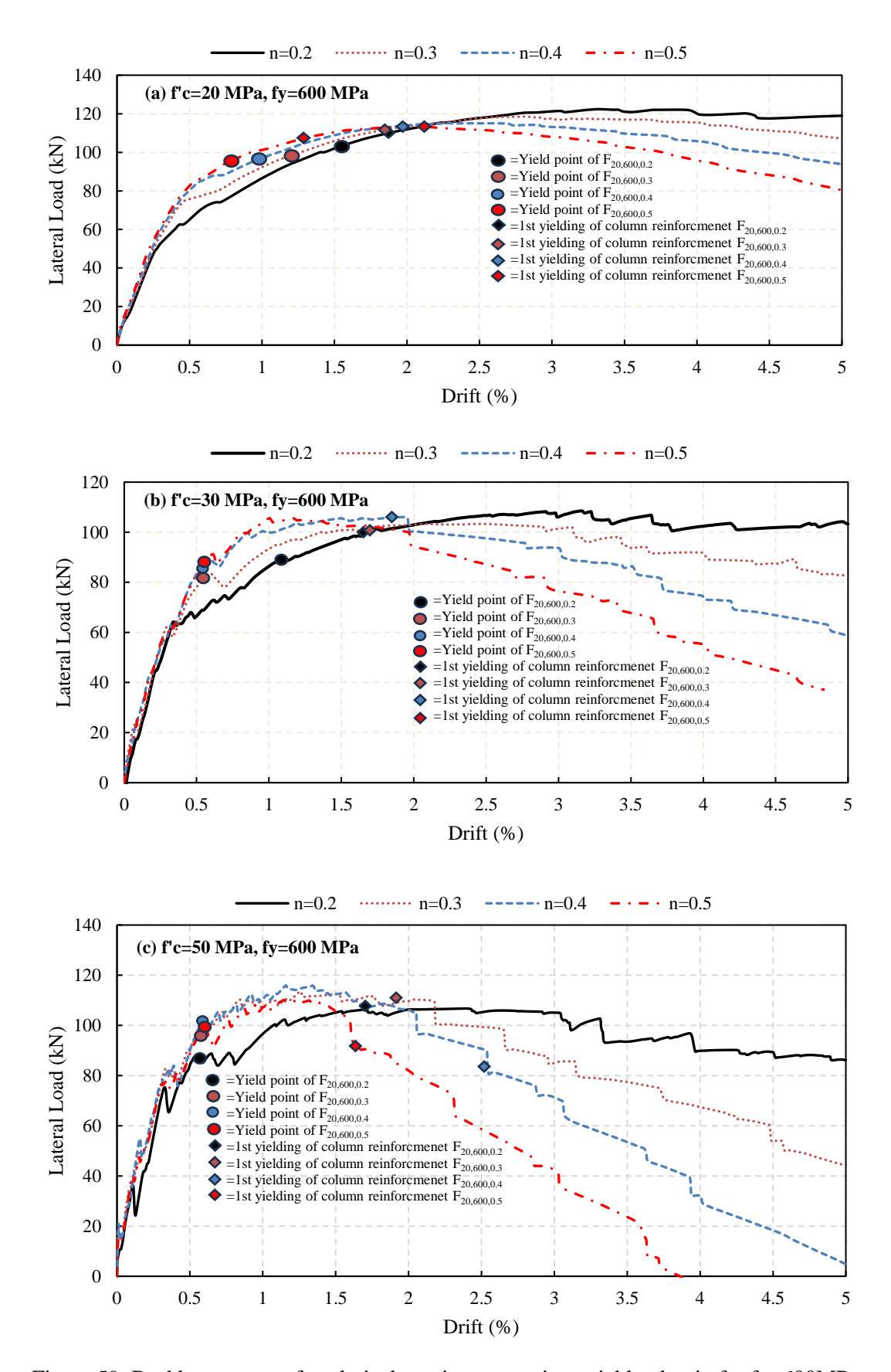


Figure 59: Backbone curve of analytical specimens varying axial load ratio for fy=600MPa

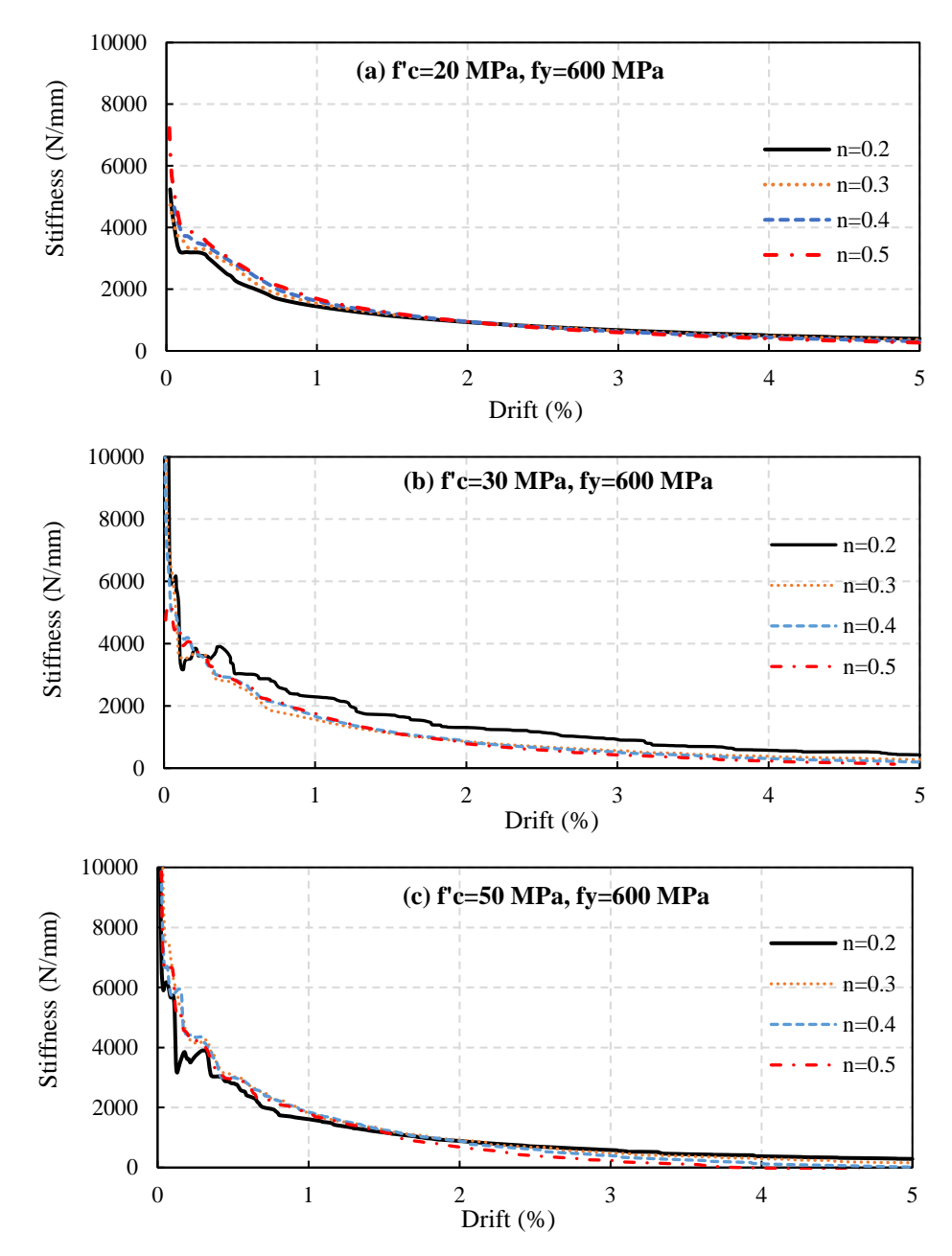


Figure 60: Stiffness degradation curve of analytical specimens varying axial load ratio

Higher load ratio has negligeable effect on ultimate lateral load capacity but exhibits significant effect on ductile property. Low strength concrete has very little sensitivity on load ratio in terms of ductility but higher concrete grade shows limited ductility at or above axial load ratio of 0.4. Structural framing with higher concrete strength results in higher initial stiffness but undergoes steeper stiffness degradation and less drift capacity with increase of axial load ratio. On the other hand, specimens with low f'c result in lower initial stiffness but milder degradation across all axial load ratios up to 0.5. Yielding of the beam occurred within a narrow drift margin in case of higher gravity load, resulting in a sudden capacity drop.

Effect of concrete strength pairing with high strength reinforcement under different axial load ratio (Set-4)

Table 30: Lateral behavior of analytical specimens varying concrete's grade

Specimen Name	At 75% of maximum lateral capacity		At 1st yielding of reinforcement of column		At maximum lateral capacity		$\frac{\delta_m}{s}$	δ_m	$\frac{V_m}{V}$	$\frac{V_{\rm m}}{V_{\rm y-col}}$
	V _y (kN)	δ _y (%)	V _{y-col} (kN)	δ _{y-col} (%)	V _m (kN)	δ _m (%)	δ_y	δ_{y-col}	$V_{\mathcal{Y}}$	
F _{20,600}	91.79	1.5	110.35	1.89	122.39	3.32	2.21	1.76		1.11
F _{30,600}	77.49	0.66	102.63	1.83	103.32	2.45	3.71	1.34	1 22	1.01
F _{40,600}	83.37	0.62	105.07	2.02	111.16	1.10	1.77	1.04	1.33	1.08
F _{50,600}	82.67	0.62	*	*	110.23	1.19	1.92	*		*

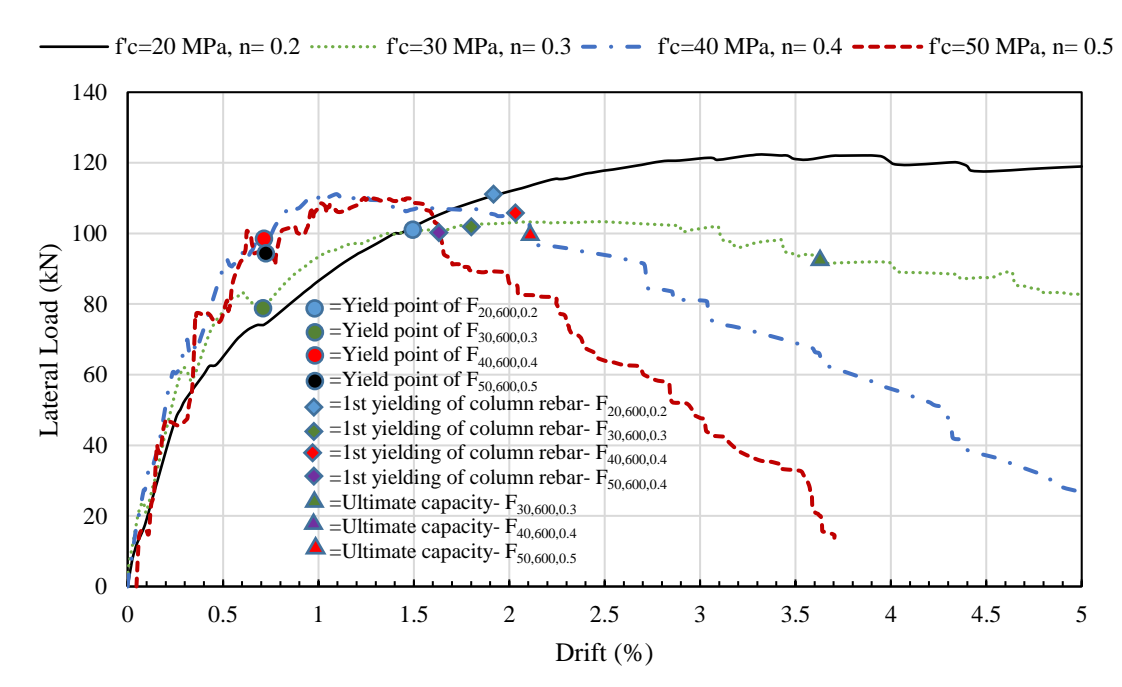


Figure 61: Backbone curve of analytical specimens varying concrete's grade

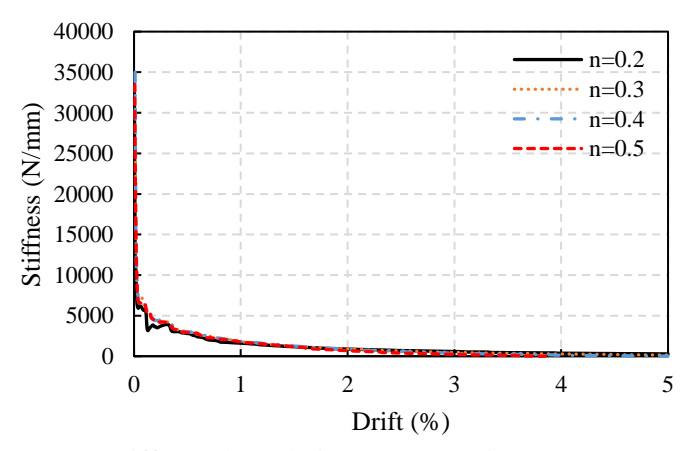


Figure 62: Stiffness degradation curve varying concrete's grade

At low axial load level, lateral capacity can be higher even with lower concrete strength. All range of concrete grade (20MPa to 50MPa) shows similar ductility and stiffness degradation pattern at lower axial load ratio but with an increased axial load ratio, higher grade concrete frame ductility reduces significantly. Higher grade concrete exhibits higher initial stiffness but it's almost overlapping at post yield stage. The combination of high strength concrete with high strength reinforcement is best at lower axial load ratio in terms of obtaining maximum lateral load capacity as well as sufficient ductility accepting least damage to the structural members. In case of using higher grade concrete, a high axial load ratio can cause limited ductility that is an unfavorable behavior at seismic event. This finding is an indication to optimum combination of material strength (concrete and reinforcement) as per seismic performance objective (operational, immediate occupancy, life safety, collapse prevention etc.) of the target structure.

6 Discussion

This study aims to assess the performance of RC structural members and sections reinforced with different grades of steel reinforcement based on the current design provisions, analytical procedure, and literature review on experimental works. Building codes like BNBC2020, ACI318-19, NZS3101:2006, and Eurocode 2 & 8 have been studied to compare the existing design provisions for higher-grade steel reinforcement. Based on existing provisions on various design considerations, parameters like flexural capacity, load-moment interaction of axial members, deflection, crack, etc. have been assessed for the sample section and compared. In addition to the design comparisons for serviceability and other states of structures under static application of external loads, lateral force resistance capacity has been assessed using non-linear static analysis over FEM of RC frame.

6.1 Comparison of Structural Member Design Parameters

\square Tensile strain and corresponding strength reduction factor (ϕ)

ACI 318-19 modified strain relationship to determine ϕ factor concerning section characteristics to be compression or tension controlled. Based on this modification, to ensure a tension-controlled section, the rebar minimum tensile strain is higher for higher yield strength of reinforcement as shown in Figure 7.

☑ Flexural capacity of Beam:

With the reduction of reinforcement with the respective increase of rebar yield strength for a particular concrete grade maintaining a constant $A_s f_y$. In other words, it is to maintain stress block depth constant concerning the grade of steel of reference (i.e. changing steel quantity A_s) to maintain section depth constant with respect to the reference steel grade that is 400. It reflects no section increase while using a higher grade of steel than Grade 400 for particular section capacity with varying ϵ_{ty} , ϵ_{cu} , ρ_b , ϵ_t . Adjusted $A_s = A_s f_{y=400}/f_y$), the flexural capacity remains almost unchanged for the same member size and reinforcement grade as found in Table 7Table 8Table 9.

☑ Member Deflection:

Deflection is a function of member stiffness and in RC section, reduction of reinforcement causes a reduction of stiffness for the same member size. Designing with high yield strength reduces reinforcement quantity for the same flexural capacity leading to reduction of stiffness. As a result, deflection usually increases with increased yield strength of reinforcement.

When deflection is a governing criterion the effect of higher-grade reinforcement can be offset either by providing an increased amount of reinforcement or increasing the depth of the section. Table 13 and Figure 8b show, that the extent of increase of deflection for higher rebar grade is higher for lower concrete strength. So, Higher grade concrete is better performing with high-strength reinforcement in terms of deflection control.

☑ Flexural crack width:

Higher-strength rebar undergoes higher tensile strain during service conditions resulting in relatively higher crack width. Crack width is a serviceability limit that is to be maintained as per building code(s) in the process of its design. The crack extent depends on rebar tensile stress at the service load level. Figure 11 shows an escalation of crack width at various percentages of steel service stress of different grades. For limiting crack width relevant to exposure conditions, rebar quantity is required to adjust after designing a section for flexure. However, flexural cracks are not that much sensitive to concrete compressive strength.

In ACI 318-19, the crack control issue has been addressed in terms of maximum rebar spacing limit. From Figure 13 it shows that at 30%, 50% and 70% of steel yield stress level (fs=% of fy) maximum allowable rebar spacing are 467mm, 255mm and 153mm for 600MPa reinforcement respectively, for a concrete section designed in flexure.

☑ Column capacity (axial load-moment interaction):

According to ACI 318-19, fy=550MPa is allowed as the upper limit for axial compression calculation. As a result, with constant $A_s f_y$ for a column section, the initial axial capacity is around 3% less with 600MPa compared to that of 400MPa and 500MPa grade. Due to the effect of axial force, in contrast, to beam flexural capacity, column flexural capacity with higher grade rebar is a little lower than lower grade rebar with constant $A_s f_y$.

☑ Confinement criteria:

ACI 318-19 has provided confinement requirement criteria for columns in special moment frames and for special RC walls. For the column, the magnitude of axial load concerning column cross-section and concrete grade (axial load ratio, P_u/A_gf_c) is a sensitive parameter. For an axial load ratio, P_u/A_gf_c higher than 0.3, the confinement requirement is higher. Use of higher grade transverse reinforcement reduces the rebar volume to comply code provision ensuring ductile performance of column. But, maximum spacing of transverse bar is relatively smaller in case of higher-grade reinforcement to resist buckling and premature failure of longitudinal reinforcement.

Eurocode 8 considers confinement for medium ductility class column (DCM) in addition to high ductility class column (DCH) whereas, ACI considers confinement rebar for SMF only. Higher grade concrete is less ductile in nature therefore requires higher confinement quantity.

☑ Development length requirement:

ACI 318-19 has introduction of reinforcement grade factor (ψ_g) in development length requirement compared to BNBC 2020 provisions. As a result, the development length demand is about 10% and 20% higher for 500MPa and 600MPa grade rebars compared to BNBC 2020 based requirement. Moreover, the development length demand is higher for higher grade reinforcement and that can be offset by using higher concrete grade. In case of end anchorage, development length can be reduced about 30% using headed deformed bar replacing conventional hooked anchorage. In general, higher-grade concrete is better to reduce development length of all types of tensile stress.

Technically, low strength concrete has no limitation to be used with high strength reinforcement in terms of design compliance if building code provisions are followed and applied entirely.

6.2 Structural member Performance comparison against Lateral Load

\square Lateral load resistance capacity of frame:

In case of constant $A_s f_y$, both parametric study under this research and literature review on experimental works exhibits that the lateral load resistance is relatively higher in case of lower grade rebar initially. But after a drift ratio of about 3.0% the lateral load capacity matches for 400, 500 and 600MPa grade rebar (Figure 52). In terms of concrete compressive strength, higher grade concrete provides higher lateral capacity as expected.

Higher grade reinforcement results slightly lower value of over strength $v_u/v_{y\text{-col}}$ compared to 400MPa grade (Table 27).

☑ Displacement ductility:

Displacement ductility decreases with increase of yield strength (fy) in general but follows similar pattern for all yield strength grade rebar. For high strength reinforcement, higher grade concrete is better to achieve higher ductility of RC frame. Our findings also reveal that the inelastic drift ratio generally achieve above 2.5~3.0% which mostly meets seismic ductility criteria of building codes.

☑ Energy dissipation:

Literature review on experimental works reveals that the hysteretic loop behavior is more or less comparable for different graded reinforcement. Since, the hysteretic loop formation is quite stable both in forward and reverse cycle, the energy dissipation ability is acceptable for higher yield strength.

☑ Stiffness degradation pattern:

For same concrete grade, higher grade steel shows similar stiffness degradation pattern compared to 400MPa steel.

☑ Cracking due to lateral deformation:

Damage level and crack formation is always remained higher for higher grade reinforcement at certain displacement level. Cracking at joints can cause brittleness within the frame behavior and can cause sudden collapse due to losing bond between concrete and reinforcement. Confinement is important

\square Effect of concrete grade and its performance criteria:

Higher compressive strength of concrete is generally exhibiting better performance with higher grade reinforcement as optimum combination to achieve higher capacity. But concrete has negligeable tensile strength and shows fragility under tensile strain. In addition, higher strength concrete is less ductile and cause faster capacity drop in lateral load due to formation of larger width cracks with higher grade rebar. For crack controlling and enhanced ductility, confinement demand is higher for higher grade concrete. Furthermore, use of steel fiber reinforcement in concrete is a very good option for controlling tensile crack in concrete. Inclusion of steel fiber can result enhanced integrity and withstand higher number of load reversal. Controlling crack also enhances durability of the structure with lessening exposure of reinforcement to moisture and ionic action. Therefore, compressive strength being a single parameter is not sufficient as performance indicator of RC frame with high strength reinforcement.

☑ Effect of axial load ratio:

From parametric study, it's observed that higher axial load ratio initially gives higher resistance to lateral load (Figure 59) but beyond 1.5% to 2.0% drift the capacity drop is steeper for the case of higher axial load compared to lower axial load level. In case of higher compressive strength of concrete, the lateral load capacity drop is sharper compared to lower grade concrete with increase of lateral displacement. For ductile seismic performance, axial load ratio needs to be limited using sufficient member size rather increasing reinforcement quantity too much to achieve design capacity.

Finally, lateral load resistance and ductility mostly depends on the cracking of concrete due to deformation at post yield stage. Low strength concrete is more ductile (due to lower cracking) but high strength concrete is desirable with high strength reinforcement to achieve efficient strength utilization and for optimum design. Having said that, design with higher strength concrete needs proper use of confinement, keeping axial load ratio at lower range, use of micro fiber reinforcement to control cracking and ensure collapse prevention during seismic event.

7 Benefits & Challenges of Utilizing High-Strength Reinforcement

7.1 Benefits

☑ Improved Structural Capacity:

- The advantage of high material strength can be availed to increase the loadcarrying capacity of RC structures.
- More suitable for high-rise buildings, and long-span bridges involving large-scale loads.

☑ Reduction in Reinforcement Quantity:

- Higher strength allows for smaller reinforcement areas, reducing congestion in beams, columns, and joints.
- Results in cost savings in reinforcement material.

☑ Cost Economy:

• Reduction in total reinforcement requirement in construction leads to reduction both in material and workmanship cost.

☑ Enhanced Durability:

 Less steel area reduces potential corrosion zones and minimizes maintenance requirements.

☑ Sustainability:

• Lower steel usage reduces the environmental footprint of steel production.

☑ Better Structural Integrity

- Reduces bar congestion by lessening rebar volume, bar diameter, increasing space enhance better workmanship opportunity.
- Compaction of concrete becomes easier because of less congestion.
- Less amount of confinement volume ensures easy placement of bars in potential hinge zones.

7.2 Challenges

☑ Bond and Anchorage Issues:

- Bond strength to concrete with high-strength reinforcement is often challenging due to high-stress concentration.
- Requires larger development lengths or use of special anchorage.

☑ Crack and Deflection control:

 Higher tensile stress causes larger crack formation in RC members both under service conditions and during lateral load experience. To control cracking, it may require closer reinforcement spacing than that is required for lower grade reinforcement. Similarly for deflection control, higher volume of reinforcement may be required than that is required from flexural demand.

☑ Ductility:

• Frame with lower quantity of reinforcement of higher yield strength is relatively less ductile than lower grade reinforcement.

☑ Compatibility with Concrete properties

- Lower concrete's compressive strength might limit the utilization of the reinforcement's full capacity or might result larger member size to fulfill capacity demand.
- Best paired with high-strength concrete to optimize performance.

7.3 Recommendations

- ☑ Mechanical splices (coupler) and anchors (headed bar) are recommended to use with high yield strength reinforcement, especially for bar dia 20mm and above so as to minimize the development length requirement and ensure sufficient bond within RC member.
- ☑ Service level axial load ratio is suggested not to exceed 0.40 for columns to avoid possible brittleness and achieve ductility of RC frame against earthquake.
- ☑ Higher compressive strength of Concrete is recommended for better performance by using higher-grade rebar.
- ☑ Controlled use of steel fiber reinforcement is suggested as per established design provision to enhance resistance against tensile splitting and disintegration of concrete.
- ☑ It's suggested not to exceed service stress level beyond 50% of yield strength for flexural members (beam and slab) to maintain better durability, and maintain serviceability.

✓ Further research recommendation:

- Test on RC frame with various parameters on high-strength rebar to fine-tune modeling parameters for finite element analysis.
- Research on using steel fiber reinforcement to incorporate its application provision in local building code and encourage manufacturing in a local capacity.
- Test the headed anchor for capacity assessment and encourage local production for economic viability.

7.4 Conclusion

The use of higher-strength reinforcement in RC structures may be a great alternative in modern structural engineering, enabling efficient detailing and design with reduced material usage. However, proper attention is necessary in designing, detailing, and code compliance to address particularly the relevant provisions of ductility and compatibility with concrete. The use of high-strength steel in reinforced concrete structures offers several advantages under gravity, and wind action as well as design against seismic responses and resistance. The use of high-strength reinforcement exhibits rational performance that is found in various experimental works. Several renowned building codes have been updated and provided guidelines and provisions on how to use high-strength reinforcement in designing structures with due diligence.

In the context of concrete compatibility, the lower boundary of design compressive strength is somewhat between 20MPa (3000psi) to 25MPa (3500psi) according to most of the building codes. In practice, for design performance aspects like development length, deflection control, workability, durability, structural longevity, economy, etc. higher-grade concrete is better performing with higher-grade reinforcement. Concrete strength of lower bound values is not preferable to maintain dimensional proportionality, economy, performance reliability, etc. From the durability point of view, the least concrete strength demand (related to density mostly) is well understood from Part-VI, Sec-8.1.7 of BNBC 2020, where, concrete compressive strength requirement starts from 20MPa up to 50MPa according to exposure type specific.

References

- [1] S.R.O. No.55-Law/2020. The Bangladesh National Building Code (BNBC) 2020., 2021.
- [2] D. R. Ahsan, "Investigation on performance of different structural members reinforced with B600C-R rebar as compared to B500CWR and B420DWR rebar.," October 2022.
- [3] J. M. R. a. S. P. H. Tavallali A.L., "Concrete beams reinforced with high-strength steel subjected to displacement reversals. ACI Structural Journal 111:. https://doi.org/10.14359/51686967," ACI Structural Journal, 2014.
- [4] S. B.M., "Design of Concrete Structures Using High-strength Steel Reinforcement. Transportation Research Board, National Research Council," Transportation Research Board, National Council for Highway Research, 2011.
- [5] Park, "Ductility Evaluation from Laboratory and Analytical Testing.," State-of-the Art Report, Tokyo-Kyoto, Japan, 1988.
- [6] A. H. M. E. K. S. I. Y. Yehia S, Recommended concrete properties for high strength steel reinforcement, 2011.
- [7] R. S. H. T. A. A. L. Jeffrey M., "Drift Capacity of Concrete Columns Reinforced with High-Strength Steel 110," ACI Structural Journal, 2013.
- [8] A. D. J. Yizhu Li SC, "Concrete Columns Reinforced with High-Strength Steel Subjected to Reversed Cycle Loading.," ACI Structural Journal, 2018.
- [9] T. T. I. G. P. R. A. A. Anggraini R, "Experimental load-drift relations of concrete beam reinforced and confined with high-strength steel bars under reversed cyclic loading," ASEAN Engineering Journal, no. 11, p. 56–69, 2021.
- [10] B. O. Abhay Kumar Jain, "The compatibility of concrete strength wit high strength reinforcing steel.," Concrete Model Code for Asia, 1999.
- [11] Z. L. W. H. Hu X, "Experimental Study on Crack Width of HRB600 Grade High-Strength Steel Bar Reinforced Concrete Beams.," 2024.
- [12] H. H. K. K. Naas AAAE, "Comparative Analytical Study on Crack Width of Reinforced Concrete Structures.," Civil Engineering Journal, 2021.
- [13] A. S. A. Harba ISI, "Numerical analysis of high-strength reinforcing steel with conventional strength in reinforced concrete beams under monotonic loading.," Open Engineering, no. 12, p. 817–833, 2022.
- [14] A. A. Shunmuga Vembu PR, "A Comprehensive Review on the Factors Affecting Bond Strength in Concrete.," no. Buildings 13:, 2023.

- [15] G. W. Slavin CM, "Testing., Defining structurally acceptable properties of high-strength steel bars through material," The University of Texas at Austin, 2015.
- [16] Lepage A, "Towards earthquake-resistant concrete structures with ultra high-strength steel reinforcement," 2008.
- [17] Sun C, "Experimental Evaluation of Effect Factors on Seismic Performance of Concrete Columns Reinforced with HTRB630 High-Strength Steel Bars.," International Journal of Concrete Structures and Materials, 2022.
- [18] "Seismic Performance of High-Strength Steel RC Bridge Columns.," Journal of Bridge Engineering, no. 21:04015044, 2016.
- [19] R. M. A. Siddique MAA, "EFFECT OF MATERIAL PROPERTIES ON DUCTILITY OF REINFORCED CONCRETE BEAMS.," in The Institution of Engineers, Malaysia 67, no.3:, 2006.
- [20] Noor M A, "Study on Grade 75 and 60 Reinforcement in RC design.," Dhaka, Bangladesh, 2008.
- [21] ACI CODE-318-19(22): Building Code Requirements for Structural Concrete and Commentary (Reapproved 2022), American Concrete Institute, ACI, 2019.
- [22] A. 224R, "Control of Cracking in Concrete Structures," ACI Committee 224, 2001.
- [23] N. Z. S. N. 3101.1:2006, "Concrete structures standard", Wellington, 2006.
- [24] "EN 1992-1-1, Eurocode 2: Design of concrete structures Part 1-1: General rules and rules for buildings," 2004.
- [25] C. Darwin D., Design of Concrete Structures, Newyork: McGraw-Hill Education, 2021.
- [26] I. 456, "Plain and Reinforced Concrete Code of Practice," 2021.
- [27] F. L. P. Paultre, "Confinement Reinforcement Design for Reinforced Concrete Columns," JOURNAL OF STRUCTURAL ENGINEERING ©ASCE, 2008.
- [28] "Eurocode 8: Design of structures for earthquake resistance," 2004.
- [29] D. Sokoli, "PLASTICITY SPREAD IN COLUMNS REINFORCED WITH HIGH STRENGTH STEEL," 16th World Conference on Earthquake, 16WCEE, no. Paper N° 234, 2017.
- [30] C. Sun, "Experimental Evaluation of Effect Factors on Seismic Performance of Concrete Columns Reinforced with HTRB630 High-Strength Steel Bars," International Journal of Concrete Structures and Materials, 2022.

- [31] S. A. Dehkordi, "Effects of high-strength reinforcing bars and concrete on seismic behavior of RC beam-column joints," Engineering Structures (ELSEVIER), 2019.
- [32] S. D. Systèmes., "https://www.3ds.com/products-services/simulia/products/abaqus/".
- [33] M. B. Vecchio, "Shear Deformations in Reinforced Concrete Frames," ACI Structural Journal, Vols. V. 89, No. 1, Jan.-Feb., pp. pp. 46-56, 1992,.
- [34] D. J. Carreira, "Stress-Strain Relationship for Plain Concrete in Compression," ACI Journal, 1985.
- [35] M. Nakano, "Guideline for post-earthquake damage evaluation and rehabilitation of RC buildings in Japan," in 13th World Conference on Earthquake Engineering, Vancouver, Canada, 2004.
- [36] Y. B. Alaee, "Drift capacity of high-strength concrete columns with mixed-grade longitudinal reinforcements," Advances in Structural Engineering, vol. 22(2), pp. 519-534, 2018.
- [37] R. Park, "Evaluation of ductility of structures and structural assemblages from laboratory testing.," Bulletin of the New Zealand Society for Earthquake Engineering, Vols. 22(3), p. 155–166., 1989.